

University of Windsor

Scholarship at UWindor

Electronic Theses and Dissertations

Theses, Dissertations, and Major Papers

2005

Functional elucidation of lactate dehydrogenase in *Toxoplasma gondii* by double-stranded RNA gene suppression mediation.

Fatme Al-Anouti
University of Windsor

Follow this and additional works at: <https://scholar.uwindsor.ca/etd>

Recommended Citation

Al-Anouti, Fatme, "Functional elucidation of lactate dehydrogenase in *Toxoplasma gondii* by double-stranded RNA gene suppression mediation." (2005). *Electronic Theses and Dissertations*. 2172.
<https://scholar.uwindsor.ca/etd/2172>

This online database contains the full-text of PhD dissertations and Masters' theses of University of Windsor students from 1954 forward. These documents are made available for personal study and research purposes only, in accordance with the Canadian Copyright Act and the Creative Commons license—CC BY-NC-ND (Attribution, Non-Commercial, No Derivative Works). Under this license, works must always be attributed to the copyright holder (original author), cannot be used for any commercial purposes, and may not be altered. Any other use would require the permission of the copyright holder. Students may inquire about withdrawing their dissertation and/or thesis from this database. For additional inquiries, please contact the repository administrator via email (scholarship@uwindsor.ca) or by telephone at 519-253-3000ext. 3208.

INFORMATION TO USERS

This manuscript has been reproduced from the microfilm master. UMI films the text directly from the original or copy submitted. Thus, some thesis and dissertation copies are in typewriter face, while others may be from any type of computer printer.

The quality of this reproduction is dependent upon the quality of the copy submitted. Broken or indistinct print, colored or poor quality illustrations and photographs, print bleedthrough, substandard margins, and improper alignment can adversely affect reproduction.

In the unlikely event that the author did not send UMI a complete manuscript and there are missing pages, these will be noted. Also, if unauthorized copyright material had to be removed, a note will indicate the deletion.

Oversize materials (e.g., maps, drawings, charts) are reproduced by sectioning the original, beginning at the upper left-hand corner and continuing from left to right in equal sections with small overlaps.

ProQuest Information and Learning
300 North Zeeb Road, Ann Arbor, MI 48106-1346 USA
800-521-0600

UMI[®]

**FUNCTIONAL ELUCIDATION OF LACTATE DEHYDROGENASE IN
TOXOPLASMA GONDII
BY DOUBLE-STRANDED RNA GENE SUPPRESSION MEDIATION**

by
Fatme Al-Anouti

A Dissertation
Submitted to the Faculty of Graduate Studies and Research
through the Department of Chemistry and Biochemistry
in Partial Fulfillment of the Requirements for
the Degree of Doctor of Philosophy at the
University of Windsor

Windsor, Ontario, Canada
2005



Library and
Archives Canada

Bibliothèque et
Archives Canada

0-494-09717-5

Published Heritage
Branch

Direction du
Patrimoine de l'édition

395 Wellington Street
Ottawa ON K1A 0N4
Canada

395, rue Wellington
Ottawa ON K1A 0N4
Canada

Your file *Votre référence*

ISBN:

Our file *Notre référence*

ISBN:

NOTICE:

The author has granted a non-exclusive license allowing Library and Archives Canada to reproduce, publish, archive, preserve, conserve, communicate to the public by telecommunication or on the Internet, loan, distribute and sell theses worldwide, for commercial or non-commercial purposes, in microform, paper, electronic and/or any other formats.

The author retains copyright ownership and moral rights in this thesis. Neither the thesis nor substantial extracts from it may be printed or otherwise reproduced without the author's permission.

AVIS:

L'auteur a accordé une licence non exclusive permettant à la Bibliothèque et Archives Canada de reproduire, publier, archiver, sauvegarder, conserver, transmettre au public par télécommunication ou par l'Internet, prêter, distribuer et vendre des thèses partout dans le monde, à des fins commerciales ou autres, sur support microforme, papier, électronique et/ou autres formats.

L'auteur conserve la propriété du droit d'auteur et des droits moraux qui protègent cette thèse. Ni la thèse ni des extraits substantiels de celle-ci ne doivent être imprimés ou autrement reproduits sans son autorisation.

In compliance with the Canadian Privacy Act some supporting forms may have been removed from this thesis.

Conformément à la loi canadienne sur la protection de la vie privée, quelques formulaires secondaires ont été enlevés de cette thèse.

While these forms may be included in the document page count, their removal does not represent any loss of content from the thesis.

Bien que ces formulaires aient inclus dans la pagination, il n'y aura aucun contenu manquant.


Canada

10070-3

©2005 Fatme Al-Anouti
All Rights Reserved

ABSTRACT

Toxoplasma gondii is an intracellular parasite of humans and other mammals which can differentiate between an active and a dormant form. Our primary interest was to modulate gene expression in *T. gondii* in order to investigate a putative gene function. The capability of double-stranded RNA to down-regulate gene expression has been demonstrated in various organisms but has yet to be demonstrated in intracellular organisms such as *T. gondii*. Therefore, the effect of *in vitro* synthesized double-stranded RNA was first investigated for the down-regulation effect of the homologous gene in *T. gondii*. Three non-essential marker genes which encode the green fluorescent protein, uracil phosphoribosyl transferase and hypoxanthine-xanthine-guanine phosphoribosyltransferase were used in the study. Double-stranded RNA was efficiently electroporated into the parasites and specifically lowered the expression of the homologous marker gene. The down-regulation effects can be observed for three successive propagations of the parasites, suggesting the potential use of double-stranded RNA in *T. gondii*.

Subsequently, the down-regulation effect of double-stranded RNA was further characterized in transgenic *T. gondii* expressing double-stranded RNA. We constructed a plasmid coding for double-stranded RNA homologous to the uracil phosphoribosyl transferase gene. A stable parasite line with down-regulated uracil phosphoribosyl transferase expression was generated and shown to have lowered levels of the corresponding transcript as compared to wild type parasites. The steady state level of the expressed double-stranded RNA was quantified and

correlated to that of the homologous mRNA in order to estimate the copy number of double-stranded RNA which can effectively exhibit the down-regulation effect.

Most importantly, the double stranded RNA was used for functional elucidation of lactate dehydrogenase which has long been hypothesized to be essential for parasite metabolism and differentiation. We generated stable transgenic parasite lines in which the expression of lactate dehydrogenase was knocked-down by double-stranded RNA. The differentiation processes of these parasite lines were impaired. *In vivo* studies in a murine model system revealed that these parasite lines were unable to establish a chronic infection. This study was the first to demonstrate that lactate dehydrogenase expression is essential for parasite differentiation.

Dedications

To my loving parents, my patient husband and my lovely kids

Acknowledgements

I wish to begin by showing gratitude to my advisor Dr. Sirinart Ananvoranich for her excellent supervision throughout my doctoral study. She has been a true mentor who guided me constantly. I thank her for all her effort and most of all for giving me a chance to continue my studies.

I also like to thank my committee members: Dr. Marc Ouellette for devoting his time to be a member, Dr. Pandey for his help and suggestions and most of all for his lovely spirit. Also thanks to Dr. Lana Lee for devoting time for being a member and for her academic and personal valuable advice. I would also like to express my gratitude to Dr. Adnan Ali for being a member in my committee and for his concern and support during my study.

Thank you Marlene Bezaire for all your help, concern and friendship. Thank you for making sure my OGS applications were always complete, for taking care of all the meeting schedules and above all for devoting your time to listen to my problems.

Special appreciation goes to Ahmad Al-Riyahi who has been really wonderful throughout my study in terms of help and support. He has been my right arm constantly without any complaint and I wish him all the best for his future career. Also thanks to Kevin Renaud, Wil and Vanuel for technical help.

I would also like to show gratitude to Shane Miersch for his critical reading and suggestions concerning my thesis and Jaafar Naderi for his help, advice and concern.

Finally, I would like to thank my previous colleagues Monique Verhaegen, Bakhos Tannous and Shirin Akhter for sharing with me all their happy and sad moments. Thank you Ju Sheng and Tom Quach for being good friends during the first two years of my study.

At the end, I would like to thank my family for putting up with me throughout the study years and for being so supportive.

TABLE OF CONTENTS

	Page
ABSTRACT	iv
DEDICATIONS	vi
ACKNOWLEDGEMENTS	vii
LIST OF FIGURES	xv
LIST OF ABBREVIATIONS	xviii
CHAPTER 1	
GENERAL INTRODUCTION	
1.1 <i>Toxoplasma gondii</i>	1
1.1.1 The parasite life cycle	2
1.1.2 Parasite growth stages in the intermediate host	3
1.1.2.1 Tachyzoites	3
1.1.2.2 Bradyzoites	4
1.1.3 <i>Toxoplasma gondii</i> cultures as paradigm for Apicomplexan parasites	7
1.1.3.1 Host cells and parasite strains	7
1.1.3.2 Bradyzoite-tachyzoite interconversion	8
1.1.4 <i>Toxoplasma gondii</i> and anti-parasitic regimens	11
1.1.5 Genetic manipulations of <i>Toxoplasma gondii</i>	12
1.1.5.1 Transient gene expression	12
1.1.5.2 Stable gene expression	13
1.1.6 Modulation of gene expression in <i>Toxoplasma gondii</i>	14
1.1.6.1 Non-homologous recombination vectors and insertional mutagenesis	14
1.1.6.2 Tetracycline repressor-based inducible system	15
1.2 RNA tools	16
1.2.1 Antisense RNA	16
1.2.1.1 Non-RNA-cleavage mechanism by preventing translation and transcription processing	17
1.2.1.2 Degradation of RNA via a chemical or enzymatic RNA-cleavage mechanism	19
1.2.2 Ribozymes	22

1.3 RNA interference	23
1.3.1 The natural phenomenon of RNA interference	23
1.3.2 Post-transcriptional gene silencing and co-suppression	23
1.3.3 The features of RNA interference	26
1.3.4 The application of RNA interference	27
1.3.5 The mechanism of RNA interference	30
1.3.6 Dicer and the RNase III family	33
1.3.7 The Argonaute protein family	33
1.3.8 RNA interference as an antiviral defense mechanism	34
1.3.9 RNA interference in mammalian cells	35
1.3.9.1 RNA interference mediated by small interfering RNAs	35
1.3.9.1.1 Gene knock-down in mammalian systems by hairpin RNAs	37
1.3.9.1.2 Gene silencing using small interfering RNA vector-based technology	38
1.3.10 Small RNAs and translational suppression	38
1.3.11 Dicer and Argonaute1 family members as mediators in both RNA interference and temporal development	40
OBJECTIVES	42

Chapter 2

MATERIALS AND GENERAL METHODS

2.1 MATERIALS	43
2.2 GENERAL METHODS	46
2.2.1 Cell culture and <i>Toxoplasma gondii</i>	46
2.2.1.1 <i>Toxoplasma gondii</i> strains	47
2.2.1.2 <i>Toxoplasma gondii</i> transformation by electroporation	47
2.2.2 DNA quantification	48
2.2.3 Protein quantification by the Bradford assay	48
2.2.4 Bacterial culturing	49
2.2.4.1 Preparation of competent bacteria	49

2.2.4.2 Transformation of competent bacteria	50
2.2.4.3 Plasmid isolation from transformed bacteria	50
2.2.5 Gel electrophoresis	50
2.2.5.1 Agarose gel electrophoresis	50
2.2.5.2 Sodium dodecyl sulfate-Polyacrylamide gel electrophoresis	51
2.2.6 Polymerase chain reaction	51
2.2.6.1 Oligonucleotide primers	51
2.2.6.2 Polymerase chain reaction with <i>Taq</i> DNA polymerase	52
2.2.6.3 Polymerase chain reaction with <i>Pfu</i> DNA polymerase	52
2.2.7 Reverse transcription polymerase chain reaction	52
2.2.8 <i>In vitro</i> transcription	53
2.2.9 Southern blot analysis	54
2.2.9.1 Genomic DNA extraction from <i>Toxoplasma gondii</i>	54
2.2.9.2 Generation of Digoxigenin-labeled probes	55
2.2.9.3 Digestion of genomic DNA, blotting and hybridization	55
2.2.9.4 Immunological detection of hybridization signal	56
2.2.10 Northern blot analysis	56
2.2.11 Dot blot analysis	57
2.2.12 Synthesis of double-stranded RNA	57

CHAPTER 3

THE EFFECT OF DOUBLE-STRANDED RNA ON THE EXPRESSION OF THE HOMOLOGOUS GENE IN *TOXOPLASMA GONDII*

SUMMARY	58
3.1 INTRODUCTION	59
3.2 EXPERIMENTAL PROCEDURES	64
3.2.1 <i>Toxoplasma gondii</i> and selection with 5-fluoro-2'-deoxyuridine	64
3.2.2 The synthesis of double-stranded RNA and electroporation	64

3.2.2.1	The generation of double-stranded RNA	64
3.2.2.2	The labeling of double-stranded RNA with fluorescein	65
3.2.2.3	Monitoring the presence of labeled double-stranded RNA in <i>Toxoplasma gondii</i>	66
3.2.3	Nucleobase incorporation assays	67
3.3	RESULTS	68
3.3.1	The introduction of <i>in vitro</i> synthesized double-stranded RNA via electroporation	68
3.3.2	Knock-down of gene expression by electroporated double-stranded RNA	69
3.3.2.1	The expression of green fluorescent protein	69
3.3.2.2	The expression of hypoxanthine-xanthine-guanine phosphoribosyl transferase	72
3.3.2.3	The expression of uracil phosphoribosyl transferase	72
3.3.2.3.1	The down-regulation of uracil phosphoribosyl transferase disables the parasite to incorporate 5-fluoro-2'-deoxyuridine	74
3.3.2.4	The expression of hypoxanthine-xanthine-guanine phosphoribosyl transferase and uracil phosphoribosyl transferase	76
3.4	DISCUSSION	77

CHAPTER 4

GENERATION AND CHARACTERISATION OF A STABLE *TOXOPLASMA GONDII* PARASITE LINE EXPRESSING DOUBLE-STRANDED RNA HOMOLOGOUS TO URACIL PHOSPHORIBOSYL TRANSFERASE

SUMMARY	89
4.1 INTRODUCTION	90
4.2 EXPERIMENTAL PROCEDURES	92
4.2.1 Plasmid construction and electroporation	92
4.2.2 Tolerance to 5-fluoro-2'-deoxyuridine and the microtiter assay	93
4.2.3 Northern, Southern and dot blot analysis	94

4.2.4 Uracil incorporation assay	94
4.2.5 Detection of the double-stranded RNA homologous to uracil phosphoribosyl transferase expression by reverse transcription and polymerase chain reaction	94
4.2.6 Quantification of the level of double-stranded RNA homologous to uracil phosphoribosyl transferase by quantitative reverse transcription and polymerase chain reaction	95
4.2.6.1 Preparation of the competitive standard	95
4.2.6.2 Quantitative reverse transcription and polymerase chain reaction	96
4.2.7 Transformation and plasmid rescue	97
4.3 RESULTS	97
4.3.1 Generation a stable parasite line resistant to 5-fluoro-2'-deoxyuridine	97
4.3.2 Detection of <i>in vivo</i> produced double-stranded RNA homologous to uracil phosphoribosyl transferase	98
4.3.3 Measurement of the steady state levels of the uracil phosphoribosyl transferase transcript	99
4.3.4 Assessment of the uracil phosphoribosyl transferase activity	99
4.3.5 Analysis of the genomic organization of the parasite line	100
4.3.6 Stability of the parasite line in the absence of 5-fluoro-2'-deoxyuridine	101
4.3.6.1 Analysis of genomic DNA from different propagations of the parasite line	101
4.3.6.2 Transformation using genomic DNA from the parasite line and plasmid rescue	102
4.3.6.3 Correlation of the steady state levels of the uracil phosphoribosyl transferase transcript and the homologous double-stranded RNA	103
4.4 DISCUSSION	105

CHAPTER 5
FUNCTIONAL ANALYSIS OF LACTATE DEHYDROGENASES IN
TOXOPLASMA GONDII

SUMMARY	121
5.1 INTRODUCTION	122
5.2 EXPERIMENTAL PROCEDURES	124
5.2.1 <i>Toxoplasma gondii</i> and cell culture	124
5.2.2 Plasmid construction and transformation	124
5.2.2.1 Bradyzoite-specific expression plasmids	124
5.2.2.2 Tachyzoite-specific expression plasmids	125
5.2.2.3 Generation of stable parasite lines	125
5.2.3 Southern and northern blot analysis	126
5.2.4 Detection of double-stranded RNA homologous to lactate dehydrogenase by reverse transcription and polymerase chain reaction	127
5.2.5 Synthesis of double-stranded RNA and hairpin RNA by <i>in vitro</i> transcription	127
5.2.6 Electroporation of double-stranded RNA and measurement of <i>Toxoplasma gondii</i> growth	129
5.2.7 Immunofluorescence assay	129
5.2.8 Lactate dehydrogenase enzymatic assay	130
5.2.9 Polyacrylamide gel electrophoresis and western blot analysis	130
5.2.10 Experimental infections in mice	131
5.3 RESULTS	132
5.3.1 Down-regulation of the expression of lactate dehydrogenase by <i>in vitro</i> produced double-stranded RNA	132
5.3.2 Reduced parasite growth with lowered lactate dehydrogenase expression	133
5.3.3 Generation of lactate dehydrogenase knock-down parasite lines	135
5.3.3.1 Analysis of the genomic arrangement of parasite lines	136

5.3.3.2 Detection of the expression of double-stranded RNA homologous to lactate dehydrogenase and transcription profile of the target mRNAs in the parasite lines	137
5.3.3.3 Protein expression and enzymatic activities of lactate dehydrogenases of the parasite lines	139
5.3.3.4 Phenotypic studies of the parasite lines	141
5.3.3.5 <i>In vitro</i> parasite differentiation	141
5.3.3.6 Assessment of virulence of the parasite lines in mice	143
5.4 DISCUSSION	145
GENERAL CONCLUSIONS	166
REFERENCES	168
APPENDICES	183
VITA AUCTORIS	192

LIST OF FIGURES

	Page
CHAPTER 1	
FIGURE 1.1 <i>Toxoplasma gondii</i> life cycle	6
FIGURE 1.2 Structures of the different types of antisense oligonucleotides	21
FIGURE 1.3 A model for the RNA interference pathway	32
CHAPTER 3	
FIGURE 3.1 The synthesis of fluorescein-labeled double-stranded RNA homologous to the green fluorescent protein	80
FIGURE 3.2 The efficiency of double-stranded RNA electroporation into <i>Toxoplasma gondii</i>	81
FIGURE 3.3 The down-regulation of the expression of the green fluorescent protein mutant version	82
FIGURE 3.4 The effect of <i>in vitro</i> synthesized double-stranded RNA homologous to hypoxanthine-xanthine-guanine phosphoribosyl transferase on expression of target transcript	84
FIGURE 3.5 The effect of <i>in vitro</i> synthesized double-stranded RNA homologous to uracil phosphoribosyl transferase on the expression of the corresponding transcript	85

FIGURE 3.6 Longevity of the effects of double-stranded RNA homologous to uracil phosphoribosyl transferase	86
FIGURE 3.7 Double-knock-down by double-stranded RNA homologous to hypoxanthine-xanthine-guanine phosphoribosyl transferase and double-stranded RNA homologous to uracil phosphoribosyl transferase	88

CHAPTER 4

FIGURE 4.1 Tolerance of the parasite line to 5-fluoro-2'-deoxyuridine	109
FIGURE 4.2 Detection of the expression of double-stranded RNA homologous to uracil phosphoribosyl transferase in the parasite line	111
FIGURE 4.3 Assessment of uracil phosphoribosyl transferase transcript steady state level in the parasite line	112
FIGURE 4.4 Uracil phosphoribosyl transferase activity and uracil assay	113
FIGURE 4.5 Analysis of the genomic organization of the parasite line	114
FIGURE 4.6 Stability of the parasite line in absence of 5-fluoro-2'-deoxyuridine	115
FIGURE 4.7 Measurement of expression level of double-stranded RNA homologous to uracil phosphoribosyl transferase	116
FIGURE 4.8 Measurement of the expression level of the double-stranded RNA homologous to uracil phosphoribosyl transferase in different propagations of the parasite line in the absence of 5-fluoro-2'- deoxyuridine	118
FIGURE 4.9 The correlation of the uracil phosphoribosyl transferase transcript and homologous double-stranded RNA expression levels	119

CHAPTER 5

FIGURE 5.1 The effect of double-stranded RNA homologous to lactate dehydrogenase on the target transcript	153
FIGURE 5.2 The effect of double-stranded RNA homologous to lactate dehydrogenase on the growth of <i>Toxoplasma gondii</i>	154
FIGURE 5.3 Analysis of the genomic arrangement of the parasite lines	156
FIGURE 5.4 Detection of the expression of double-stranded RNA homologous to lactate dehydrogenase and the transcription profile of target mRNAs in the parasite lines	157
FIGURE 5.5 Assessment of lactate dehydrogenase protein expression in the parasite lines	159
FIGURE 5.6 Growth and replication of the parasite lines	160
FIGURE 5.7 <i>In vitro</i> differentiation of the parasite lines	162
FIGURE 5.8 Assessment of the virulence of the parasite lines <i>in vivo</i>	164

LIST OF ABBREVIATIONS

ATP	Adenosine triphosphate
bp	base pair
BAG1	bradyzoite surface antigen 1
BSA	bovine serum albumin
CAT	chloramphenicol acetyl transferase
CST1	cyst wall glycoprotein 1
Cfu	colony forming unit
cDNA	complementary DNA
CMV	Cytomegalo virus
DAPI	4', 6 diamidino-2-phenylindole
DEPC	diethylpyrocarbonate
DHFR-TS	dihydrofolate reductase-thymidylate synthase
DIG	digoxigenin
DMEM	Dulbecco's Modified Eagle Medium
DMSO	dimethylsulfoxide
DNA	deoxyribonucleic acid
DNase	deoxyribonuclease
dNTP	deoxyribonucleoside triphosphate
DPBS	Dulbecco's phosphate-buffered saline
dsRNA	Double-stranded RNA
dUMP	deoxy uridine monophosphate
<i>E. coli</i>	<i>Escherichia coli</i>
EDTA	ethylenediaminetetra-acetic acid disodium salt
ENO	enolase
FBS	fetal bovine serum
FDUR	5 fluoro-2'-deoxyuridine
FITC	Fluorescein iso-thiocyanate
GFP	Green fluorescent protein
HFF	human foreskin fibroblasts
hpRNA	hairpin RNA
HXGPRT	Hypoxanthine-guanine phosphoribosyltransferase
HDV	Hepatitis delta virus
HBV	Hepatitis B virus
INF	Interferon
IPTG	isopropyl thiogalactopyranoside
LDH	lactate dehydrogenase
LacZ	B-galactosidase
Min	Minutes
M-MLV RT	Moloney murine leukemia virus reverse transcriptase
mM	Millimolar
MOPS	3-(N-Morpholino)propane-sulfonic acid
MPA	mycophenolic acid

mRNA	Messenger RNA
miRNA	Micro-RNA
Nt	nucleotide
NTP	ribonucleoside triphosphate
Oligo	Oligonucleotide
PAGE	polyacrylamide gel electrophoresis
PNA	peptide nucleic acid
PBS	phosphate buffered saline
PCR	polymerase chain reaction
<i>Pfu</i>	<i>Pyrococcus furiosus</i>
PRPP	α -D-5-phosphoribosyl-1-pyrophosphate
QC-RT-PCR	Quantitative-Competitive-RT-PCR
RNA	ribonucleic acid
RNAi	RNA interference
RNase	Ribonuclease
ROP1	rhoptry protein 1
RT	reverse transcription
RT-PCR	reverse transcription PCR
RISC	RNA induced silencing complex
rfu	relative fluorescence units
siRNA	small interfering RNA
SAG1	surface antigen 1
SAG4	surface antigen 4
Sec	Second
SSC	sodium chloride-sodium citrate
TAE	Tris-Acetate-EDTA
<i>Taq</i>	<i>Thermus Aquaticus</i>
<i>T. gondii</i>	<i>Toxoplasma gondii</i>
<i>T. brucei</i>	<i>Trypanosoma brucei</i>
TBE	Tris Borate EDTA
Trp	Tryptophan
TET	Tetracycline
TetR	Tetracycline repressor protein
tTA	Transactivator
TCA	trichloroacetic acid
TEMED	N,N,N',N'-Tetramethylethylenediamine
TMP	Thymidine monophosphate
tRNA	transfer RNA
TUB	Tubulin
6TX	6 thioxanthine
UMP	Uridine monophosphate
UPRT	uracil phosphoribosyltransferase
UV	Ultraviolet
UTR	Untranslated region
VP16	Transcriptional activator domain of CMV

CHAPTER 1

GENERAL INTRODUCTION

1.1 *Toxoplasma gondii*

Toxoplasma gondii is a ubiquitous protozoan parasite that can infect a variety of warm-blooded vertebrates including humans (Dubey, 1994). It is estimated that 30% of the human population in North America are carriers for *T. gondii* (Soete *et al.*, 1993). This pathogen is closely related to other medically important protozoan parasites of the phylum Apicomplexa, such as *Plasmodium* and *Cryptosporidium* (Dubey, 1994). *Toxoplasma gondii* can exist in humans in one of two different growth forms; the rapidly dividing tachyzoite or slowly replicating bradyzoite. Infections in healthy individuals are usually asymptomatic because the tachyzoites are normally cleared by the host immune response (Dubey, 1994). When an acute infection is acquired during pregnancy, congenital malformations often occur. In most cases of human toxoplasmosis, the infection ultimately becomes chronic when tachyzoites differentiate into bradyzoites (Freyre, 1995). The bradyzoites can remain dormant within tissue cysts protected from the host immune response for the remainder of the host's lifespan (Soete *et al.*, 1993). In infected patients with immune deficiencies such as AIDS, bradyzoites are released from the tissue cysts and differentiate into tachyzoites giving rise to a recurrent infection which can prove fatal. No effective treatment for chronic toxoplasmosis is available to date (Boothroyd *et al.*, 1997, Black and Boothroyd, 2000). Therefore, cell culture and animal models are crucial for the study of chronic *Toxoplasma* infection and development of new strategies which aim at eliminating the dormant tissue cyst.

1.1.1 The parasite life cycle

The parasite *T. gondii* has a complex life cycle involving both sexual and asexual replication (Fig. 1.1). The asexual phase can occur in any nucleated cell and involves the two forms: the tachyzoite and the bradyzoite (Dubey, 1994). The sexual component on the other hand can occur exclusively in the feline intestinal epithelium and eventually leads to the generation of oocysts (diploid zygotes). Non-feline hosts including humans are called “intermediate” because they can not harbor the sexual phase of the parasite. The sexual phase of *T.gondii* begins when a cat feeds on infected animals harboring tissue cysts (Dubey, 1994, Soete *et al.*, 1993). The tissue cysts are ingested, and the bradyzoites are released in the digestive system where they initiate gametogenesis and differentiate into micro and macrogametes. Consequently, a fusion between these two gametes leads to the formation of the diploid zygote also known as oocyst. The oocyst later develops a thick impermeable cyst wall and is shed in the feline feces (Soete *et al.*, 1993). Upon exposure to the atmosphere, the oocyst undergoes a proliferation process known as sporogony. This process which consists of two meiotic divisions followed by a single mitotic division culminates in the generation of eight haploid structures called the sporozoites. Each four sporozoites sub-compartmentalize as a single group in a sac-like sporocyst within the oocyst wall. The mature haploid oocyst is very stable in the environment and can survive for many months in the soil (Dubey, 1994, Soete *et al.*, 1993). Transmission occurs when this infectious form is ingested by animals. The ingested sporozoites then rapidly initiate an infection which is first dominated by tachyzoites. As the infection proceeds however, tissue cysts with numerous bradyzoites are formed and act as a reservoir for

the transmission of parasite *T. gondii* to other animals through carnivorousism. Humans often acquire *T. gondii* infection by ingestion of under-cooked meat which harbors the parasite cyst or by contact with infected cats (Dubey *et al.*, 1994).

1.1.2 Parasite growth stages in the intermediate host

1.1.2.1 Tachyzoites

The word tachyzoite originates from the term “tachos” which means “speed” in Latin. This term was first used to describe the rapidly proliferating growth form of *T. gondii*. Tachyzoites are also called endodyozoites because they divide by endodyogeny which produces two daughter parasites from one parasite (Luft *et al.*, 1992). Ultrastructurally, tachyzoites are crescent-shaped unicellular organisms approximately 2 by 6 μm in length, possessing subcellular organelles including an apicoplast, a single mitochondrion, a nucleus, an endoplasmic reticulum and inclusion bodies (Freyre, 1995). The apicoplast is a non-photosynthetic plastid which is surrounded by four membranes and has its own genomic DNA. The exact function of this organelle is still unidentified but several studies indicate that the synthesis of lipids and heme could be among the possible roles of this plastid (Dzierszynski *et al.*, 2001). The nucleus usually occupies the central area of the cell and contains chromatin clumps. The parasite has two membranes, an outer plasma-membrane and an inner membrane which is discontinuous at both the anterior and posterior ends (Tomavo, 2001). The membranes are embraced by a network of microtubules which are arranged in a spiral form. The anterior end is often full of club-shaped and rod-like excretory organelles called the rhoptries and micronemes, respectively (Soldati *et*

al., 1995). It is speculated that these structures are involved in host cell invasion and parasite development (Soldati *et al.*, 1995). The tachyzoite can undergo only asexual replication for proliferation. It is responsible for host-cell invasion which commences by attachment to the host cell, penetration by phagocytosis, and multiplication by endodyogeny which produces two daughter parasites in each division. The last step involves host cell rupture as a result of the mechanical stress exerted by the extending and growing parasites on the host cell membrane (Freyre, 1995). Following entry by phagocytosis, the tachyzoite gets surrounded by a sac-like membrane, the parasitophorous vacuole, which originates from both the host and parasite cell membranes. Parasites within a single vacuole divide usually synchronously, leading to the formation of rosettes. The growth rate of tachyzoites can vary according to the strain of *T. gondii* (Dubey, 1994).

1.1.2.2 Bradyzoites

The term bradyzoite; which is derived from the word “brados” for “slow” in Latin; was first coined to describe the slowly replicating form of the parasite. Bradyzoites are also known as cystozoites because they usually form tissue cysts in chronic infections (Dubey, 1994, Tomavo, 2001). Tissue cysts can develop within any organ, but are more common in the neural and muscular systems like the brain and skeletal muscles. Bradyzoites can multiply by endodyogeny but at a very slow rate compared to tachyzoites (Tomavo, 2001). Tissue cysts vary in size depending on the number of resident bradyzoites. Brain tissue cysts are often spheroidal and usually small with a maximum diameter of 70 µm. In contrast,

intramuscular cysts are elongated and may reach a 100 μm in length (Freyre, 1995, Tomavo, 2001). The tissue cyst is surrounded by an elastic thin wall which is devoid of glycogen and other polysaccharides, but rather contains β -(1, 4) linkaged N-acetylglucosamine residues called chitin. As a result of this composition, the cyst wall can bind lectins such as those found in the seed of *Dolichos biflorus* and wheat-germ (Boothroyd *et al.*, 1997, Tomavo, 2001, Cleary *et al.*, 2002). Recently, a monoclonal antibody that reacts with the cyst wall has been described (Zhang *et al.*, 2001). Using this antibody, a 116 kDa glycoprotein called CST1 has been identified and shown to be one of the glycoproteins that could bind *Dolichos biflorus* (Zhang *et al.*, 2001). The cyst wall allows the bradyzoites to be less susceptible to destruction by proteolytic enzymes and gastric acid (pepsin-HCl) (Freyre *et al.*, 1995).

Bradyzoites differ structurally from tachyzoites because they accumulate numerous amylopectin granules (for glucose storage) within the cytoplasm and have a posteriorly located nucleus. Amylopectin is hypothesized to act as an energy source for the bradyzoite (Boothroyd *et al.*, 1997, Tomavo, 2001). The bradyzoite contains other organelles like those of the tachyzoite including rhoptries and a single mitochondrion. The rhoptries are more numerous and electron dense in comparison to those found in the tachyzoite. Interestingly, the mitochondrion is not functional in the bradyzoite, thus anaerobic respiration is the only source for supplying the energy needed by this form of the parasite. The tachyzoite on the other hand exhibits both aerobic and anaerobic respiration (Denton, *et al.*, 1996, Dando *et al.*, 2001).

Figure 1.1

Toxoplasma gondii life cycle

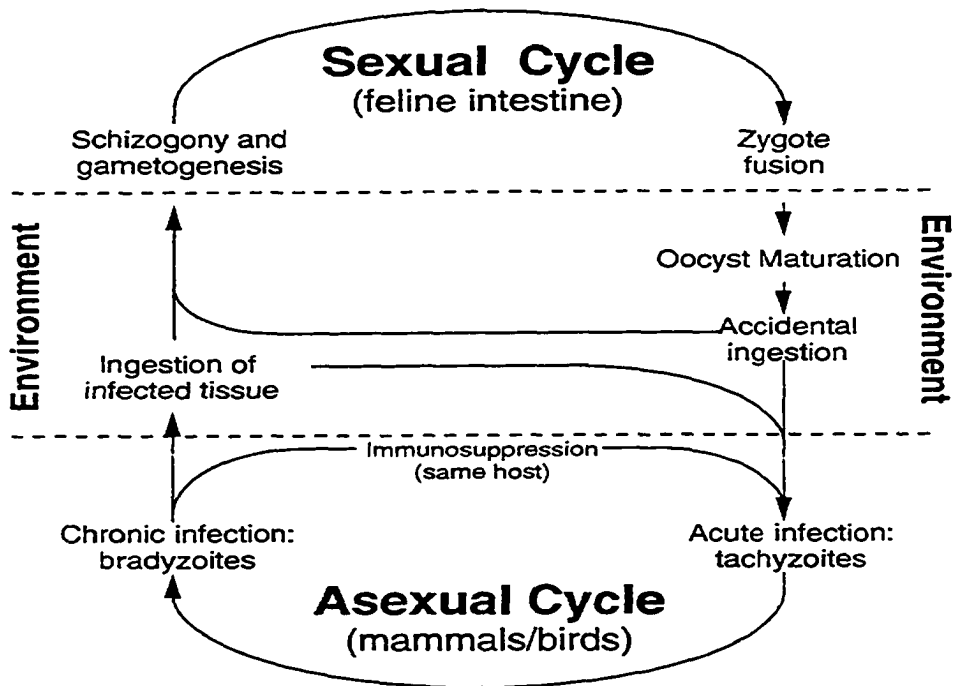


(Figure adapted from Black and Boothroyd, 2000)

Figure 1.1. The life cycle of *Toxoplasma gondii* consists of two phases: sexual and asexual. The asexual component can occur in any warm-blooded animal (intermediate host) including mammals, but the sexual component can occur in only the feline host (definite host) and culminates in the generation of the oocyst.

1.1.3 *Toxoplasma gondii* cultures as paradigm for Apicomplexan parasites

Many protozoan parasites like *Plasmodium spp.* are difficult to culture and maintain in the laboratory. Studying the mechanism of virulence of these pathogens is thus difficult (Sibley *et al.*, 1996). Unlike other Apicomplexan parasites, *T. gondii*, can be easily cultured using standard cell culture techniques and may therefore be used as an experimental model to study the other closely related Apicomplexans (Roos *et al.*, 1994, Black and Boothroyd, 2000). Furthermore, this parasite is amenable for molecular transformation and is thus ideal for genetic manipulation. *Toxoplasma gondii* has an 80 Mb haploid genome consisting of 11 chromosomes (Black and Boothroyd, 1998). Many *T. gondii* genes have been sequenced and the results of sequencing efforts have been deposited in the genome database ToxoDB (<http://toxodb.org>; Kissinger *et al.*, 2003).

1.1.3.1 Host cells and parasite strains

Numerous types of host cells could be used for *in vitro* studies of *T. gondii* (Roos *et al.*, 1994 and Freyre, 1995). Human fibroblasts are commonly used because they are easy to grow and provide an extensive area that allows the parasite to replicate for many cycles within the same cell before being lysed. In addition, the ability of fibroblasts to withstand the action of many growth inhibitors including some drugs allows selection for chemical resistance when needed (Roos *et al.*, 1994, Freyre, 1995). In addition to fibroblasts, Vero cells, macrophages and T cells are sometimes used for the parasite propagation (Boothroyd *et al.*, 1997, Cleary *et al.*, 2002).

There are several strains of *T. gondii* which are commonly propagated in cultures. These strains differ in virulence and replication rates. Most strains can produce tissue cysts *in vitro*, but with variable efficiencies (Soete *et al.*, 1993, Freyre, 1995). The RH strain is one of the most commonly used in culture due to its fast replication, ease of propagation in cell culture and efficient lysis of host cells which releases ample numbers of parasites sufficient for purification (Freyre, 1995). This strain is primarily utilized for biochemical experiments, particularly in the characterization of parasite virulence and drug-resistant mutants (Roos *et al.*, 1994, Freyre, 1995). The main disadvantage for the use of the RH strain is its poor cyst formation. Only few tissue cysts are formed in mice when RH parasites are cultured *in vitro*. In addition, the RH strain fails to undergo sexual replication in feline hosts (Freyre, 1995). Other strains such as, ME-49 and Prugniaud, produce more tissue cysts than the RH strain (Soete *et al.*, 1993). Thus, these two strains are excellent for experiments which focus on bradyzoite development and differentiation. Most researchers alternatively use PLK strain, a subclone of the ME49 strain, to perform genetic crosses in feline hosts because it can undergo a complete sexual cycle (Soete *et al.*, 1993, Boothroyd *et al.*, 1997).

1.1.3.2 Bradyzoite-tachyzoite interconversion

During infection in the intermediate host, *T. gondii* undergoes stage conversion from the tachyzoite to the encysted bradyzoite stage, thus establishing a chronic infection (Freyre, 1995). This reversible process plays a key role in the pathogenesis of infection because a chronic infection could later trigger disease

reactivation. Understanding the mechanism of interconversion could help in designing new chemotherapeutic agents to control toxoplasmic reactivation (Boothroyd *et al.*, 1997). Recently, scientists have focused on the development of *in vitro* systems for studying cyst formation to circumvent the limitations of obtaining enough cysts *in vivo* and the complexity of host response. Most *T. gondii* strains undergo spontaneous conversion from tachyzoites to bradyzoites in cell culture. However, only a small fraction (10-20%) of cysts results from spontaneous conversion. External stresses to infected host cells are shown to increase the cyst formation in cultures. The *in vitro* stress is thought to mimic the host immune response which induces tissue cyst formation *in vivo* (Soete *et al.*, 1993). The most commonly used *in vitro* system involves growing the parasites in alkaline medium (pH 8.3) to force the conversion of tachyzoites into bradyzoites (Soete *et al.*, 1993, Boothroyd *et al.*, 1997 and Cleary *et al.*, 2002). In addition, temperature stress (culture at 42°C instead of 37°C) and sodium arsenite treatment could be utilized (Soete *et al.*, 1993, Weiss *et al.*, 1998). Treatment with the immunological factor interferon- γ (IFN- γ) also promotes bradyzoite development in macrophages indirectly by triggering the endogenous release of nitric oxide. In fact, the highest level of bradyzoite formation is found in macrophages which are manipulated to release 40-60% nitric oxide (Bohne *et al.*, 1994). Nitroprusside, an exogenous source of nitric oxide, also reduces tachyzoite replication and induces the expression of bradyzoite-specific antigens (Soete *et al.*, 1993, Bohne *et al.*, 1994). The effect of nitric oxide on *T. gondii* differentiation is attributed to its ability to react with the iron-sulfur centers of the proteins involved in the electron transport system of the aerobic respiration (Bohne *et al.*, 1994). The

mitochondrial inhibitors oligomycin, antimycin A, atovaquone and rotenone also induce tachyzoite-bradyzoite stage conversion (Soete *et al.*, 1993, Denton *et al.*, 1996). Studies involving host cells with non-functional mitochondria demonstrated that the mitochondrial inhibitors promote tissue cyst development in culture because of their effects on the parasite mitochondrion and not the host cell mitochondria (Soete *et al.*, 1993).

Cell culture growth conditions which favor the formation of bradyzoites are associated with the up-regulation of heat shock proteins (HSPs). HSPs seem to be essential during stress-induced stage conversion (Weiss *et al.*, 1998) However, it has been recently shown that the disruption of the bradyzoite specific antigen BAG1 (also known as hsp30) decreases, but does not completely prevent *in vivo* cyst formation (Bohne *et al.*, 1998).

Although the differentiation of the tachyzoite to bradyzoite can be successfully induced *in vitro*, the genetic regulatory signals that control this process are still unknown (Boothroyd *et al.*, 1997, Tomavo, 2001, Cleary *et al.*, 2002). Stage interconversion is associated with morphological and molecular biological changes including stage-specific antigen expression and alterations to metabolism. Several studies have identified stage-specific proteins including the surface antigens CST1 (Zhang *et al.*, 1997, Cleary *et al.*, 2002), BAG1 (Bohne *et al.*, 1995), SAG4A (Manger *et al.*, 2000); metabolic enzymes, lactate dehydrogenase (LDH) and enolase (ENO) (Yang and Parmley, 1997, Tomavo, 2001, Dzierszinski *et al.*, 2001). Some of these genes are developmentally regulated and suspected to be crucial for bradyzoite differentiation (Boothroyd *et al.*, 1997, Yihiaoui *et al.*, 1999).

1.1.4 *Toxoplasma gondii* and anti-parasitic regimens

Acute parasitic infections of *T. gondii* are normally controlled by the immune system in healthy individuals (Pfefferkoron and Pfefferkorn, 1980). Antibiotics like sulfadiazine could also be used to clear the infections (luft *et al.*, 1992). Chronic infections however, which are characterized by the presence of tissue cysts are not affected by the action of sulfadiazine and other anti-parasitic agents because tissue cysts are dormant, and shielded by a cyst wall (Tomavo, 2001). Recently, genetic manipulations have offered a new way to control toxoplasmosis. Several potential targets for the development of antiparasitic drugs like genes involved in parasite attachment, gliding, invasion and growth have been identified by the generation of knock-out mutants. Among these targets, the gene encoding the surface antigen 3 (SAG3) is promising (Dzierenski *et al.*, 2000). Parasite lines with disrupted SAG3 display at least two fold reduction in host cell invasion when compared with the wild type parasites. In addition, these mutants show attenuated virulence with a reduced ability to cause mortality in mice (Dzierenski *et al.*, 2000). The RNA-based technology of antisense RNAs and ribozymes, has recently been used in the *T. gondii* system to manipulate the expression profile of essential genes. One of the important *T. gondii* metabolic genes, nucleoside triphosphate hydrolase (NTP) had been targeted by an endogenous chimeric antisense NTP RNA-hammerhead ribozyme (Nakaar *et al.*, 1999). The attenuation of NTP gene expression drastically reduced parasite proliferation but did not prevent cyst formation. Despite all the progress with tachyzoite research, the challenge for the future lies in the identification of genes that are crucial for the development the tissue cyst.

1.1.5 Genetic manipulations of *Toxoplasma gondii*

Genetic manipulations by molecular transformation of *T. gondii* have been extensively employed as a tool to verify gene function and molecular events at various stages of the parasite life cycle (Boothroyd *et al.*, 1995, Roos *et al.*, 1994). Electroporation is one of the most efficient means to introduce plasmids and nucleic acids into *T. gondii*. It is speculated that the pulse of current employed in electroporation causes the formation of small pores within the parasite's cell membrane thus allowing the plasmid or nucleic acid to be taken up. Once inside the parasite, plasmids act as vehicles for either transient or stable gene expression depending on whether or not they integrate into the parasite genome or replicate as episomal DNA (Boothroyd *et al.*, 1995, Roos *et al.*, 1994).

1.1.5.1 Transient gene expression

The expression of genes harbored by a transforming plasmid vector for only a short limited time (generally a few days) is termed transient. Transient gene expression occurs when the utilized vectors lack an origin of replication or fail to integrate into the parasite genome (Roos *et al.*, 1994).

A reporter gene whose product can be assayed is used as an indicator of the plasmid being introduced. Numerous reporter genes including β -galactosidase (*LacZ*), luciferase, β -glucouronidase and chloramphenicol acetyltransferase (*CAT*) have been employed for transient expression in *T. gondii* (Soldati *et al.*, 1995, Roos *et al.*, 1994, Dzierszynski *et al.*, 2001). Among these reporter systems, the *CAT* and *LacZ* have demonstrated greater activity when their expression was driven by

Toxoplasma promoters, such as those of the surface antigen (SAG1), the rhostry protein (ROP1) and the β -tubulin (TUB1) (Roos *et al.*, 1994, Soldati *et al.*, 1995). Despite the usefulness of transient expression for genetic manipulations, this strategy has some limitations due to the short duration of expression. In the most efficient transformation, there is significant variation in the amount of genetic material taken up by the cells, giving rise to a heterogenous population (Roos *et al.*, 1994, Soldati *et al.*, 1995).

1.1.5.2 Stable gene expression

Several strategies allowing the stable expression of transgenes have been established. Stable transformation leads to the generation of parasite lines permanently expressing transgenes by directed or random integration into the parasite genome (Donald and Roos, 1994, Roos *et al.*, 1994). One approach for stable transformation involves the complementation of an auxotrophic condition by transforming the parasite with a transgene whose expression converts the phenotype to prototrophy. (Sibley *et al.*, 1994). In one study, complementation was achieved by expressing the *E. coli* tryptophan (*trp*) gene which encodes the tryptophan synthase, an enzyme that catalyzes the production of tryptophan from supplemented indole. It was demonstrated that the transforming vector encoding the *trp* gene integrated into the parasite genome by non-homologous recombination at high efficiency (Sibley *et al.*, 1994).

1.1.6 Modulation of gene expression in *Toxoplasma gondii*

Various molecular tools such as insertional mutagenesis, tetracycline-repressor-based inducible systems and RNA-based modulators have been employed for the characterization of gene function in *T. gondii* (Donald and Roos, 1995, Black *et al.*, 1995, Meissner *et al.*, 2001, Nakaar *et al.*, 1999, Al-Anouti and Ananvoranich, 2002, Sheng *et al.*, 2003).

1.1.6.1 Non-homologous recombination vectors and insertional mutagenesis

Vectors lacking long stretches of continuous genomic DNA usually integrate by non-homologous or random recombination (Sibley *et al.*, 1994 and Tomavo, 2001). A number of transformation vectors based on sequences from the dihydrofolate reductase-thymidylate synthase gene (DHFR-TS) have been developed for *T. gondii* genetic transformations (Donald and Roos, 1993). The DHFR-TS gene was engineered to harbor mutations analogous to those found in the DHFR-TS gene of pyrimethamine-resistant *Plasmodium falciparum* (Donald and Roos, 1993). Vectors carrying the DHFR-TS minigene were shown to integrate into the genome by non-homologous recombination in more than 5% of the transformed parasites. Several investigators have used the DHFR-TS minigene to disrupt non-essential genes by insertional mutagenesis (Donald and Roos, 1995, Donald *et al.*, 1996). The insertion at the uracil phosphoribosyl transferase (*UPRT*) and hypoxanthine-xanthine-guanine phosphoribosyl transferase (*HXGPRT*) loci which code for enzymes of the

pyrimidine and purine salvage pathways, respectively, were successfully generated (Donald and Roos, 1995, Donald *et al.*, 1996).

Insertional mutagenesis has its limitations when essential genes are being investigated. The functions of essential genes could be compensated for by complementation. Complementation is often achieved by stable episomal shuttle vectors. A 500-bp sequence that permits the maintenance of bacterial plasmids as episomal DNA has been identified (Black and Boothroyd, 1998). This sequence which could be incorporated into vectors bearing fragments of the parasite genome allows these vectors to replicate autonomously within *T. gondii* (Black and Boothroyd, 1998).

1.1.6.2 Tetracycline repressor-based inducible system

The tetracycline repressor-based system for gene control developed by Bujard and Gossen provides tightly regulated control of transgene expression and is based on the *E. coli* tetracycline resistance operon (Bujard *et al.*, 1990). This system utilizes a chimeric transactivator protein (tTA) that consists of the *E. coli* TET repressor (TetR) fused to a strong viral domain termed VP16. The VP16 is a potent activator of transcription. The tetR mediates the binding of VP16 to a synthetic promoter with a TATA box (derived from the cytomegalovirus (CMV) promoter) and seven tetR binding sites (tetO). The addition of tetracycline or its analogues prevents the tTA from binding the promoter and initiating transcription (Bujard *et al.*, 1990). This system for the control of gene expression is important for the study of function of essential genes which can not be disrupted using the repertoire of

molecular tools for *T. gondii*.

An inducible system based on the tetracycline repressor (TetR) has been reported for the control of gene expression in many protozoan systems but is best optimized in *Trypanosoma brucei* (Wang *et al.*, 2000, Cottrell and Doering, 2003). This system was used for modulating gene expression in *T. gondii* (Meissner *et al.*, 2001). Using this strategy, the myosin A gene has been conditionally disrupted. Disruption of this gene caused severe impairment in host cell invasion and parasite spreading in culture (Meissner *et al.*, 2001).

1.2 RNA tools

The RNA-based tools antisense RNA and ribozymes are unique methods for studying essential genes because they do not disrupt gene expression at the DNA level (Lamond and Sproat, 1993). These RNA-based modulators have been extensively used for the down-regulation of gene expression in many organisms including *T. gondii* (Nakaar *et al.*, 1999, Al-Anouti and Ananvoranich, 2002, Sheng *et al.*, 2003).

1.2.1 Antisense RNA

Antisense RNA interrupts protein expression at the post-transcriptional level. Within the past decade, antisense RNA has emerged as a powerful technology for sequence-specific modulation of gene expression (Baker and Monia, 1999). Considering the several processing steps to which RNA is usually subjected (including splicing, polyadenylation, translation and degradation) prior to being

translated into a protein, it is possible to modify gene expression with antisense RNA by interfering with any of these steps (Baker and Monia, 1999).

The antisense RNA down-regulates the gene expression by two different methods; non-RNA-cleavage mechanism and cleavage mechanism. In a non-RNA cleavage, the antisense RNA interacts with target mRNA sequences by base pair interactions and subsequently prevents the docking of important proteins which mediate transcript processing and translation (Hostomsky *et al.*, 1993). The antisense RNA can induce the degradation of RNA *via* a cleavage mechanism (Lamond and Sproat, 1993). Antisense-mediated RNA cleavage is accomplished by either the recruitment of nucleases such as RNase H, or by the attachment of synthetic residues like metal complexes (to the antisense RNA) which subsequently cleave the RNA backbone by chemical degradation (Baker *et al.*, 2002).

1.2.1.1 Non-RNA-cleavage mechanism by preventing translation and transcript processing

One site at which antisense RNA can interfere with mRNA processing is at the 5' capping step. The 5' cap which is a N7 methylated guanosine with a 5'-5' triphosphate linkage to the 5' terminus of the mRNA acts as a signal for mRNA splicing, transport and translation (Hostomsky *et al.*, 1993). In addition, the cap structure shields the transcript from degradation by the 5' exonucleases. Capping of the mRNA is mediated by the enzyme guanylyl transferase which adds a guanylyl monophosphate to the 5' phosphorylated mRNA. The antisense RNA could be designed to bind the 5' diphosphorylated mRNA and interrupt the capping process.

The antisense-directed interference with capping renders the mRNA extremely unstable (Baker *et al.*, 2002). Interfering with mRNA processing at the polyadenylation site is also feasible with the antisense RNA-based technology (Baker *et al.*, 2002). The mRNA precursors are polyadenylated in three successive steps: the assembly of a 3' end-processing protein complex onto the polyadenylation signal AAUAAA, the cleavage of the precursor transcript 10-30 nt downstream the polyadenylation signal and finally the addition of a poly(A) tail. The poly (A) tail is necessary for mRNA transport from the nucleus, stability and initiation of translation (Taylor *et al.*, 1996). Therefore, interrupting any of the polyadenylation steps (like base-pairing with the polyadenylation signal) could knock-down protein expression.

Inhibition of RNA translation into protein is one of the most common approaches for antisense RNA. The antisense is used to block the initiation, elongation or termination step (Baker *et al.*, 1999). Translation normally begins upon the recognition of the 5' cap by translation protein factors which recruit the ribosomal subunits onto the transcript. A sequence called the internal ribosomal entry site (IRES) residing within the 5'UTR is crucial for this process (Baker and Monia, 1999). In a study performed to compare the effectiveness of the antisense activity of different synthetic oligonucleotides against the *CAT* mRNA, it was demonstrated that the oligonucleotide which specifically targeted the 5' UTR site was the most effective (Taylor *et al.*, 1996).

1.2.1.2 Degradation of RNA via a chemical or enzymatic cleavage mechanism

Following the formation of DNA and RNA hetero-duplex between the antisense DNA and target mRNA, the destruction of the mRNA is mediated by an abundant enzyme, RNase H present in most mammalian cells (Baker and Monia, 1999, Baker, 2002). In this regard, the antisense-based drug Vitravene (Ciba Vision) which is recommended for the treatment of CMV retinitis is designed to act through RNase H-dependent cleavage of mRNA (Baker *et al.*, 1999).

RNase H-independent RNA cleavage could be mediated by either enzymes (like double-stranded RNases) or by chemicals (Baker and Monia, 1999). One class of the RNase III known as the double-stranded RNase, can bind and degrade double-stranded RNA structures like the antisense: sense RNA duplex (Filippov *et al.*, 1999). These RNases were first identified in bacteria, but were recently discovered in human and other mammalian cells. Several investigators successfully employed these RNases in combination with modified oligonucleotides for target RNA cleavage (Wu *et al.*, 1998).

In addition to the enzymatic RNA cleavage mechanisms, the use of chemical degradation as an alternative strategy has been explored by several research groups. To implement this strategy, synthetic chemical residues have been either incorporated or used in combination with an antisense oligonucleotide (Haner *et al.*, 1998). Following the base pair interaction between the antisense oligonucleotide and the target transcript, the chemical moieties induce the degradation of the RNA by activating its nucleophilic 2'-OH group. For this reason, these strategies are referred

to as artificial ribonucleases. Metal complexes including those of lanthanides have demonstrated the greatest potential with respect to RNA cleavage rate (Haner *et al.*, 1998). Using this strategy, the proliferation of *Plasmodium falciparum* was inhibited *in vitro* by antisense RNA directed against the DHFR gene (Barker *et al.*, 1996).

Over the last few years, numerous modifications to the sugar and backbone of the antisense RNA have imparted greater stability to the antisense-RNA complex. Currently, there are three different classes of modified oligonucleotides (Figure 1.2): those with modified sugar residues, modified phosphodiester linkage and modified sugar phosphate backbone. The first category is represented by the 2'-O-methyl oligo-deoxynucleotides, the second category includes oligonucleotides which replace the phosphate group by 3'-C-N-O-C-4' linkage or the 3'-O by a nitrogen. The third class has a neutral six membered morpholino phosphorodiamidate, replacing the ribose structure; this type of antisense is called morpholinos. In another subclass, a polyamide chain replacing the backbone generates an antisense class called peptide nucleic acids (Taylor *et al.*, 1996, Baker *et al.*, 1999).

Figure 1.2

Structures of the different types of antisense oligonucleotides

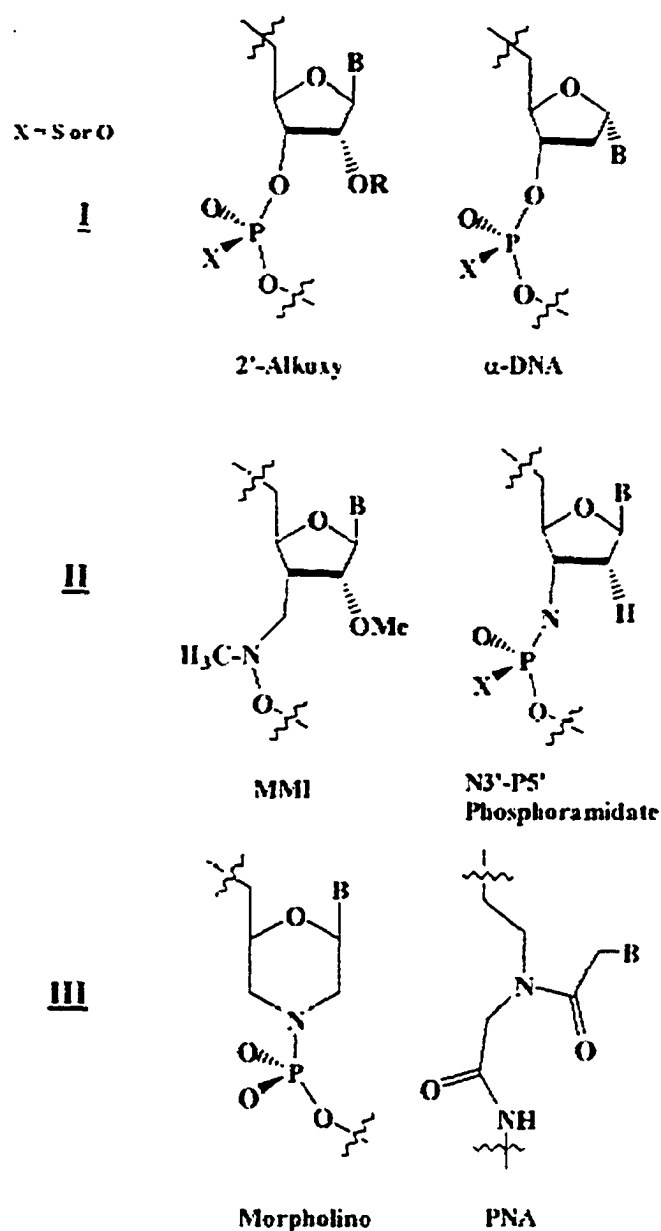


(Figure adapted from Baker and Monia, 1999)

Figure 1.2. Modifications to the oligonucleotide structure include those of the sugar residues (I), those of the phosphodiester linkage (II) and those of the entire oligonucleotide backbone (III).

1.2.2 Ribozymes

The most recent improvement to the antisense RNA-based approach implements nucleases which can cleave target RNA. Ribozymes are RNA molecules which can cleave RNA and have been utilized as ribonucleases either in conjunction with the antisense RNA or by themselves for the modulation of gene expression (Jaeger *et al.*, 1997). The notion that RNA could be catalytic was first given by Francis Crick in the 1960s, but it was not before the early 1980s that the first experimental proof was provided by Cech and Altman concerning the catalytic activity of some naturally occurring RNA molecules (Kruger *et al.*, 1982, Guerrier *et al.*, 1997). Cech and his colleagues identified an intron (later named group I intron) within the rRNA precursor of the protozoan *Tetrahymena thermophila* which exhibited a self-excising ability. Shortly after the identification of group I introns, another ribozyme *E. coli* RNase P was discovered by Sidney Altman group. The *E. coli* RNase P (which consisted of both protein and RNA moieties) was able to catalyze the hydrolytic cleavage of the 5' termini of tRNAs using the RNA moiety of the ribonuclease. Subsequent research led to the identification and characterization of several other naturally occurring ribozymes in plants, bacteria, viruses and lower eukaryotes (Jaeger *et al.*, 1997). These ribozymes can be specifically engineered to cleave target RNAs and used as valuable tools to modify gene expression in both *in vivo* and *in vitro* (Guerrier *et al.*, 1997).

1.3 RNA interference

1.3.1 The natural phenomenon of RNA interference

One of the remarkable discoveries in biology over the last decade was the finding that double-stranded RNA (dsRNA) can mediate specific silencing of genes in many eukaryotic organisms, a phenomenon termed RNA interference (RNAi) (Novina and Sharp, 2004). The use of dsRNA has unraveled a universal mechanism for RNAi which has tremendous potential for genomics studies and other fields including medicine (Hannon, 2002). Today, RNAi is one of the most powerful and convenient tools for the knock-down of gene expression in most systems (Novina and Sharp, 2004).

1.3.2 Post-transcriptional gene silencing and co-suppression

Although RNAi as a natural phenomenon of gene silencing was first reported by Andrew Fire in 1998 (Fire *et al.*, 1998), the first manifestations of RNA silencing were observed long before this discovery (Napoli *et al.*, 1990, Sijen and Kooter, 2000). In an attempt to deepen the purple color of the petunia plant, scientists introduced numerous copies of a gene that codes for deep purple flowers. The investigators were puzzled by the generation of white patchy flowers instead of the expected increased flower pigmentation. They concluded that (transgenes) silenced the expression of the plant purple-flower genes (Napoli *et al.*, 1990, Sijen and Kooter, 2000, Carthew, 2001, Tijsterman *et al.*, 2002). This finding was originally termed co-suppression because foreign transgenes could silence not only themselves but also homologous loci (Sijen and Kooter, 2000).

Co-suppression (also known as homology-dependent gene-silencing) can occur in two different modes with one operating at a transcriptional level and the other at a post-transcriptional level. Modulation of gene expression at the transcriptional level, also known as transcriptional gene silencing (TGS), involves DNA methylation of the chromatin template at cytosine residues thus preventing the modified genes from being transcribed (Hannon, 2002). A heteroduplex of RNA might act as a substrate for certain enzymes which recognize these duplexes as substrates for the methylation of cytosine or another DNA modification such as histone deacetylation both of which convert chromatin into heterochromatin; the silenced form of DNA (Hannon, 2002). The RNA-triggered methylation is restricted to gene sequences with homology to the triggering dsRNA. If the promoter and enhancers are unaffected, gene expression might either proceed with minimal effect or not proceed at all. If coding sequences within the gene are homologous, gene transcription into RNA is absolutely impeded (Sijen and Kooter, 2000, Carthew, 2001). In post-transcriptional gene silencing (PTGS), transgenes are transcribed, but their transcripts are degraded. This form of gene silencing is often associated with repetitive loci in which multicopy transgenic arrays are arranged as repeats or inverted repeats (Carthew, 2001). Later, it was discovered that the triggering cause for PTGS-mediated target degradation is a homologous dsRNA (Hannon, 2002). The generation of dsRNA might occur when transgenes are super-expressed by using a strong endogenous promoter integrated into the genome (after transformation) or from the head-to-head organization of the transcription units in the multicopy transgenic arrays. The production of dsRNA directly or an antisense strand (which

can later pair with its complementary sense strand to form dsRNA) thus invokes PTGS (Carthew, 2001). It was later shown that the need for repeated transgenic arrays could be bypassed by using *in vitro* synthesized dsRNA (Tijsterman *et al.*, 2002).

Post-transcriptional gene silencing exists not only in plants but also other organisms including *Drosophila*, *C. elegans*, *Neurospora crassa*. In fungi, PTGS is referred to as quelling (Kuwabara and Coulson, 2000). One interesting feature of PTGS, is its ability to generate signals which spread through the whole system or organism. This systemic silencing suggested that initial signals that invoke the silencing mechanism are amplifiable. The first suggestion regarding a source for signal amplification was raised after the first RNA-directed RNA polymerase (RdRP) which converts a single-stranded RNA template into a dsRNA product was cloned from tomato plants and later from other plants (Sijen *et al.*, 2001). It was hypothesized that the RdRP might be a candidate enzyme for amplifying the silencing signal by synthesizing an endogenous pool of dsRNA (Kuwabara and Coulson, 2000, Carthew, 2001). Later, it was shown, however, that mutants for the gene *ego-1* which encodes a *C. elegans* RdRP homologue could undergo RNAi as effectively when compared to the wild type. In addition, *Drosophila* which contains no RdRP homologues in its genome exhibits potent gene silencing at the post-transcriptional level (Sijen *et al.*, 2001, Cottrell and Doering, 2003). An alternative model which predicted an interaction between the dsRNA and a catalytic protein or ribonucleoprotein was later proposed (Zamore *et al.*, 2000, Hammond *et al.*, 2000).

The existence of PTGS in many organisms as a natural phenomenon is considered as a genome surveillance system which blocks the expression of harmful or aberrant genes like viruses and transposons (Bosher and Labouesse, 2000). Because normal gene expression within the organism does not usually produce dsRNA, this duplex is considered as aberrant by the surveillance system and is tagged for destruction (Fire *et al.*, 1998, Bosher and Labouesse, 2000).

1.3.3 The features of RNA interference

For decades, RNA was thought to have only two major roles in the cell. The mRNAs act as messages between genes and their protein products; and the ribosomal/transfer RNAs are involved in protein synthesis (Novina and Sharp, 2004). The picture became increasingly complicated with the discovery of RNAi in the nematode *Caenorhabditis elegans* (Fire *et al.*, 1998). Since then, RNAi has been demonstrated for many other organisms including insects (Yang *et al.*, 2000), protozoa (Ngo *et al.*, 1998) and mammals (Elbashir *et al.*, 2001, Paddison *et al.*, 2002, Doi *et al.*, 2003), suggesting that this phenomenon might be conserved through evolution.

The effect of RNAi on gene silencing is capable of persisting for a long time through cell division rounds and growth, until it eventually subsides as the input dsRNA pool becomes diluted. In fact, experimental studies in *C. elegans*, *Drosophila* and mouse models demonstrated that RNAi maintains its potency up to a 50-fold increase in cell mass (Fire *et al.*, 1998, Wianny and Zernicka, 2000, Svoboda *et al.*, 2000). RNAi could also be inheritable and transmissible (Fire *et al.*, 1998). In *C.*

elegans, subsequent generations can inherit the RNAi from their germlines which were originally treated with dsRNA (Fire *et al.*, 1998, Tabara *et al.*, 1998). These RNAi features indicate that even few molecules of the dsRNA could effectively degrade a large pool of the homologous transcript (Tabara *et al.*, 1998).

1.3.4 The application of RNA interference

In planning an experiment involving the use of RNAi, there are different parameters that must be considered, such as the sequence of the dsRNA, the duration of the effect and the method of delivery into the system (Sharp *et al.*, 2001, Hannon, 2002). Regarding the first parameter, specificity is critical because only the gene(s) with sequences homologous to that of the dsRNA should be affected. Therefore, the sequence of the dsRNA must be accurately selected to specifically knock-down the expression of the homologous gene so as to avoid cross-interference with other genes which harbor some homologous sequences (Bosher and Labouesse, 2000, Kamath and Ahringer, 2003). For instance, in *C. elegans*, there are six closely related genes encoding the myosin heavy chain with 87% nucleotide identity. A dsRNA homologous to the highly conserved region of one of these genes generates a lethal phenotype presumably because of knock-down of expression of all six genes. On the other hand, if the dsRNA is designed against a non-conserved region of one of the six genes, the organism survives but develops paralysis as a result of silencing of the targeted myosin heavy chain gene normally expressed in the body wall muscle (Ketting *et al.*, 2001). Recent investigations have demonstrated that an approximately 80% identity within a 200 nucleotide region could lead to the down-regulation of the

expression of non-target genes by the dsRNA (Novina and Sharp, 2004). The length of the dsRNA also has an important effect on the potency of RNAi. Although the minimal length of the dsRNA required to trigger an effective RNAi is still not definite, several studies have shown that dsRNA less than 500 bp might not be optimal in some systems (Tabara *et al.*, 1999, Kuwabara and Coulson, 2000).

RNA interference could be invoked by either endogenous or exogenous dsRNA. Both types of dsRNA are equally efficient in mediating gene silencing. However, the means of delivery of the dsRNA contributes to variability in its efficiency (Parrish and Fire, 1999, Elbashir *et al.*, 2001). In *C. elegans*, microinjection into the embryo, germ line or body parts is most commonly employed for administering dsRNA. Feeding worms with bacteria expressing dsRNA homologous to the gene of interest, or even soaking the worms in a solution of dsRNA is also amazingly effective (Tabara *et al.*, 1998, Tabara *et al.*, 1999, Sijen and Kooter, 2000). Electroporation is another potential route for delivering dsRNA into the system and is usually the method of choice for mammalian cells (Tabara *et al.*, 1999, Elbashir *et al.*, 2001).

The long duration of the RNAi effect is an interesting feature. Injected dsRNA is remarkably long-lived, such that its effects can persist throughout the entire life cycle of the progeny of injected animals (Novina and Sharp, 2004). Investigations have demonstrated that when dsRNA is introduced into early embryos in *C. elegans*, it becomes gradually diluted as the organism proceeds through development such that early genes are more easily down-regulated compared to late-acting genes. In animals with small number of cells like *C. elegans*, the dsRNA dilution does not pose a

problem to gene silencing (Parrish and Fire, 2001). In more complex organisms such as *Drosophila* and mammals, the dsRNA amount could be indeed a limiting factor (Wianny and Zernicka, 2000, Sharp, 2001). Injection of dsRNA homologous to the green fluorescent protein (*GFP*) into a mouse zygote constitutively expressing the *GFP*, was effective until the embryo reached a developmental stage of approximately 50 fold increase in cell mass (Wianny and Zernicka, 2000, Svoboda *et al.*, 2000).

The reversibility of gene silencing with exogenous dsRNA; which is not stably inheritable could be an asset for certain research objectives. However, this reversibility could also be a limitation to some investigations. To circumvent this problem, and make RNAi inheritable, stable transformation with dsRNA-expressing plasmids is implemented. Some plasmids are engineered to contain the target sequence as inverted repeats so that the dsRNA is expressed as a hairpin dsRNA *in vivo*. Such constructs have been successfully used for many systems including mammalian cells (Sui *et al.*, 2002, Paddison *et al.*, 2002). Another plasmid system with two promoters arranged in a head-to-head fashion flanking the target cDNA was first utilized for *T. brucei* but later adopted for stable dsRNA expression in other systems (Ngo *et al.*, 1998, LaCount *et al.*, 2000, Wang *et al.*, 2000 and Tschudi *et al.*, 2003). In addition, a tetracycline-inducible promoter in *T. brucei* led to the development of inducible dsRNA expression constructs (Wang *et al.*, 2000, Cottrell and Doering, 2003). Stable expression of dsRNA is advantageous because it bypasses the need for a delivery method and is inheritable throughout the generations of the transgenic lines. In addition, the expression of dsRNA could be regulated in a stage-

specific manner (depending on the promoter) to achieve a controlled gene silencing at a determined time and stage (Sharp, 2003).

1.3.5 The mechanism of RNA interference

Both genetic and biochemical approaches have tremendously contributed to the understanding of the mechanism of RNAi. Using extracts from *Drosophila* embryos and tissue-cultured cells transfected with dsRNA, a nuclease activity which degrades an exogenous homologous mRNA, was partially purified *in vitro* (Tuschl *et al.*, 1998, Tuschl *et al.*, 1999, Yang *et al.*, 2000, Nykanen *et al.*, 2001). It was also observed that this nuclease activity co-purifies with small RNAs 21-25 nt long consisting of sense and antisense portions identical to sequences within the used dsRNA (Tuschl *et al.*, 1998, Tuschl *et al.*, 1999). Further experiments showed that extracts from *Drosophila* embryos generate small 21-25 nt RNAs only when they are supplemented with the homologous dsRNA (Clemens *et al.*, 1999, Hammond *et al.*, 2000). Also, incubation of a cell-free system with the dsRNA and its homologous mRNA exhibit RNAi features *in vivo*. (Hammond *et al.*, 2000, Clemens *et al.*, 2000, Zamore *et al.*, 2000). Interestingly, preincubation of the cell-free lysate with the dsRNA potentiated the degrading activity of the lysate on the target mRNA (Clemens *et al.*, 2000, Zamore *et al.*, 2000, Ketting *et al.*, 2001). All these *in vitro* studies led to the generation of a model for the pathway of RNAi. The model (Fig. 1.3) starts with the dsRNA being diced through an ATP-dependent step by an enzyme called Dicer into small interfering RNAs (siRNAs) (Elbashir *et al.*, 2001). These 21-23 nt siRNAs with 2-nt overhanging 3' ends are later incorporated into a 360 kDa ribonucleoprotein

nuclease-complex called the RNA induced silencing complex (RISC). The RISC contains RNA and some proteins belonging to a family called the “Argonaute” family (Bernstein *et al.*, 2001, Hutavagner and Zamore, 2002). Unwinding of the siRNA duplex in the presence of ATP renders the complex capable of destroying the homologous mRNA by an associated nuclease termed slicer (Bernstein *et al.*, 2001, Hutavagner and Zamore, 2002). The RNAi reaction consists of four steps: ATP-dependent dsRNA processing, ATP-independent incorporation of siRNAs into the RISC, ATP-dependent unwinding of the siRNA duplex and finally the ATP-independent recognition and cleavage of the target transcript. An ATP-dependent RNA helicase unwinds the two strands of the siRNA before they associate with the target mRNA. The 5' phosphate on the siRNA is essential for assembly with the RISC and subsequent target cleavage (Hammond *et al.*, 2001). Moreover, the addition of nucleotides to the 5' end of the antisense strand of the siRNA shifts the cleavage site correspondingly (Elbashir *et al.*, 2001, Nykanen *et al.*, 2001, Hannon, 2002).

Figure 1.3

A model for the RNA interference pathway

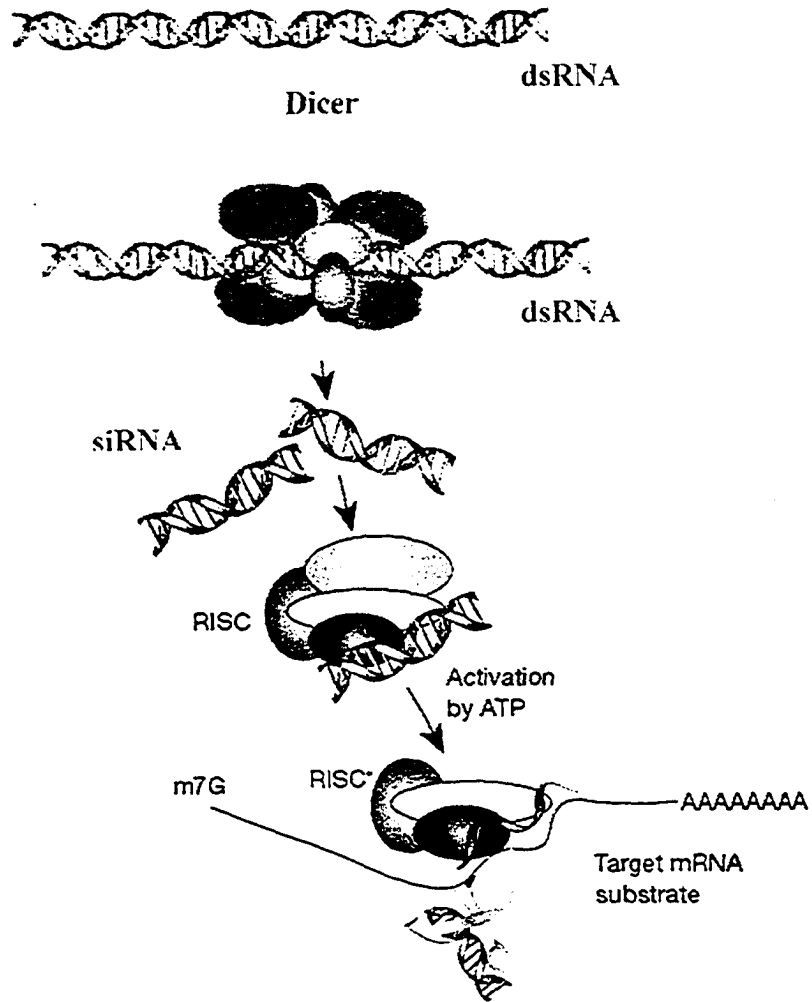


(Figure adapted from Hannon, 2002)

Figure 1.3 The RNA interference pathway starts with Dicer acting on the dsRNA to generate the active siRNAs. These siRNAs in turn trigger destruction of the complementary target mRNA by the slicer activity of the RISC which is activated upon association with the siRNA.

1.3.6 Dicer and the RNase III family

Dicer is a member of the RNase III family which has the ability to degrade dsRNA (Filippov *et al.*, 2000). The RNase III enzymes which are commonly found in prokaryotes and eukaryotes cleave their dsRNA substrate into smaller duplexes with 5' phosphate and 3' hydroxyl termini with 2 single-stranded nucleotides (overhang) at the 3' ends (Filippov *et al.*, 1999). Dicer has an ATP-dependent RNA helicase domain at the amino terminus which is speculated to act as a translocase that drags the Dicer along the dsRNA as it is being cleaved.

Dicer is evolutionarily conserved in worms, flies, plants, fungi and mammals (Bernstein *et al.*, 2001). There are three types of RNase III: the canonical, the Drosha-like and Dicer. The canonical RNase III members contain a dsRNA-binding domain (dsRBD) and a catalytic center with a highly conserved stretch of nine amino acid residues known as the RNase III signature motif. The second class, known as the Drosha family, has two RNase signature motifs and a single dsRBD. The last class of RNase III to which Dicer belongs has dual signature domains and a dsRBD with an RNA-helicase domain (Filippov *et al.*, 1999, Ketting *et al.*, 2001).

1.3.7 The Argonaute protein family

The Argonautes are a group of closely related proteins which act as key components of the RISC in mammals, fungi, worms, plants and protozoa (Bartel, 2004, Liu *et al.*, 2004). The Argonaute family was first linked to the RISC by genetic studies in *C. elegans*, which revealed the gene *rde-1* (for RNAi defective) as an essential gene for the silencing process. The Argonautes are divided into Argonaute1-

like (after the *Arabidopsis* Argonaute1) or into Piwi-like (after the *Drosophila* Piwi) depending on the presence of either conserved domains (Liu *et al.*, 2004, Bartel, 2004). Mammals contain four members (Argonaute1 to 4) in the Argonaute1 subfamily (Tabara *et al.*, 1999). It has been shown by extensive experimentation that Argonaute1 is associated with translational suppression while Argonaute2 is the catalytic slicer of the RISC that mediates RNAi (Tabara *et al.*, 1999, Bartel, 2004). In concordance, mammalian cells lacking Argonaute 2 are not capable of mounting responses to siRNA (Liu *et al.*, 2004).

1.3.8 RNA interference as an antiviral defense mechanism

The presence of duplexes of RNA within the cell is often indicative of a viral infection or other mobile genetic elements including transposons. RNA interference has an antiviral role (Fire *et al.*, 1998, Parrish and Fire, 1999, Sharp, 2001). The eukaryotic cells have evolved a protective system to respond to dsRNA: activation of PKR, activation of the RNase L/oligo 2'5' synthetase system and the interferon signal transduction pathway (Sharp, 1999, Cottrell and Doering, 2003).

Cells normally contain a basal level of dsRNA-dependent PKR in the inactive unphosphorylated form. Autophosphorylation and subsequent activation are triggered upon the binding of the dsRNA to PKR. Subsequently, the activated PKR phosphorylates the eukaryotic initiation factor (EIF2 α) and results in halting of host cell protein translation. In addition, the activated PKR phosphorylates I κ B-NF- κ B and causes the transcription factor NF- κ B to separate and translocate into the nucleus where it is involved in the interferon (IFN) pathway. Also, dsRNA induces a

conformational change in the 2', 5' oligoadenylate synthetase upon binding. The active synthetase polymerizes ATP and other nucleotides into 2', 5' oligoadenylate which is metabolized into a cofactor for the non-specific ribonuclease RNase L that degrades both viral and cellular RNA transcripts (Sharp, 1999, Cottrell and Doering, 2003).

The IFN- α /IFN- β signaling cascade pathway is a physiological reaction to viral genetic elements. It is activated both directly and indirectly by the dsRNA. The IFNs are multifunctional cytokines (glycoproteins released by cells of the immune system) that modulate host immunological functions and can inhibit viral replication. The IFN regulatory factor-1 (IRF-1) is activated by the dsRNA and assembles with another activated transcription factor NF- κ B into a complex called the enhanceosome onto IFN- β promoter. This complex then activates the transcription of IFN- β gene. Following their synthesis, the IFN- β s are secreted surrounding cells where they bind their receptors and stimulate the expression of IFN- α and other IFN-stimulated genes (Sharp, 1999).

1.3.9 RNA interference in mammalian cells

1.3.9.1 RNA interference mediated by small interfering RNAs

RNA interference is evidently conserved in many diverse organisms including plants, fungi, metazoans and many protozoans. Homologs of the proteins that are involved in this silencing process are identified in the genomes of most organisms to date (Hannon, 2002). Despite the usefulness of this phenomenon as a tool to study gene function in various organisms, experimental work with dsRNA in

mammalian systems has been difficult (Tabara *et al.*, 1999, Sharp *et al.*, 1999, Nykanen *et al.*, 2001). Mammals possess a protective antiviral response system which leads to a general inhibition of host gene expression (Yang *et al.*, 2002). During early embryonic development, however, these responses could be alleviated. Several studies have reported a successful specific RNAi silencing upon the injection of long dsRNA into early stage-mouse embryos (Tabara *et al.*, 1999). Other research has demonstrated a potent and specific down-regulation of gene expression in human embryonic fibroblasts and kidney cells 293 and correlated this effect with the appearance of 22 nt siRNAs homologous to the gene that was targeted for suppression (Nykanen *et al.*, 2001, Yang *et al.*, 2002). In some human cell lines, the non-specific PFR and INF responses could be blocked by the use of viral inhibitors. Some viruses like adeno viruses express RNAs that mimic dsRNA binding but not action. Also, Vaccinia virus expresses two inhibitory proteins: E3L which has the ability to bind dsRNA and K3L which binds and inhibits PKR (Elbashir *et al.*, 2001). Recently, researchers have demonstrated that specific RNAi responses could be induced in non-embryonic mammalian cell lines through the direct introduction of synthetic siRNAs (Elbashir *et al.*, 2001, Yang *et al.*, 2002). Moreover, some investigators demonstrated that long dsRNAs hydrolyzed by *E. coli* RNase III into short RNAs are able to specifically silence gene expression in cultured mammalian cells (Yang *et al.*, 2002 and Doi *et al.*, 2003). The direct introduction of siRNA into the system to invoke RNAi has been successfully implemented for non-mammalian organisms as well including *C. elegans* and *Drosophila* (Yang *et al.*, 2002, Doi *et al.*, 2003). The power of RNAi is enhanced by the ability to engineer stable silencing of

gene expression. Stable silencing in mammalian systems could be provoked by the expression of either hairpin RNA or siRNA (Sharp *et al.*, 1999, Bernstein *et al.*, 2001).

1.3.9.1.1 Gene knock-down in mammalian systems by hairpin RNAs

In lower organisms, *in vivo* systems that express long dsRNA hairpins have been effectively used for RNAi (Novina and Sharp, 2004). In mammals, such expression systems could not be used because they induce a non-specific effect on gene expression triggered by the dsRNA-interferon related pathways (Wang *et al.*, 2000, Liu *et al.*, 2004, Novina and Sharp, 2004). Mammalian RNAi was first described in mouse embryos using dsRNA. Then following the analysis of the intermediates of the dsRNA, siRNAs have been utilized for the down-regulation of gene expression in mammalian tissue cultures. The direct use of siRNA bypasses non-specific gene suppression and has been shown to be suitable for RNAi (Tabara *et al.*, 1999). In addition to siRNAs, short hairpin dsRNAs (hairpins) have been shown to trigger specific inhibition of gene expression in mammals and lower organisms (McManus *et al.*, 2002). Two different classes of hairpins could be distinguished: class I, which consists of two siRNA strands covalently linked at the 5' and 3' end, class II, consists of an approximately 70 nt long stem with a 12 nt loop. Both classes contain 19 nt of uninterrupted RNA duplex and 5' hydroxyl termini. The activity of class I hairpins depends on the position of the linkage on which end (McManus *et al.*, 2002). Studies have shown that the hairpins are as effective as

siRNAs for mammalian cells if the linkage is on the antisense 3' end (Sui *et al.*, 2002, McManus *et al.*, 2002).

1.3.9.1.2 Gene silencing using small interfering RNA vector-based technology

The restricted availability of the short synthetic RNAs and the lack of guaranteed efficacy of synthetic siRNA present major drawbacks to this technology. An alternative method is to obtain stable expression of siRNA by implementing vectors with opposing T7 RNA polymerase promoters (Donze and Picard, 2002). Among other vectors used for *in vivo* siRNA expression are those which utilize the RNA polymerase III (Pol III) promoter (or U6 promoter in mice) to drive the expression of short RNAs whose 3' ends are terminated with a stretch of 4-5 thymidines (Sui *et al.*, 2002). The resultant RNA from such vectors is composed of two complementary 21 nt sequences arranged in an inverted orientation with an intervening 6 bp non-homologous spacer sequence. The RNA is predicted to fold back and form a hairpin dsRNA with an overhang of thymidines (Sui *et al.*, 2002).

1.3.10 Small RNAs and translational suppression

Although the cellular functions of the RNAi pathway are not completely understood, the identification of a new large class of small non-coding RNAs which are not translated in different organisms implicates that this pathway is regulated to a great extent. Small temporal RNAs (stRNAs) and micro-RNAs (miRNAs) are 21-23 nt RNAs single-stranded RNAs which could vary from a few thousand to 40,000

molecules per cell (Banerjee and Slack, 2002, Novina and Sharp, 2004). They are processed by Dicer from endogenous hairpin precursor transcripts that are approximately 70 nt long with a 4-15 nt loop and stem regions. A perfect duplex is sometimes formed within the hairpin, but more often multiple bulges disrupt this duplex. The stRNAs and miRNAs are indistinguishable in structure and they are both capable of effective gene silencing through translational suppression (Banerjee and Slack, 2002, Novina and Sharp, 2004).

The stRNAs exert post-transcriptional repression by binding to complementary 3'UTR sites on the target genes. Their role is to control the timing of the cell fate determination during the postembryonic development and hence the name temporal (Elbashir *et al.*, 2001). The genes of temporal development have been studied extensively in *C. elegans*. Many members of the stRNA genes including *lin-4* and *let-7*; the most studied; are conserved in other animal species (*Drosophila*, humans and others) suggesting that these are evolutionarily ancient genes (Parrish and Fire, 2001, Elbashir *et al.*, 2001). *Drosophila* has a single gene identical to *C. elegans let-7* while humans have at least three (Yang *et al.*, 2000, Hutvagner and Zamore, 2002). The target transcripts of *lin-4* and *let-7* are referred to as *lin-14/28* and *lin-41*, respectively, and they contain complementary sites in their 3'UTRs. Studies have shown that if these sites were modified or deleted, down-regulation of the expression of these genes would be lost. The single bulged cytosine on *lin-4* has been defined as essential by site-directed mutagenesis for halting the translation of *lin-14* mRNA by *lin-4* stRNA (Hutvagner and Zamore, 2002).

1.3.11 Dicer and Argonaute family members as mediators in both RNA interference and temporal development

There is a tight connection between the RNAi and stRNA/miRNA machineries. Today, it is clear that silencing by RISC can be exhibited in different ways. In flies, plants and fungi, dsRNA can trigger both TGS by chromatin remodeling and PTGS (Liu *et al.*, 2004). The RISC can also disturb protein synthesis by translational suppression in mammals and other organisms (Bartel, 2004, Liu *et al.*, 2004). When the small RNAs (siRNAs) are fully complementary to the target mRNA, RISC degrades the substrate RNA. If the small RNAs (miRNAs and stRNAs) contain mismatched duplexes and some degree of uncomplementarity to the target mRNA, translational suppression is the outcome (Bartel, 2004).

The Arabidopsis ortholog of Dicer, denoted as SIN-1/CARPEL FACTORY (*sin-1/caf-1*), is needed for normal floral development, suggesting that the RNAi pathway components may be involved in temporal development. Also, the *C. elegans* ortholog of Dicer, *dcr-1* has been shown to be involved in temporal control because the RNAi of *dcr-1* results in abnormal developmental timing and a phenotype which resembles *lin-4* and *let-7* loss-of-function mutations. Moreover, the human ortholog of Dicer, Helicase-MOI, is required for the processing of *let-7* in cultured human cells (Hutvagner and Zamore, 2002, Novina and Sharp, 2004).

Members of the *Rde-1* (for RNAi defective) and Argonaute gene family function in RNAi. Recent studies have demonstrated that many members of this family are also involved in the stRNA pathway (Tabara *et al.*, 1999, Bastin *et al.*, 2001, Liu *et al.*, 2004). In *Drosophila*, *ago-2*, a close homolog of *ago-1*, is needed for

embryogenesis (Tabara *et al.*, 1999). In addition, *C. elegans* has 24 *rde-1* homologs, of which 14 were examined for a role in the stRNA temporal pathway using RNAi. Two of these, *alg-1* and *alg-2* (for argonaute like genes) were found to cause phenotypes like those of *lin-4* and *let-7* loss-of-function mutations (Liu *et al.*, 2004).

Despite the fact that the RNAi and developmental pathways intersect through Dicer and the involvement of small RNAs, there are numerous differences between them (Bastin *et al.*, 2001). The most striking difference concerns the outcome of each pathway, RNA degradation by RNAi versus translational inhibition with stRNAs. The specificity of one pathway versus the other has been suggested to be dictated by members of the RDE-1 family in *C. elegans* (Bastin *et al.*, 2001, Liu *et al.*, 2004). Based on this, Dicer could be directed to either the dsRNA by RDE-1 or the stRNA precursors by members of the families ALG-1 and ALG-2. The decision between mRNA degradation and translational suppression could be mediated by the interaction of RDE-1 family members and the small RNAs. Nearly perfect duplexing is a requirement for mRNA cleavage, and because stRNAs do not completely duplex to the target mRNA, they cannot activate the degradation pathway (Yang *et al.*, 2000, Bastin *et al.*, 2002). Another remarkable difference between RNAi and the temporal pathway is that following stRNA processing, only a single strand of the RNA duplex is stable (Novina and Sharp, 2004). On the other hand, processing of the dsRNA in the RNAi pathway yields siRNAs which are double stranded. The stRNAs bind specific complementary sites in the 3'UTR of the target gene, whereas siRNAs can target complementary sequences anywhere in the mRNA (Tabara *et al.*, 1999, Sharp *et al.*, 1999, Nykanen *et al.*, 2001).

OBJECTIVES

RNA interference has revolutionized studies in versatile systems ranging from nematodes to trypanosomes (Ullu *et al.*, 2004). Prior to our study, there has been no report about RNAi or the use of dsRNA in *T. gondii*. The first goal of this study was to investigate whether dsRNA could be used to down-regulate gene expression in *T. gondii*. Non-essential marker genes were initially targeted by *in vitro* synthesized homologous dsRNA. The second purpose was to proceed to the application of dsRNA (if it exhibits ability to inhibit gene expression) in order to elucidate the putative role of genes in *T. gondii*. Genes which are essential for *T. gondii* differentiation and growth are particularly important for the development of new drugs which might prevent tissue cyst formation. In the second part of the study, the gene encoding lactate dehydrogenase was selected as a target for down-regulation because of its speculated significant role in parasite development and differentiation.

CHAPTER 2

MATERIALS AND GENERAL METHODS

2.1 MATERIALS

The chemicals and reagents used in the study were obtained from different companies. The following is a list of the companies and the reagents purchased from them:

Alpha Innotech (San Leandro, CA)

Chemi-glow detection kit

Amersham-Pharmacia Biotech (Baie d'Urfe, Quebec).

Calf intestinal Alkaline phosphatase (CIAP), T7 RNA polymerase, 2'-deoxyribonucleoside 5'-triphosphates (dNTPs), ribonucleoside triphosphates (rNTPs), nitrocellulose membranes, and Hybond N⁺ nylon membranes

Baxter Diagnostics Corp. (Toronto, ON)

Nalgene™ disposable 25 mm syringe filters (0.2 um pore size) and glass Pasteur pipettes

Bio-Rad Laboratories (Mississauga, ON)

Bromophenol Blue, Coomassie brilliant blue R-250, Xylene Cyanol, medium range protein molecular weight standards, and Bio-Rad protein assay dye reagents

Gelman Sciences (Ann Arbor, MI)

The Vacuicap™ disposable bottle-top filter for sterilization of cell media

GibcoBRL Invitrogen (Burlington, ON)

Cell culture media Dulbecco's modified medium (DMEM), minimal essential medium (MEM), phosphate buffer supplemented with calcium, trypsin, penicillin-streptomycin (10 u/ml) and L-glutamine

Hyclone (Logan, UT)

10% Cosmic calf serum

Invitrogen Corporation (Burlington, ON)

Proteinase K, Trizol, and RNase out ribonuclease inhibitor

MBI Fermentas (Burlington, ON)

Restriction enzymes *HincII*, *SacII*, *SmaI* and *EcoRI*

Molecular Probes (Eugene, OR)

PicoGreen, SYBR-gold, trypan blue and goat anti-rabbit IgG conjugated to rhodamine

Perkin Elmer (Norwalk, CT)

[³H] uracil and [³H] hypoxanthine monohydrogen chloride

Promega (Madison, WI)

Agarose , Mung Bean Nuclease, T4 DNA ligase, Moloney murine leukemia virus reverse transcriptase (M-MLV), RQ1 RNase-free DNase, Wizard ® PCR Preps DNA Purification System, DNA ladders 1 kb and 100 bp, Multicore buffer, and restriction enzymes *BamHI*, *KpnI*, *SacI*, *XbaI* and *XhoI*

Qiagen (Mississauga, ON)

The Qiaex ® I and the Plasmid midiprep kits for DNA purification

Roche Diagnostics (Laval, Qubec)

Digoxigenin-11-dUTP (DIG-dUTP), anti-digoxigenin alkaline phosphatase Fab antibody, blocking reagent, *Taq* DNA polymerase, fluorescein-labeling kit, and CSPD chemiluminescent substrate

Sarstedt Incorporation (Newton, NC, USA)

Conical 15 ml and 50 ml graduated polypropylene centrifuge tubes, disposable pipette tips, 24 and 96 well plates, Petri dishes, cell scrapers, and T75 and T25 tissue culture flasks

Sigma-Aldrich (Oakville, ON)

Acetic acid, ampicillin, chloroform, DNA ladders (λ , 100 bp and 1 kb) 4',6 diamidino-2-phenylindole (DAPI), *Dolichos biflorus* conjugated to fluorescein isothiocyanate, dimethylsulfoxide (DMSO), dithiothreitol (DTT), diethylpolycarbonate (DEPC), ethanol, ethylenediaminetetra-acetic acid disodium salt (EDTA), ethidium bromide, fluoro-deoxyuridine (FDUR) formamide, formaldehyde, glycine, glycerol, hydrochloric acid, methanol, morpholinopropanesulfonic acid (MOPS), mycophenolic acid (MPA), nicotinamide adenine dinucleotide in reduced form (NADH), pepsin, polyoxyethylene sorbitan monolaurate (Tween-20), 2-propanol, phenylmethyl sulfonyl fluoride (PMSF), pyruvate, scintillation fluid, sodium citrate, sodium chloride, sodium acetate, N,N,N',N' tetramethyl ethylenediamine (TEMED), tris-hydroxymethylaminomethane (Tris), Triton X-100, Trichloroacetic acid, xanthine

Stratagene (La Jolla, CA)

Pfu turbo DNA polymerase, XL1BL bacterial strain and pBluescript (SK+) plasmid

USB (Cleveland, OH)

Acrylamide, bis-acrylamide, ammonium persulfate (APS), equilibrated phenol, RNase A and sodium dodecyl sulphate (SDS)

Nucleopore (ON)

Polycarbonate filters (3 µm pore size)

Wisent (Montreal)

Dialyzed fetal bovine serum (FBS)

2.2 GENERAL METHODS

General procedures commonly used are described in this chapter. Specific procedures pertaining to each project are described in the experimental procedures of each chapter. General solutions and buffers are listed in Appendix A.

2.2.1 Cell culture and *Toxoplasma gondii*

Cell and parasite culturing was always conducted under sterile conditions in the Class II type A/B3 Biosafety cabinet (Jouan, SA), and all cultures were maintained in a CO₂ incubator (Thermo Forma). All cell culture experiments were carried out using human foreskin fibroblasts (HFF) that were grown in DMEM medium with L-glutamine, supplemented with 10% cosmic calf serum, 5 µg/ml streptomycin and 5 units/ml penicillin in a 5% CO₂ atmosphere. *T. gondii* was propagated in HFF grown in MEM medium with L-glutamine, supplemented with 1% dialyzed fetal bovine serum. Parasites were scraped from infected monolayers and used to infect a new monolayer of HFF grown in MEM medium. When 500 µl of

scraped parasites were used to infect HFF grown in 4 ml culture medium, complete cell lysis was observed in three days (Donald and Roos, 1994).

2.2.1.1 *Toxoplasma gondii* strains

Wild type *Toxoplasma gondii* strain RH was used in Chapters 3 and 4 while the PLK and PLK Δ HXGPRT strain was used in only Chapter 5. Both strains were obtained from the AIDS Research and Reference Reagent Program, NIH.

2.2.1.2 *Toxoplasma gondii* transformation by electroporation

Toxoplasma gondii tachyzoites that had lysed out of a confluent HFF monolayer were scraped from culture plates, syringed through a 21-G needle twice, filtered through a 3 μ m membrane to remove host cellular debris and sedimented by centrifugation at 15,000xg for 10 min at room temperature. The collected pellet was washed twice with Dulbecco's phosphate-buffered saline supplemented with 0.1 g/l Ca⁺² (DPBS) prior to electroporation. For electroporation, the pellet was resuspended in 800 μ l cytomix buffer (120 mM KCl, 0.15 mM CaCl₂, 10 mM K₂HPO₄, KH₂PO₄, pH 7.6, 25 mM HEPES, pH7.6, 2 mM EDTA, 5 mM MgCl₂) freshly supplemented with 2 mM ATP and 5 mM glutathione. Transforming DNA or RNA was added to the resuspended *Toxoplasma* pellet in 4 mm electroporation cuvettes and subjected to electroporation using BTX model 600 Electro Cell Manipulator (Genetronics) (current of 25 Ω , 25 μ F and 1.8 kEV). After a 15 min incubation period at room temperature, the electroporated parasites were inoculated into confluent HFF cells (Donald and Roos, 1994).

2.2.2 DNA quantification

DNA quantification was done using PicoGreen (Molecular Probes) according to manufacturer's instructions. The DNA sample (diluted in TE buffer up to a total volume of 50 μ l) was mixed with an equivalent amount of diluted PicoGreen (1/200) in a microtiter well. Following an incubation period of 5 min, the sample fluorescence was measured (excitation 480 nm, emission 520 nm) using the SPECTRA max GEMINI XS dual-scanning microplate spectrofluorometer with the Soft max[®] PRO software. DNA standards (Molecular Probes) were used to plot a standard curve which was utilized for calculating the concentration of the sample DNA. Alternatively, DNA quantification was performed using the Agilent UV-visible spectrophotometer (Agilent Technologies, Mississauga, ON) by measuring the absorbance of the DNA sample at 260 nm (Sambrook, 1989). In order to determine the purity of DNA from proteins, the absorbance was also measured at 280 nm and compared to that at 260 nm. The DNA concentration was then calculated from the equation $[\text{DNA}] = (A_{260\text{nm}})(\text{dilution factor})(50 \mu\text{g/ml})$.

2.2.3 Protein quantification by the Bradford assay

Protein concentration was determined by the Bradford method using the Agilent UV-visible spectrophotometer. The protein sample was diluted and mixed with 0.5 ml of Bradford reagent. After incubation at room temperature for 10 min, spectrophotometric measurements were carried out at 595 nm using the Bradford Reagent as a blank. A standard curve made with standard protein solutions of BSA

was used to determine the unknown concentration of protein in the sample (Sambrook, 1989).

2.2.4 Bacterial culturing

To maintain sterile conditions throughout bacterial culturing procedures, all broth solutions and glassware were autoclaved prior to use. Any mentioned centrifugations in the following sections were carried out in either the BR4i centrifuge (Jouan, SA) (maximum speed of 4,000xg) or the desktop Eppendorf Model 5415C microcentrifuge from Desaga (Sarstedt Gruppe, Germany, maximum speed of 13000xg).

2.2.4.1 Preparation of competent bacteria

XL₁BL *E. coli* was grown on an agar plate containing tetracycline (0.1 g/l). A single colony was inoculated from the plate into 3 ml LB broth with tetracycline and grown overnight in the shaker incubator at 37°C. The second day, only 1 ml was used from that culture to inoculate a 100 ml LB broth. After three hours of vigorous shaking, the bacteria was chilled on ice for 30 min and then pelleted at 5000xg for 15 min. Cold sterile CaCl₂ (100 ml of 100 mM solution) was then added to the cell pellet. The suspended pellet was centrifuged again at 5,000xg for 15 min. The pellet was washed with 50 ml CaCl₂ solution and centrifuged again as before. The final wash was with 10 ml 100 mM CaCl₂. The pelleted bacteria was finally resuspended in a solution containing 100 mM CaCl₂ and 25% glycerol and aliquoted into microfuge tubes and finally stored at -80°C until use (Sambrook, 1989).

2.2.4.2 Transformation of competent bacteria

Eight μl of ligation reaction products were added to 25 μl of freshly thawed competent *E. coli*. Following 30 min incubation on ice, the cell suspension was heat shocked at 42°C for 60 sec, followed by another 2 min incubation on ice. After the addition of 400 μl LB broth, the bacteria was allowed to recover for 45 min at 37 °C with shaking. Approximately 50 μl of this culture was spread on LB agar plates containing 0.1 g/l ampicillin. Plates were then incubated overnight at 37 °C (Sambrook, 1989).

2.2.4.3 Plasmid isolation from transformed bacteria

Plasmid mini-preparations were performed to isolate the recombinant plasmids from the transformed bacteria (Sambrook, 1989).

2.2.5 Gel electrophoresis

2.2.5.1 Agarose gel electrophoresis

Agarose gels were electrophoresed using the Miniature Horizontal Gel System MLB-06 (Tyler Research Instruments, Edmonton). Agarose was dissolved in Tris acetate EDTA (TAE) buffer and ethidium bromide was later added to a final concentration of 10 ng/ml. After the gel had solidified, it was immersed into the electrophoresis tank filled with TAE buffer. The DNA samples were loaded into the wells after mixing with the gel loading buffer and run for 40 min at 90 V (Sambrook, 1989). The gels were visualized using the Benchtop Ultraviolet Transilluminator

(VWR Scientific, Mississauga, ON). Gel images were captured by the Alpha Imager™ 2200 Light Imaging System with Alpha Ease software for photography of ethidium bromide stained agarose gels (Alpha Innotech Corporation, San Leandro).

2.2.5.2 Sodium dodecyl sulfate-Polyacrylamide gel electrophoresis

Sodium dodecyl sulfate-Polyacrylamide gel electrophoresis (SDS-PAGE) was conducted with a discontinuous buffer system (Laemmli, 1970). The stacking and resolving gels were cast using the vertical gel electrophoresis system BRL (Bethesda Research Laboratories). The resolving solution was poured first and left to polymerize before being overlaid by the stacking gel. Samples were mixed with the gel loading buffer and boiled for 10 min before being loaded into the wells. The gel was run with the Tris-glycine running buffer at 150 volts until the bromophenol blue dye reached the end of the gel. After electrophoresis, the gel was first soaked in the staining solution for 1 h and then in the destaining solution for 3 h (Laemmli, 1970, Sambrook, 1989). Gels were finally photographed by the Alpha Imager system.

2.2.6 Polymerase chain reaction

Polymerase chain reaction (PCR) was performed using either the 48-well Perkin Elmer Cetus DNA thermal cycler (Perkin Elmer, Norwalk, CT) or the 20-well Techgene thermal cycler (Techne, Cambridge, UK). PCR using genomic DNA as template was always performed with *Pyrococcus furiosus* (*Pfu*) DNA Polymerase,

while PCR using plasmid or cDNA as template was performed with *Thermus aquaticus* (*Taq*) DNA polymerase.

2.2.6.1 Oligonucleotide primers

All the oligonucleotide primers used in the study were synthesized by Sigma-Genosys. The sequences of all the oligonucleotide primers used in the study are listed in Appendix B.

2.2.6.2 Polymerase chain reaction with *Taq* DNA polymerase

PCR was carried out in a total volume of 100 μ l containing 20 mM ammonium sulfate, 75 mM Tris-HCl (pH 8.8), 2 mM MgCl₂, 20 μ M of each dNTP, 50 pmol of each primer, the proper DNA template and 2 u of *Taq* DNA polymerase. PCR was run for 30 cycles (95°C for 30 sec, 55°C for 40 sec, 72°C for 1 min). Samples were subjected to a final extension step at 72°C for 10 min and finally stored at 4°C until use (Gibbs, 1990).

2.2.6.3 Polymerase chain reaction with *Pfu* DNA polymerase

Polymerase chain reaction (PCR) was carried out in a total volume of 100 μ l containing 10 mM KCl, 20 mM Tris-HCl (pH 8.8), 0.1% Triton X-100, 2 mM MgSO₄, 10 mM (NH₄)₂SO₄, 0.15 mM of each dNTP, 50 pmol of each primer, proper DNA template and 2.5 u *Pfu* Turbo DNA polymerase. PCR was performed for 30 cycles, each consisting of denaturation (95°C, 1 min), annealing (60°C, 1 min) and

extension (72°C, 1 min). Samples were then incubated at 72°C for 10 min and cooled to 4°C until use (Gibbs, 1990).

2.2.7 Reverse transcription polymerase chain reaction

Reverse transcription polymerase chain reaction (RT-PCR) was performed in two steps. The first was a RT reaction while the second was a PCR. Extracted RNA was treated with 2 u of RQ1 RNase-free DNase for 15 min at 37°C, and the DNase was inactivated by heating at 75°C for 5 min. The RT reactions were then carried out using 2 µg of treated total RNA as initial template, 10 pmoles of oligonucleotide primer in a total volume of 20 µl containing 50 mM Tris-HCl pH 8.3, 75 mM KCl, 10 mM DTT, 3 mM MgCl₂, 0.5 mM of each dNTP, 50 u of RNase out RNase inhibitor and 200 u of M-MLV reverse transcriptase. The reactions were incubated at 37°C for 60 min. Eight µl of the RT reaction mixtures were later used for the subsequent PCR amplification. The PCR was performed in a total volume of 100 µl containing 75 mM Tris-HCl pH 8.8, 50 mM KCl, 2 mM MgCl₂, 50 uM dNTPs, 10 pmoles of each oligonucleotide primer, and 2 u of *Taq* DNA polymerase. The reactions were programmed for 30 amplification cycles each consisting of: denaturation at 94°C for 30 s; annealing at 56°C for 30 s and extension at 72°C for 1 min. The products were stored at -20°C until use (Sambrook, 1989).

2.2.8 *In vitro* transcription

The 17 nucleotide long T7 promoter was incorporated upstream the DNA templates by PCR using the T7 promoter containing oligonucleotides as specified in

each chapter. The T7-bearing DNA templates were then used for the synthesis of RNA by *in vitro* transcription. The transcription reaction was carried out in a total volume of 100 µl containing 40 mM Tris-HCl (pH 8.0), 6 mM MgCl₂, 10 mM NaCl, 10 mM DTT, 50 u RNase inhibitor, 2.5 mM rNTP, 200 u T7 RNA polymerase, and 1/100 dilution pyrophosphate. Transcription was allowed to proceed at 37°C for 2.5 hrs. At the end of the incubation period, the transcribed RNA was treated with 2 units of RNase free RQ1 DNase and further incubated for 30 min to degrade DNA. The product was finally subjected to phenol:chloroform extraction and the integrity of the RNA was always confirmed by running it on 1% agarose gel stained with ethidium bromide (Sambrook, 1989).

2.2.9 Southern blot analysis

2.2.9.1 Extraction of genomic DNA from *Toxoplasma gondii*

Toxoplasma gondii tachyzoites that had lysed out of a confluent HFF monolayer were scraped from culture plates, syringed through a 21-G needle twice, filtered through a 3 µm membrane to remove host cellular debris and sedimented by centrifugation at 15,000xg for 10 min at room temperature. The collected pellet was washed twice with DPBS and used for genomic DNA and RNA extraction. *Toxoplasma gondii* genomic DNA was recovered by suspending the pelleted tachyzoites in 1 ml lysis buffer (100 mM EDTA, 10 mM Tris, pH 8.0, 1% SDS) plus 2 mg/ml Proteinase K and an overnight incubation at 43°C. The suspension was then extracted three times each with an equal volume of phenol:chloroform and twice with an equal volume of chloroform. Genomic DNA was finally recovered from the

aqueous phase by precipitating with two volumes of 95% ethanol and a 15 min centrifugation at 14,000xg (Bohne *et al.*, 1994, Bohne and Roos, 1997).

2.2.9.2 Generation of Digoxigenin-labeled probes

DNA probes labeled with Digoxigenin (DIG-dUTP) were generated by PCR using the specific primers and template specified in each. Reactions were performed as explained in the PCR section with the addition of 50 μ M DIG-dUTP to the final mixture.

2.2.9.3 Digestion of genomic DNA, blotting and hybridization

Hybridization assays were performed using either the ProBlot hybridization oven obtained from Labnet (Mandel) or the Bambino hybridization oven. Approximately 10 μ g of genomic DNA was digested with the specified restriction enzyme overnight at 37°C in the appropriate restriction buffer and electrophoresed at 30 volts on 0.7% agarose gel overnight. The gel was transferred by the vacuum blotting system (Boekel Scientific, PA), to Hybond N⁺ nylon membrane using 10x SSC as a transfer buffer. The membrane was UV cross-linked using the CL-1000 UV crosslinker (Upland, CA) at 500 mJ setting for 1 min and prehybridized in hybridization oven (Boekel Scientific, PA) at 68°C with 20 ml prehybridization buffer (1x blocking solution, 4x SSC). The membrane was then hybridized for 12-16 h with 3 ml fresh prehybridization buffer containing 8 μ l heat denatured probe. The membrane was finally washed twice each with 4x SSC/0.5% SDS and 2x SSC/0.1% SDS 64 °C (Sambrook, 1989).

2.2.9.4 Immunological detection of hybridization signal

The hybridization signal was detected using alkaline phosphatase conjugated anti-DIG Fab fragments and CSPD chemiluminescent substrate. The blot was soaked in 20 ml maleic acid buffer for 5 min and then immersed into 20 ml blocking solution for one hour. The blot was then treated with 20 ml antibody solution for one hour followed by three different washes each 15 min using 15 ml wash buffer. After soaking the blot in 15 ml detection buffer for 5 min, CSPD was added and the blot was incubated at 37°C for 5 min. The signal was finally revealed by using the chemiluminescence filter wheel in the Alpha Imager system. The blot was later stripped by being soaked in 50 ml blot denaturation buffer at 37°C for 30 min and reprobed with the second probe under the same conditions described above (Roche kit instructions).

2.2.10 Northern blot analysis

Toxoplasma gondii RNA was extracted from tachyzoite pellet using Trizol reagent. Reagents and equipment were treated with 0.1% DEPC whenever possible prior to RNA extraction. Approximately 7 ug of total RNA in 2 volumes RNA loading buffer was heat denatured at 70° C for 15 min and chilled on ice before being loaded on 1% agarose /2.7% formaldehyde gel run in 1x MOPS buffer at 50 volts (Sambrook, 1989). The gel was transferred to Hybond-N⁺ membrane and probed as for southern blot except that the hybridization was performed at 58° C and the washes at 54° C. Immunological detection of hybridization signal was performed as described before.

2.2.11 Dot blot analysis

This method was used because it allowed the rapid analysis of samples extracted in little amounts for the sequence of interest. Dot blots were done using the dot blot apparatus from Invitrogen. Approximately 2 µg of each RNA sample was mixed with 2 volumes of RNA loading buffer and heat denatured at 70°C for 10 min. The samples were chilled on ice for 5 min, loaded onto the nylon membrane placed within the dot blot apparatus, and aspirated under vacuum. The membrane was UV-crosslinked and used for hybridization as described before.

2.2.12 Synthesis of double-stranded RNA

For the production of T7 promoter-bearing DNA templates for the double-stranded RNA (dsRNA), PCR with the T7 RNA polymerase promoter sequence appended to the specific oligonucleotide primers (as specified in each Chapter) was performed. The resultant T7 promoter-bearing DNA templates were used for the synthesis of the dsRNA by *in vitro* transcription. The dsRNA produced was phenol:chloroform extracted and suspended in DEPC water and stored at – 80°C until use (Ngo *et al.*, 1998).

CHAPTER 3

THE EFFECT OF DOUBLE-STRANDED RNA ON THE EXPRESSION OF THE HOMOLOGOUS GENE IN *TOXOPLASMA GONDII*

SUMMARY

The double-stranded RNA has been used in many organisms to interrupt gene expression at the post-transcriptional level. We have explored the use of *in vitro* synthesized double-stranded RNA for gene expression study in *Toxoplasma gondii*. We produced double-stranded RNAs homologous to the three well documented selectable markers the green fluorescent protein, the uracil phosphoribosyl transferase and the hypoxanthine-xanthine-guanine phosphoribosyltransferase. Each double-stranded RNA was efficiently electroporated into the parasites and monitored for its effect on the expression of the homologous gene. The parasites electroporated with the double-stranded RNA homologous to the green fluorescent protein exhibited reduced fluorescence for the green fluorescent protein. The parasites electroporated with the double-stranded RNA homologous to the uracil phosphoribosyl transferase had low enzymatic activity for the uracil phosphoribosyl transferase, while the parasites electroporated with the double-stranded RNA homologous to the hypoxanthine-xanthine-guanine phosphoribosyl transferase had low enzymatic activity for the hypoxanthine-xanthine-guanine phosphoribosyl transferase. To investigate the *in vivo* longevity of the effects of the electroporated double-stranded RNA, we utilized the uracil phosphoribosyl transferase. An operative uracil phosphoribosyl transferase assimilates 5-fluoro-2'-deoxyuridine ultimately leading to parasite

clearance. Parasites electroporated with the double-stranded RNA homologous to the uracil phosphoribosyl transferase became resistant to 5-fluoro-2'-deoxyuridine as a result of inhibited uracil phosphoribosyl transferase expression. Moreover, the effects of the double-stranded RNA homologous to uracil phosphoribosyl transferase persisted for three successive propagations of the parasites. Our study suggests that the double-stranded RNA could be a useful tool for gene silencing in *T. gondii*.

3.1 INTRODUCTION

Among the RNA technologies used to modulate gene expression, double-stranded RNA (dsRNA) has been successfully used to suppress gene expression in many systems by post-transcriptional silencing of the homologous genes. The dsRNA can induce a specific degradation of the target mRNA *via* RNAi, resulting in the down-regulation of gene expression (Fire *et al.*, 1998, Yang *et al.*, 2000, Novina and Sharp, 2004). Prior to our study, no reports on RNAi in *T. gondii* were documented. In the closely related *Plasmodium*, there are controversial results regarding RNAi. Some studies demonstrated that treatment with dsRNAs homologous to dihydroorotate dehydrogenase and cysteine protease specifically inhibited the expression of these target genes in *Plasmodium* (McRobert and McConkey, 2001, Malhotra *et al.*, 2002).

In this study, three well documented selectable marker genes, including the green fluorescent protein (*GFP*), the hypoxanthine-xanthine-guanine phosphoribosyl transferase (*HXGPRT*) and the uracil phosphoribosyl transferase

(*UPRT*), were chosen as targets to investigate whether the dsRNA can induce gene silencing in *T. gondii*. All of these markers have been extensively used for genetic manipulations in *T. gondii* (Donald and Roos, 1995, Donald *et al.*, 1996, Striepen *et al.*, 1998). We generated dsRNA homologous to each of these selectable marker genes and examined the effect on target gene expression upon electroporation into the parasites.

The green fluorescent protein, a 238 amino acid protein of the jellyfish *Aequoria victoria* is a naturally fluorescent protein that has been used for studies on gene expression and protein trafficking in many systems (Cubbit *et al.*, 1995, Marra *et al.*, 1998). This protein is an excellent marker because its fluorescence could be observed in the absence of any exogenous substrate thus permitting observations *in vivo*, without fixation or complicated manipulation of experimental samples. Moreover, GFP fluorescence could be detected using standard fluorescein isothio-cyanate (FITC) excitation/emission filters. Fluorescence of GFP is dependent on protein expression which requires proper folding and post-translational formation of the chromophore (Cormack *et al.*, 1996). Various investigators have produced GFP mutations in order to improve protein expression and fluorescence emission (Cormack *et al.*, 1996, Marra *et al.*, 1998). The GFP version that we used in this study is called GFPmut2. This GFPmut2 version harbors the mutations S65A, V68L and S72A and exhibits brighter fluorescence in *E. coli* compared to the wild type GFP (Cormack *et al.*, 1996, Marra *et al.*, 1998). Moreover, GFPmut2 excitation characteristics are more closely matched to conventional FITC filters than the wild type *A. victoria* protein

protein (Marra *et al.*, 1998). The expression of this GFP mutant has been explored in the protozoan parasite *T. gondii* as a potential tool for the analysis of its cell biological processes (Striepen *et al.*, 1998). A transgenic parasite line *P30GFP* with stable GFPmut2 expression was first generated for the study of *T. gondii* protein secretory pathway. The *P30GFP* parasites constitutively express GFPmut2 as a fusion to the P30 major surface antigen and thus display strong intrinsic green fluorescence within the parasitophorous vacuoles (Striepen *et al.*, 1998). In this study, the expression of *GFPmut2* in the *P30GFP* parasites was targeted for silencing by the homologous dsRNA because the modulation of the expression could be conveniently monitored by fluorescence microscopy.

The 244 a.a protein UPRT is the only enzyme of the pyrimidine salvage pathway in *T. gondii*. This parasite mainly relies on the *de novo* pathway for the synthesis of pyrimidines. UPRT has been utilized as a negative selectable marker for *T. gondii* genetic transformations (Donald and Roos, 1995). This enzyme is non-essential for the survival of *T. gondii* and is not expressed in mammalian cells. UPRT normally catalyzes the conversion of uracil to uridine monophosphate during pyrimidine salvage (Donald and Roos, 1995). Upon growing the parasites in the presence of uridine analogs such as 5-fluoro-2'-deoxyuridine (FDUR), the incorporated fluoro-deoxyuridine is metabolized into 5-fluorouracil. A functional UPRT enzyme would catalyze the phosphoribosylation of 5-fluorouracil to 5-fluorouridine, leading to the synthesis of 5-fluoro-deoxyuridine monophosphate. The latter is lethal to the parasites because it inhibits the synthesis of thymidine monophosphate. Only parasites with

disrupted UPRT selectively survive the toxic effects of FDUR because they can not metabolize the compound into 5-fluoruracil but rather resort to the *de novo* pathway for the synthesis of thymidine monophosphate (Donald and Roos, 1995). Therefore, upon the electroporation of the dsRNA homologous to *UPRT* (*dsUPRT*) into *T. gondii*, the selection for resistance to FDUR would permit the identification of parasites in which the expression of *UPRT* has been silenced by the action of the *dsUPRT*. In addition, the knock-down of *UPRT* would lower the parasite's ability to assimilate the radioactive pyrimidine analog of uracil, allowing a feasible assessment of the down-regulation effect exerted by the *dsUPRT*.

The multifunctional enzyme HXGPRT plays a key role in the purine salvage pathway. *Toxoplasma gondii* like other protozoans has no *de novo* enzymes for purine synthesis (Donald *et al.*, 1996). Thus, the parasite salvages purines from the host in order to meet its nutritional needs. The salvage activities of *T. gondii* are accounted for by the two enzymes HXGPRT and adenosine kinase (AK). *Toxoplasma gondii* expresses two different isoforms of HXGPRT denoted as I and II of molecular weights 26 and 31 kDa, respectively. HXGPRT catalyzes the conversion of hypoxanthine and guanine to inosine monophosphate (IMP) and guanine-xanthine monophosphate (GXP), respectively (Donald *et al.*, 1996). HXGPRT also converts xanthine to xanthine monophosphate (XMP), a reaction which is not catalyzed by its mammalian analogue HGPRT. The feasibility of HXGPRT as both a negative and positive selectable marker for transformations makes it unique (Nakaar *et al.*, 2000). *T. gondii* parasites with disrupted HXGPRT

gene do not display any apparent phenotype, because adenosine provides an adequate source of adenine nucleotides which can be converted into guanine nucleotides. Parasites with functional HXGPRT are eliminated by the drug 6-thioxanthine, whereas those with disrupted HXGPRT can tolerate the toxic action of this drug. The mechanism by which the 6-thioxanthine causes parasite elimination is still not fully understood. One hypothesis is that the drug inhibits purine salvage in the parasite by acting as a substrate for HXGPRT. It is converted into 6-thioxanthine riboside-5'phosphate, a poor substrate of GMP synthase. Inhibition of this enzyme is detrimental to the growth of the parasite because all the adenine and adenosine salvage pathways require the conversion of XMP to GMP (Pfefferkorn *et al.*, 1983). Alternatively, if 6-thioxanthine riboside-5'phosphate is converted by GMP synthase to 6-thioguanic acid, this analog of GMP could have detrimental effects if further phosphorylated into a 6-thioguanine riboside triphosphate and then used for RNA synthesis (Pfefferkorn and Borotz, 1994). Using HXGPRT as a positive selectable marker requires selection in medium containing mycophenolic acid (MPA) and xanthine. MPA is a cytotoxic base analog which inhibits IMP dehydrogenase and thus prevents the formation of XMP and eventually GMP. Supplementing the medium with xanthine circumvents the effect of MPA because the parasites can use HXGPRT to convert the xanthine into XMP and GMP (Donald *et al.*, 1996). In this chapter, *HXGPRT* was selected for the gene silencing study by the dsRNA homologous to *HXGPRT* (*dsHXGPRT*). The knock-down of *HXGPRT* would decrease the

parasite's ability to uptake radioactive purine analogs thus providing a suitable means to assess the effect of the *dsHXGPRT* on the expression of *HXGPRT*.

Here, we show that *in vitro* synthesized dsRNA could be efficiently introduced into *T. gondii* by electroporation. The dsRNA can specifically modulate gene expression. In addition, when two genes were targeted by two different dsRNAs, the expression of both genes was attenuated. However, the attenuated expression was not to the same level as when each individual dsRNA was used. We therefore believe that dsRNA should be useful as a tool for the study of gene expression in *T. gondii*.

3.2 EXPERIMENTAL PROCEDURES

3.2.1 *Toxoplasma gondii* and selection with 5-fluoro-2'-deoxyuridine

Toxoplasma gondii strain RH was used for all the experiments unless specified. The parasites were maintained in culture as described in the general methods. The *dsUPRT* electroporated parasites were selected in media containing FDUR at 5 μ M final concentration.

3.2.2 The synthesis of double-stranded RNA and electroporation

3.2.2.1 The generation of double-stranded RNA

All the dsRNAs used were produced *in vitro* by transcriptions using DNA templates to which the T7 polymerase promoter sequence has been appended by PCR. The synthesis of the DNA template for *dsGFP* (accession number AF420592, nts 1-515) was performed with T7on5'GFP and T7on3'GFP

oligonucleotides and plasmid peGFP-N1 (Clontech). For the production of *dsGFPmut2* (AF302837, nts 21-604), the primers T7on5'GFPmut2 and T7on3'mut2 were used and the template for PCR was *GFPmut2* cDNA obtained by RT-PCR from *T. gondii* RNA. The plasmid pTUB5-LacZ (obtained from Dr. Soldati, University of Geneva, Switzerland) with oligonucleotides T7on5'LacZ and T7on3'LacZ were utilized for the synthesis of the template for *dsLacZ* (AE005174, nts 12-612). The DNA templates for the generation of *dsUPRT* (U10246, nts 1-724), sense and antisense *UPRT* RNA were synthesized by PCR using plasmid pUPRT (obtained from Dr. Ullman, Oregon Health and Science University, USA) as template. T7AntisenseUP and BamHIUP primers were used for the production of the *UPRT* DNA templates for the synthesis of the antisense RNA, while HindIII-T7GGG and AgeIUP primers were used for the production of *UPRT* DNA templates for the synthesis of sense RNA. The DNA template for the production *dsUPRT* was synthesized using the *UPRT* specific oligonucleotides with the T7 polymerase promoter sequences (mentioned above). The plasmid pTub8myc-His-GFP-HXGPRT (obtained from Dr. Soldati, University of Geneva, Switzerland) was utilized for the production of the DNA template for the *dsHXGPRT* (U10247, nts 1-535) with the oligonucleotide primers T7on5'HXGPRT and T7on3'HXGPRT. T7on5'HXGPRT and HXGPRT forward were used for the synthesis of HXGPRT DNA for the generation of *HXGPRT* sense RNA. For the production of *HXGPRT* antisense RNA, the primers T7on3'HXGPRT and HXGPRT forward were used. All generated dsRNAs were

3.2.2.2 The labeling of double-stranded RNA with fluorescein

The *dsGFP* labeled with fluorescein was produced by using the fluorescein labeling kit (Roche) in an *in vitro* transcription reaction according to manufacturer's instructions. The fluorescein labeled *dsGFP* was resolved on 1% agarose gel which was scanned using the Biorad Molecular-Imager system for gel documentation with a fluorophore scanning setting for fluorescein (excitation and emission maxima 490 and 518 nm, respectively). To reveal unlabeled nucleic acids on the same gel, the gel was stained with SYBR-gold (Molecular probes) and scanned using the Molecular-Imager with a scanning setting for SYBR-gold (Fig. 3.1). The fluorescence was quantified using the Cary eclipse spectrofluorometer (Variant, USA); excitation and emission maxima at 490 and 518 nm, respectively.

3.2.2.3 Monitoring the presence of labeled double-stranded RNA in *Toxoplasma gondii*

The labeled dsRNA electroporation was performed using the conditions described in the general methods. Following electroporation, the parasites were washed twice and finally resuspended in the cytomix buffer. The wash fractions were collected for the determination of the amount of labeled *dsGFP* remaining in solution using the spectrofluorometer. To determine the percentage of parasite survival following electroporation, the viable parasites (which appear as colorless under the microscope because they exclude the trypan

blue dye in contrast to the blue-stained dead parasites) were counted. The presence of fluorescein labeled *dsGFP* in the electroporated parasites was monitored using the Leica DMIRB fluorescence microscope under the FITC filter.

3.2.3 Nucleobase incorporation assays

The electroporated parasites were used for the infection of HFF monolayer grown on 24-well plates at approximately 10^4 parasites per well. Unattached parasites were removed by replacing the media with fresh media four hours later. Twenty four hours post-infection, 2 μ Ci of either ^3H -uracil or ^3H -hypoxanthine were added to each well, and the plates further incubated at 37 °C for two hours. The plates were chilled at -20°C for 2 min, and then trichloroacetic acid (TCA, 10%) was added to the existing medium. The monolayers were fixed by incubation with the acid for 1 h on ice. The unincorporated nucleobase was removed from the monolayers by extensive rinsing with water. The amount of incorporated nucleobase was measured from the radioactivity remaining in the TCA precipitate using a scintillation counter (Beckman LS6500). The data obtained from at least two independent experiments were calculated for average values and standard deviations for each tested RNA species. A hairpin RNA, called R31L-32, which is a substrate for RNase III, was used as the control RNA species (Lebars *et al.*, 2001). R31L-32 is 70-nt RNA and has a nucleotide sequence unrelated to the *UPRT* gene.

species (Lebars *et al.*, 2001). R31L-32 is 70-nt RNA and has a nucleotide sequence unrelated to the *UPRT* gene.

3.3 RESULTS

3.3.1 The introduction of *in vitro* synthesized double-stranded RNA via electroporation

Electroporation is the most effective means of transformation used in *T. gondii* for genetic studies (Roos *et al.*, 1994). This method is therefore used for our study to deliver the dsRNA into *T. gondii*. The efficiency of electroporation was initially determined. Fluorescein labeled dsRNA homologous to GFP (*dsGFP*) was used because GFP is not expressed by *T. gondii* RH parasites. Hence, the dsRNA would presumably not affect the parasite cell biology. We electroporated 10 μg *dsGFP* into 4×10^5 viable parasites. The amount of labeled *dsGFP* had 274×10^3 relative fluorescence units (RFU). Immediately after electroporation, the parasites were stained by Trypan blue and counted again in order to determine viability. The percentage of the parasites which survived the electroporation was 74%. The parasites were then washed twice and resuspended in the electroporation buffer. The amount of fluorescein labeled *dsGFP* remaining in solution was calculated based on RFU/ μg to be approximately 4.8 μg . Thus, from the initial *dsGFP* (10 μg) used, approximately 5.2 μg *dsGFP* (52% of the electroporated *dsGFP*) successfully entered the parasites. Using fluorescence microscopy, approximately 108 parasites were counted in each microscopic field (a diameter of 0.25 m, or area of 0.049m^2). Five independent fields were counted

which displayed fluorescence. An aliquot of the electroporated parasites was stained with Trypan blue and then analyzed for fluorescence. We were not able to detect fluorescence signals in that same aliquot. Presumably it is due to the interference effect of trypan blue on GFP signal.

3.3.2 Knock-down of gene expression by electroporated double-stranded RNA

The expression of the marker genes *GFP*, *HXGPRT* and *UPRT* was monitored following the electroporation of their homologous dsRNAs. The following sections describe the results obtained.

3.3.2.1 The expression of green fluorescent protein

We used strain *P30GFP* (Striepen *et al.*, 1998) which exhibits strong intrinsic green fluorescence signal within the parasitophorous vacuoles. Synthesized *dsGFPmut2* (10 µg) was electroporated into these green transgenic parasites in order to evaluate its ability to block *GFPmut2* expression and consequently reduce fluorescence signals. Additional control electroporations with the buffer (mock electroporation) and unrelated dsRNA were performed to verify whether the electroporation had non-specific effects in lowering fluorescence signals. The unrelated dsRNA utilized was dsRNA homologous to the bacterial β galactosidase gene (*LacZ*) which has no sequence homology to *GFPmut2*. Following electroporation, the parasites were subjected to a time course analysis of *GFPmut2* fluorescence signal. At 24 h post-electroporation, the

intensity of GFP fluorescence signal in parasitophorous vacuoles was monitored from independent tests to be comparable and almost invariable to the intensity of fluorescence from vacuoles of the unelectroporated *P30GFP* parasites. However, at 48 h post-electroporation, the parasites electroporated with the *dsGFPmut2* showed a notable reduction in fluorescence as compared to the parasites with mock electroporation (Fig. 3.3A, upper panel: parasites with mock electroporation, lower panel: parasites electroporated with the *dsGFPmut2*). The parasites electroporated with the dsRNA homologous to *LacZ* (*dsLacZ*) did not show any significant reduction in fluorescence at that same time interval.

We further attempted to quantify the extent to which the tested dsRNAs could knock-down *GFPmut2* gene expression. The fluorescence signal from 50 independent parasitophorous vacuoles was measured for each set of electroporated parasites. The fluorescence signal of examined vacuoles ranged from 22 units (the weakest) to 242 units (the brightest). Based on the value of relative fluorescence units (RFU), the fluorescence signal was classified into five different categories: very low (0-50), low (51-100), medium (101-150), high (151-200) and very high (201-250). Vacuoles were then grouped based on their RFU values. The majority (94%) of the vacuoles from parasites electroporated with buffer containing no RNA displayed strong fluorescence signals with RFU values ranging from 101 to 250 (Mock, Fig. 3.3B). Some of the vacuoles from these parasites however exhibited fluorescence with lower RFU values which ranged between 0-50 (1%) and 51-100 (5%). Therefore, we suspected that 6% of the parasites electroporated with buffer had lowered GFP expression due to

electrical shock. The distribution of vacuoles for the parasites electroporated with *dsLacZ* showed a similar pattern to that of the parasites electroporated with buffer. Approximately 91% of vacuoles from the parasites electroporated with *dsLacZ* exhibited strong fluorescence with RFU values ranging from 101 to 250 (*dsLacZ*, Fig 3.3B). Some of the vacuoles (9%) from these parasites displayed fluorescence with lower RFU values below 151. In concordance with the results obtained from mock electroporations, we speculated that 9% of the parasites electroporated with *dsLacZ* expressed GFP at a lower level because of the current pulse. This indicated that the *dsLacZ* did not likely affect the expression of GFP. As for the parasites electroporated with *dsGFPmut2*, the majority (61.5%) of the vacuoles exhibited fluorescence with lower RFU values below 101 (*dsGFPmut2*, Fig 3.3B). The fact that the majority (61.5%) of vacuoles exhibited lowered GFP expression strongly implicated that the *dsGFPmut2* besides the effect of shocking the parasites during electroporation caused a significant down-regulation of GFP expression. However, some (38.5%) of the vacuoles showed undisturbed fluorescence signals with higher RFU values. A plausible explanation is that these parasites did not have a successful introduction of *dsGFP* into their intracellular compartment (in correlation to the 68% electroporation efficiency determined in the previous section).

3.3.2.2 The expression of hypoxanthine-xanthine-guanine phosphoribosyl transferase

The second target chosen to test for the effect of dsRNA on the gene expression in *T. gondii* was *HXGPRT*. Because *HXGPRT* has enzymatic activity, the down-regulation effect can be assessed by the nucleobase incorporation assay. The *dsHXGPRT* was generated and electroporated into freshly lysed parasites which were then assayed for ^3H -hypoxanthine incorporation as an indicator of *HXGPRT* activity. In addition to electroporation with the *dsHXGPRT*, parasites were individually electroporated with the equal amount (4 μg) of *dsGFP*, *dsUPRT*, sense and antisense RNA homologous to *HXGPRT* RNA. The mock electroporated parasites were able to incorporate ^3H -hypoxanthine by 21300 ± 1864 (Mock, Fig. 3.4). The HFF did not assimilate ^3H -hypoxanthine (128 ± 16 cpm, HFF, Fig 3.6) The *dsHXGPRT* treatment notably lowered ^3H -hypoxanthine uptake by the parasites as compared to mock (12765 ± 2180 cpm, *dsHXGPRT*, Fig. 3.4). The antisense RNA homologous to *HXGPRT* repressed the *HXGPRT* activity (16885 ± 2180 , *asHXGPRT*, Fig. 3.4), while the *dsGFP*, *dsUPRT* and sense RNA homologous to *HXGPRT* did not exert an effect on the activity of *HXGPRT* (Fig. 3.4).

3.3.2.3 The expression of uracil phosphoribosyl transferase

The third target gene selected for the down-regulation study by the dsRNA was *UPRT*. The protein *UPRT* has enzymatic activity which can be measured and used for monitoring the down-regulation effect on *UPRT*

expression. In order to verify whether the *dsUPRT* can directly affect the expression of *UPRT* and the *UPRT* gene product, we introduced the *in vitro* synthesized dsRNA into purified *T. gondii* via electroporation and subsequently monitored the *UPRT* enzymatic activity. To standardize the test conditions, the purified *T. gondii* parasites were resuspended in the electroporation buffer and subjected to electroporation in the absence of RNA, mock electroporation. The mock electroporated parasites were able to infect the host cells and to incorporate ³H-uracil (16963 ± 1312 cpm, Mock, Fig. 3.6), while the host HFF had no ability to incorporate ³H-uracil (23 ± 6 cpm, HFF, Fig. 3.6). When 4 μ g of the *dsUPRT* was electroporated into the parasites, the electroporated parasites exhibited a drastically lower *UPRT* activity (632 ± 57 cpm, dsUPRTx1, Fig. 3.6), as compared to mock electroporation. The equal amounts (4 μ g) of other RNA species, including (i) the sense RNA, (ii) the antisense RNA derived from the *UPRT* gene, (iii) an unrelated RNA containing a hairpin structure, (iv) the *dsGFP*, were individually electroporated and assayed for their effect on the *UPRT* activity. The sense and antisense RNAs homologous to *UPRT* acted as specific controls for the *dsUPRT*, while the *dsGFP* and hairpin were included as general controls for the dsRNA. The sense RNA homologous to the *UPRT* mRNA did not result in an increase in the *UPRT* activity, although the sense RNA contained the whole ORF of *UPRT* mRNA, but lacking 5'- and 3'-UTRs. We observed no significant effect by the sense RNA homologous to the *UPRT* gene on the *UPRT* activity (15315 ± 860 cpm, ssUPRT, Fig. 3.6). The antisense RNA was able to lower the *UPRT* activity (8874 ± 1642 , asUPRT, Fig 3.4). The hairpin RNA

containing no sequence homologous to the *UPRT* gene slightly decreased the UPRT activity (12185 ± 534 cpm, hpRNA), as compared to the mock electroporation. The *dsGFP* did not affect the UPRT activity (15549 ± 4179 , dsGFP, Fig 3.4). When varying concentrations of *dsUPRT* (0.4 μ g to 4 pg) were introduced into purified *T. gondii*, the UPRT activity was lowered in a dose-response manner.

3.3.2.3.1 The down-regulation of uracil phosphoribosyl transferase disables the parasite to incorporate 5-fluoro-2'-deoxyuridine

We were interested to learn how long the suppressing effect of *dsUPRT* on UPRT activity would last. Since UPRT is a negative selectable marker, parasites with non-functional UPRT or suppressed UPRT activity are resistant to the presence of FDUR, whereas parasites with intact UPRT are eliminated in the presence of FDUR. Therefore the parasite resistance to FDUR can be correlated to the *dsUPRT* gene silencing effect. Ten μ g of *dsUPRT* were introduced into *T. gondii* by electroporation. Following the electroporation, the parasites (termed passage one) were divided into two portions: one was used to infect HFF (Fig. 3.6A) and the other assayed for UPRT activity by the uracil uptake assay. Twenty-four hours post-electroporation, the inoculated parasites were exposed to 5 μ M FDUR. If the electroporated parasites managed to lyse the host monolayer in the presence of FDUR, they were again aliquoted for uracil incorporation and infection in the presence of FDUR. The parasites of passage

one incorporated uracil at a drastically low reading of 170 cpm (*dsUPRT*, passage one, Fig. 3.6B). In parallel, these parasites were able to lyse the HFF monolayer in the presence of FDUR, indicating that they exhibited an FDUR^r (*FDUR*^r) phenotype. The parasites of passage two assimilated uracil at a reading of 2161 cpm (*dsUPRT*, passage two, Fig. 3.6B) and were also able to lyse the HFF monolayer in the presence of FDUR. The uracil incorporation of the parasites of the third passage was 6995 cpm (*dsUPRT*, passage three, Fig. 3.6B). These parasites like those of the previous two passages exhibited an FDUR^r phenotype. Therefore, the parasites of the first three successive passages had a suppressed UPRT activity presumably due to the effect of the electroporated *dsUPRT* from the first passage. The parasites of the fourth passage were never able to grow in the presence of FDUR, indicating that they were not FDUR^r. We speculated that the UPRT of these parasites would have been functional because the parasites were eliminated by the FDUR. Moreover, the functional UPRT was because the effect of the electroporated *dsUPRT* did not last in the fourth passage. As a control for the experiment, mock electroporations (with the buffer alone) were carried out to rule out the possibility of any random FDUR^r. The mock electroporated parasites were completely eliminated by the FDUR, indicating that the electroporation with buffer did not inhibit UPRT activity. No FDUR^r parasites emerged with the mock electroporations which were repeated at least three times. In another control test, mock electroporated parasites were grown in the absence of FDUR and continuously propagated and assayed for UPRT activity following lysis. The mock electroporated parasites of the first passage were able to

assimilate uracil at a high reading of 20489 cpm (mock, passage one, Fig. 3.6B). Similarly, the mock electroporated parasites of passages two and three incorporated uracil at high readings of 17890 and 16500 cpm, respectively (mock, passage two and passage three, respectively, Fig. 3.6B). This implicated that the mock electroporated parasites of the three successive passages had an intact UPRT activity.

3.3.2.4 The expression of hypoxanthine-xanthine-guanine phosphoribosyl transferase and uracil phosphoribosyl transferase

We questioned whether a combination of the *dsHXGPRT* and *dsUPRT* could be used to simultaneously down-regulate the two independent genes *HXGPRT* and *UPRT*. We electroporated a mixture of equal amounts of *dsHXGPRT* and *dsUPRT* (1 µg each) into purified parasites and monitored the ³H-uracil and ³H-hypoxanthine incorporation. As expected the individual dsRNA showed down-regulation effects on the individual gene. The *dsUPRT* did not affect ³H-hypoxanthine assimilation, but significantly lowered the ³H-uracil uptake, as compared to the mock electroporation (*dsUPRT*, Fig. 3.7). The *dsHXGPRT* did not reduce the incorporation of ³H-uracil but caused that of ³H-hypoxanthine to drop drastically as compared to the mock electroporation (*dsHXGPRT*, Fig. 3.7). The mixture of *dsUPRT* and *dsHXGPRT* could simultaneously lower the ³H-uracil and ³H-hypoxanthine assimilation but was not as effective as when each individual dsRNA was tested (*dsHXGPRT* + *dsUPRT*, Fig. 3.7).

3.4 DISSCUSSION

The focus of this study was to investigate whether the dsRNA could lower gene expression in *T. gondii*. The dsRNA can be used as a modulator of *T. gondii* gene expression.

We first demonstrated that the dsRNA can be efficiently introduced into *T. gondii* intracellular compartment by electroporation. We subsequently investigated the effect of dsRNA on gene expression. We showed that the *dsGFPmut2* could specifically modulate the *GFPmut2* expression, leading to reduced fluorescence by the parasitophorous vacuoles of the *P30GFP* parasites. There was a delay time of almost 48 h before observing a change in the fluorescence signal. This delay could be probably attributed to the pre-existing GFP. It is therefore likely that the half-life of the GFP is the factor here.

The down-regulation effect of the dsRNA was reproduced on the other two genes *UPRT* and *HXGPRT*. The *dsHXGPRT* was successful in inhibiting the expression of its homologous gene *HXGPRT*, as indicated by the low hypoxanthine uptake (Fig. 3.4). For all tested dsRNAs, the gene silencing effect was specific to the homologous gene. The *dsUPRT* could directly down-regulate the *UPRT* gene expression, resulting in a decreased UPRT activity. In addition, a dose-response curve could be drawn when the varying amounts of the *dsUPRT* was tested. The greater the *dsUPRT* amount used, the lower the uracil incorporation (Fig. 3.6). The antisense RNA of the *UPRT* gene could also lower the UPRT activity but not to the same level as per the dsRNA. Interestingly the hairpin RNA having an unrelated sequence to the UPRT gene can lower the

UPRT activity. We speculate that the presence of hairpin RNA might slowly induce mRNA degradation.

One of the interesting features of the electroporated *dsUPRT* was the longevity of its effect *in vivo*. The down-regulation effect lasted long enough to lower the *UPRT* gene expression for three successive propagations of the parasites, as indicated by the low UPRT activity, when compared to the mock electroporated parasites (Fig. 3.6). The FDUR^r phenotype maintained by these passages was a direct result of the attenuated UPRT activity by the *dsUPRT*. The parasites from passage four were eliminated by the FDUR. For this passage, we speculate that the *dsUPRT* amount was insufficiently low that it failed to knock-down *UPRT* gene expression.

The *dsUPRT* can be used in combination with the *dsHXGPRT* to inhibit the expression of *UPRT* and *HXGPRT* genes (double-knock down). However, the down-regulation was not as effective as when the individual dsRNA was utilized. The *dsUPRT* and *dsHXGPRT* were presumably processed into siRNAs. The siRNAs as the products of *dsUPRT* and *dsHXGPRT* would be recruited into the complex called RNA-induced silencing complex for the degradation of the target RNAs. Since the dsRNA mixture was less potent in lowering the nucleobase incorporation, we speculate that the responsible elements for the siRNA formation or the silencing complex could be the limiting factor. It is highly likely that the dsRNAs compete for the RNAi machinery. The end result of such a competition is a reduction in the extent of down-regulation exerted by the individual dsRNA. Therefore, the dsRNA can effectively knock-down gene expression but is not

ideal for the knock-down of two or more independent genes. In order to have a better understanding of the RNAi process, more experiments should be performed to dissect the individual steps of the silencing process.

The decrease in hypoxanthine incorporation as a result of electroporation with 1 μg *dsHXGPRT* (^3H -hypoxanthine, Fig. 3.7) was more drastic than when 4 μg *dsHXGPRT* were used under the same conditions (Fig. 3.4). The reason for this could be probably attributed to the low specificity and selectivity of the HXGPRT enzyme (Donald *et al.*, 1996). It is possible that 1 μg *dsHXGPRT* is the optimal amount which could induce *HXGPRT* down-regulation. We suspect that the RNA electroporation with an excess amount (4 μg) of *dsHXGPRT* might give rise to a higher level of nucleobases following the degradation of the nucleic acids. Since the enzyme HXGPRT can bind and metabolize a number of nucleobase analogues as substrates (Donald *et al.*, 1996, Nakaar *et al.*, 1999), the elevated level of nucleobases might activate HXGPRT activity. Such activation would in turn alleviate the down-regulation effect caused by the *dsHXGPRT* and thus lead to a higher hypoxanthine uptake by the parasite as compared to hypoxanthine uptake following the electroporation with 1 μg *dsHXGPRT*.

In conclusion, we have shown that the dsRNA could be successfully used as a tool for gene silencing in *T. gondii*. Although the effects of *in vitro* synthesized dsRNAs are only transient, the dsRNA could be engineered into an expression system with a chosen *T. gondii* specific promoter in order to control its stable *in vivo* synthesis.

Figure 3.1

**The synthesis of fluorescein-labeled double-stranded RNA homologous
to the green fluorescent protein**

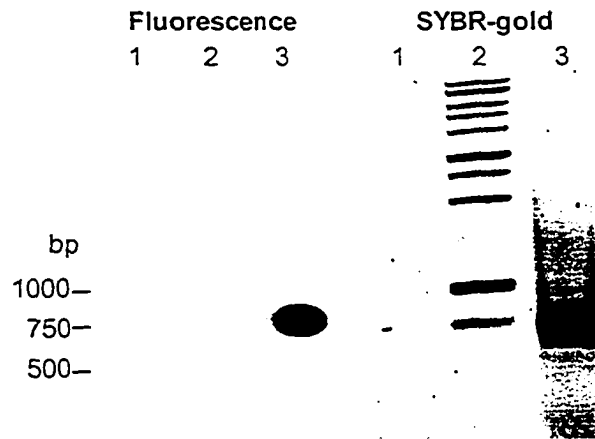


Figure 3.1. The fluorescein labeled *dsGFP* was synthesized by *in vitro* transcription and resolved on 1% agarose gel. The gel was scanned with the Molecular-Imager for gel documentation (Biorad) using the fluorescein filter and then stained with SYBR-gold to reveal both fluorescein-labeled RNA and non-labeled RNA. Lane1, A *dsGFP* sample; lane2: 1 kb marker and lane 3: A fluorescein-labeled *dsGFP* sample.

Figure 3.2

The efficiency of double-stranded RNA electroporation
into *Toxoplasma gondii*

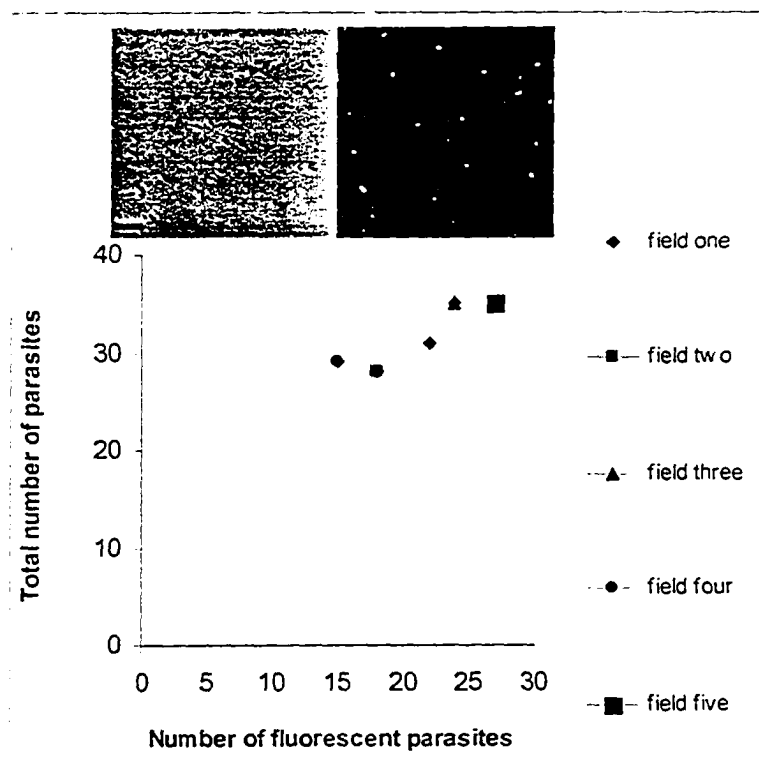
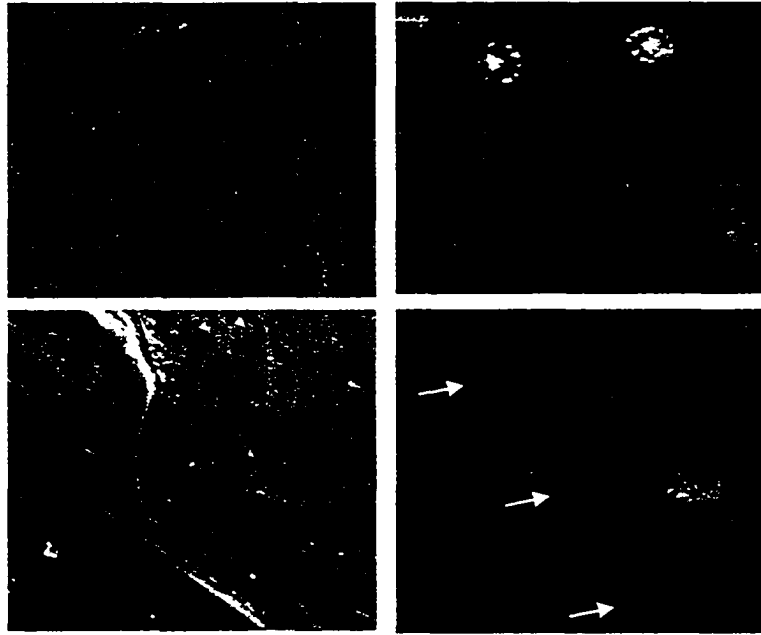


Figure 3.2. Freshly lysed and purified RH *T. gondii* parasites were electroporated with fluorescein labeled *dsGFP* and subsequently monitored for fluorescence. The efficiency of electroporation was determined by comparing the number of fluorescent parasites to the total number of parasites in five microscopic fields. The insets are the phase and fluorescence images of these electroporated parasites. Almost 70 % of the total parasites were fluorescing in this microscopic field as a result of *dsGFP* uptake by electroporation. The bar on the phase image is 10 μ m.

Figure 3.3

The down-regulation of the expression of the green fluorescent protein mutant

A



B

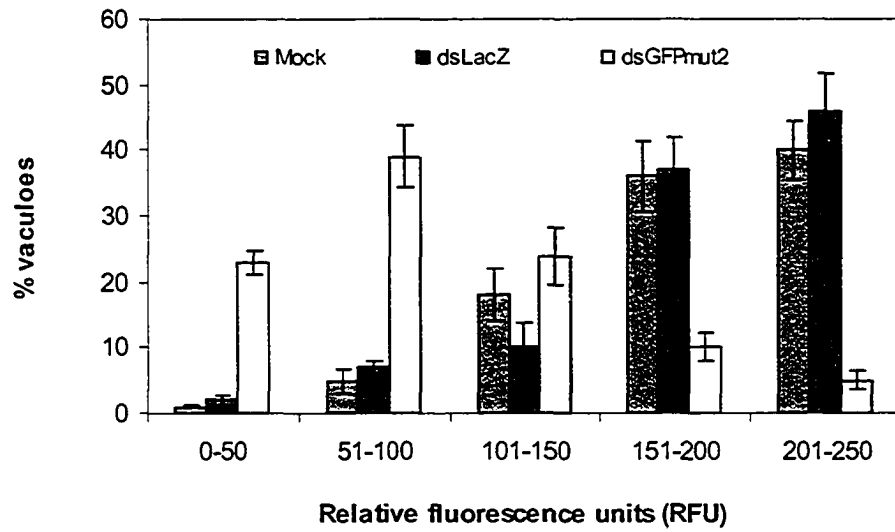


Figure 3.3. A. The *P30GFP* parasites were electroporated with buffer or the tested dsRNA and then monitored for GFPmut2 fluorescence at 48 h following the electroporation. The micrographs in the upper panel are the phase and fluorescence images from the parasites electroporated with the buffer. Micrographs in the lower panel are the phase and fluorescence images from the parasites electroporated with the *dsGFPmut2*; the arrows point to vacuoles with faint fluorescence. Bars on the micrographs are 20 μm . **B.** Distribution of the vacuoles depending on the values of relative fluorescence units. A total of 50 parasitophorous vacuoles for each set of electroporated parasites were analyzed. The experiment was performed in duplicate and the error bars represent deviation from the mean.

Figure 3.4

The effect of *in vitro* synthesized double-stranded RNA homologous to hypoxanthine-xanthine-guanine phosphoribosyl transferase on the expression of the target transcript

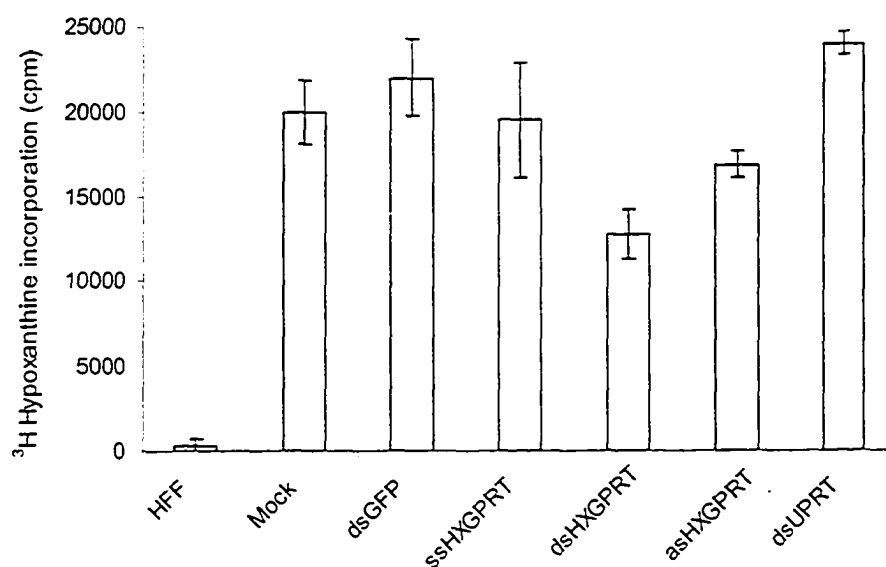


Figure 3.4. The enzymatic activity was measured by the level of ³H-hypoxanthine incorporation at 24 hours following the infection of the electroporated parasites. Various RNA species (4 µg each) were electroporated into the isolated parasites as controls. At least two independent experiments were performed. [ssHXGPRT; sense strand RNA homologous to *HXGPRT*, asHXGPRT; antisense strand RNA homologous to *HXGPRT*].

Figure 3.5

The effect of *in vitro* synthesized double-stranded RNA homologous to uracil phosphoribosyl transferase on the expression of the corresponding transcript

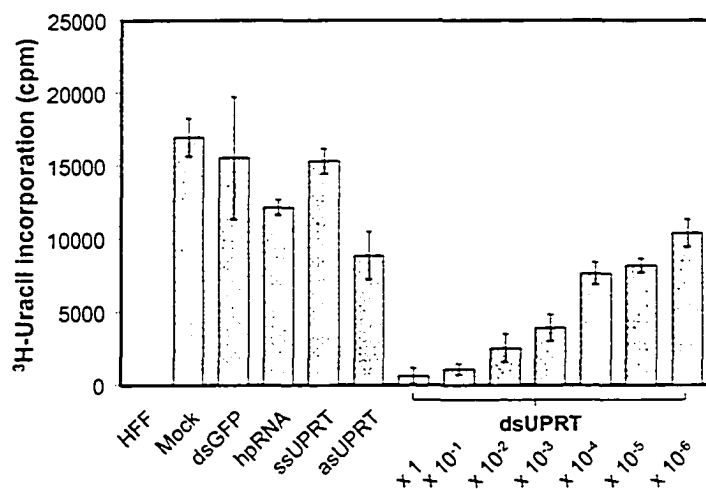


Figure 3.5. The UPRT enzymatic activity was measured by the level of ³H uracil incorporation at 24 hours following the infection of the electroporated parasites. Various RNA species (4 µg each) were electroporated into the purified parasites. At least two independent experiments were performed, and plotted values are averages and standard deviations. [hp RNA; hairpin RNA, ssUPRT; sense strand RNA homologous to *UPRT*, asUPRT; antisense strand RNA homologous to *UPRT*].

Figure 3.6

Longevity of the effects of double-stranded RNA homologous to uracil
phosphoribosyl transferase

A

Parasites lyse out



Reinfection of new HFF
in medium with FDUR



B

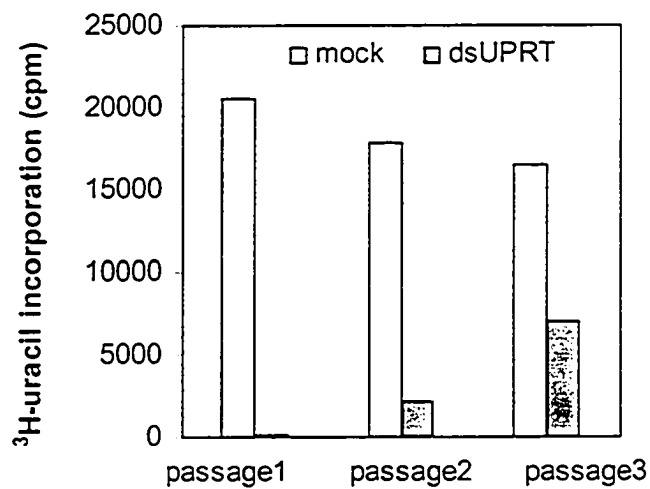


Figure 3.6. A. A schematic diagram of the passage of *dsUPRT* electroporated parasites in the presence of FDUR. **B.** The UPRT activity was assessed by the uracil incorporation assay for the FDUR^r passages and the mock electroporated parasites. The FDUR^r phenotype is the result of *UPRT* knock-down by the *dsUPRT*.

Figure 3.7

Double-knock-down by double-stranded RNA homologous to hypoxanthine-xanthine-guanine phosphoribosyl transferase and double-stranded RNA homologous to uracil phosphoribosyl transferase

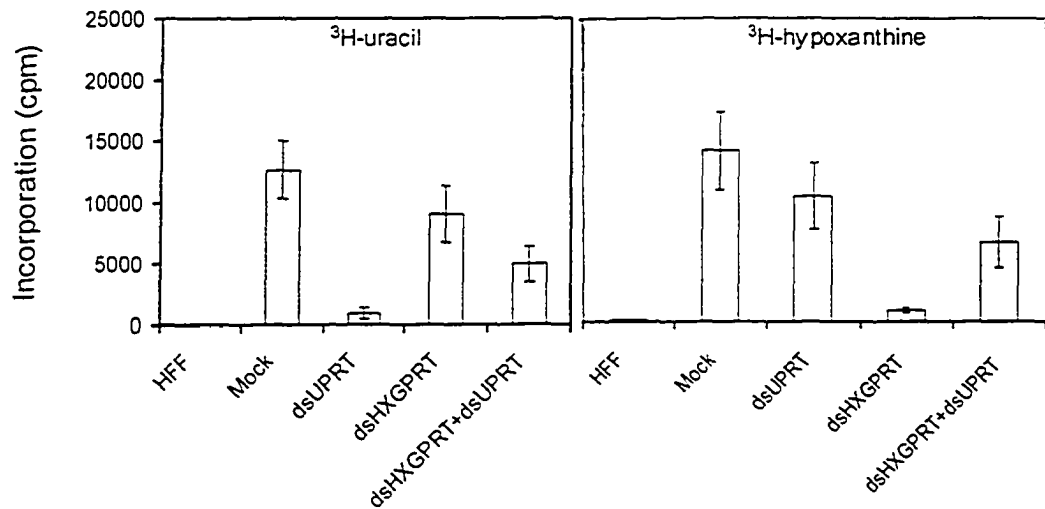


Figure 3.7. A combination of *dsHXGPRT* and *dsUPRT* (1 μ g each) were simultaneously used for the double-knock-down of the two target genes. The activities of the HXGPRT and UPRT were assessed by their corresponding nucleobase incorporation assays. Experiments were repeated 3x; error bars represent the deviation from the mean.

CHAPTER 4

**GENERATION AND CHARACTERIZATION OF A STABLE
TOXOPLASMA GONDII PARASITE LINE EXPRESSING DOUBLE-
STRANDED RNA HOMOLOGOUS TO URACIL PHOSPHORIBOSYL
TRANSFERASE**

SUMMARY

Previously, we have showed that *in vitro* produced double-stranded RNA could down-regulate the expression of the homologous gene in *Toxoplasma gondii*. In order to further characterize this double-stranded RNA and have a better understanding of the mechanism by which it modulates gene expression in the parasite, we engineered a plasmid construct to express double-stranded RNA homologous to the gene encoding uracil phosphoribosyl transferase (*UPRT*). A stable parasite line with down-regulated *UPRT* expression was generated. The uracil phosphoribosyl transferase catalyzes the conversion of uracil to uridine for the salvage of preformed pyrimidines, and is absent in the mammalian host cells. In the presence of 5-fluoro-2'-deoxyuridine (FDUR), lethal metabolites are synthesized, allowing selection for resistance and the identification of transformed parasites in which *UPRT* expression has been inhibited. In this study, a stable parasite line capable of growing in the presence of FDUR was characterized. The parasite line expressed double-stranded RNA homologous to *UPRT* and had lowered levels of the corresponding transcript as compared to wild type parasites. The parasite line appeared to maintain the engineered plasmid as an extra-chromosomal DNA.

We further demonstrated that the expressed double-stranded RNA is important for the emergence of the FDUR-resistance phenotype. When the FDUR-resistant parasites were cultured in the absence of FUDR for ten serial propagations, parasites gradually lost the plasmid encoding the double-stranded RNA and reversed to the sensitive phenotype. Using quantitative competitive reverse transcription polymerase chain reaction, the steady state level of double-stranded RNA expression in different propagations was quantified and correlated to that of *UPRT* transcript. Our study presents a thorough characterization of the behavior of *in vivo* produced double-stranded RNA in *T. gondii*.

4.1 INTRODUCTION

We have previously demonstrated that the expression of the uracil phosphoribosyl transferase (*UPRT*) was successfully down-regulated by the action of *in vitro* synthesized double-stranded RNA homologous to *UPRT* (*dsUPRT*) (Chapter 3, Al-Anouti *et al.*, 2003). Although the electroporated *dsUPRT* exhibited long-lasting effects within the intracellular *T. gondii* compartment, the down-regulation was only transient. A more thorough characterization of the dsRNA (such as the quantification of the relative levels the dsRNA and its possible intermediates against those of the target transcript) is needed to have a better understanding of the mechanism by which the dsRNA inhibits gene expression. Such characterization should be feasible in systems with stable expression of the dsRNA. Stable *T. gondii* transformants expressing the

dsRNA *in vivo* were therefore generated in this project. From literature review, there were several expression vectors engineered to express dsRNA *in vivo* (Sui *et al.*, 2002). Among these, a plasmid which has two promoters arranged in a head-to-head fashion flanking the target cDNA has been first adopted for the generation of stable *Trypanosoma brucei* parasite lines (LaCount *et al.*, 2000). We therefore adopted a similar strategy for our study. We engineered an expression vector for generating a stable *T. gondii* parasite line with down-regulated *UPRT* expression.

As reviewed in section 3.1, Chapter 3, *UPRT* is an ideal negative selectable marker marker for *T. gondii* (Donald and Roos, 1995). A functional *UPRT* assimilates 5-fluoro-2'-deoxyuridine (FDUR) ultimately leading to parasite clearance. Therefore, the selection for tolerance to FDUR allows the identification of parasites with halted expression of *UPRT* (Donald and Roos, 1995). The parasites were transformed by the constructed expression vector and then selected in the presence of FDUR for the emergence of the stably transformed parasite line with inhibited *UPRT* activity. The stably transformed parasite line (denoted *U_i* for UPRT and RNA_i) expressed the *dsUPRT* and exhibited high tolerance to the presence of FDUR as compared to the RH wild type strain. The *U_i* parasites had lower levels of the steady state *UPRT* mRNA and a lower *UPRT* activity than the RH parasites. Southern blot analysis using *U_i* genomic DNA suggested that the transforming plasmid did not undergo genomic integration but was likely maintained as an episome. This extra-chromosomal DNA was replicated and expressed to produce the *dsUPRT* which was likely to be responsible for a specific degradation of the target *UPRT*. Here, we report the generation and

characterization of the Ui parasites expressing the *dsUPRT*. First, the expression levels of both the *UPRT* mRNA and the *dsUPRT* were monitored in these parasites. Second, the stability of the Ui parasites exhibiting resistance to FDUR was investigated with respect to the presence of putative extra-chromosomal DNA. Finally, the existence of the extra-chromosomal DNA was correlated to the estimated level of the *dsUPRT* produced by these parasites and to that of the *UPRT* mRNA.

4.2 EXPERIMENTAL PROCEDURES

4.2.1 Plasmid construction and electroporation

To generate the plasmid p30/11UP30/11, the *UPRT* cDNA fragment (nts 1-724) was amplified from pUPRT (obtained from Dr. Ullman, Oregon Health and Science University) using the oligonucleotide primers AgeIUP and BamHIUP. The obtained fragment was digested with the corresponding restriction endonucleases and cloned into predigested p30/11CAT (Soldati and Boothroyd, 1995) to replace the ORF of the CAT. The generated plasmid was named p30/11UPas. Subsequently, the second modified *T. gondii* promoter SAG1 was isolated from the plasmid p30/11CAT (obtained from Dr. D. Soldati, University of Geneva, Switzerland) and cloned into p30/11UPas downstream from *UPRT* cDNA. The resultant plasmid p30/11UP30/11 had two SAG1 promoters arranged in a head-to-head fashion flanking *UPRT* cDNA. In addition to plasmid p30/11UP30/11, the parental plasmid p30/11CAT was used as a control in the transformation experiments. The plasmids were purified using the endotoxin-free

in the general methods using the RH strain. Twenty four hours post-electroporation, the transformed parasites were selected by 5 μ M FDUR. The medium was replaced every two days with fresh FDUR until the parasite stable cell lines emerged.

4.2.2 Tolerance to 5-fluoro-2'-deoxyuridine and the microtiter assay

The analysis of FUDR resistance was performed using the microtiter assay (Roos *et al.*, 1994) in order to determine the degree of tolerance of parasites to the presence of FDUR. In addition to FDUR, 6-thioxanthine was included in the study as a control to validate that nucleobase resistance did not result from spontaneous mutation. At least two independent experiments were conducted for the same tested compound. Either FDUR or 6-thioxanthine was added to HFF monolayers grown in 96-well plates and infected with 10^3 parasites per well. The series dilutions of either FDUR (0.25 to 500 μ M) or 6-thioxanthine (0.5 to 1000 μ M) were added into the second to the twelfth rows. The first rows served as the control sets which contained no tested compounds. The plates were monitored constantly until the host monolayers in the control set were completely lysed. Subsequently, the plate monolayers were stained with crystal violet (Roos *et al.*, 1994). The color intensity of the stained monolayers was determined using the Alpha Imager system (Alpha Innotech) and correlated with the extent of monolayer destruction. The values obtained from the control set (completely lysed monolayers) were given an arbitrary unit of 100% parasite survival. The

calculated data were then plotted as a function of concentration of the tested compound.

4.2.3 Northern, Southern and dot blot analysis

The Southern, northern and dot blot analysis were carried out as explained in the general methods (Chapter 2). The blots were hybridized to DIG-labeled probes specific to either the *UPRT* or *ROP1* gene. The *UPRT* (U10246, nts 1-724) specific probe was synthesized by PCR under the conditions specified in the general methods (Chapter 2) using the oligonucleotide primers AgeIUP and BamHIUP with plasmid pUPRT to produce a DIG-labeled *UPRT* (U10246, nts 1-724) specific probe. The plasmid pBS-ROP1 and primer pair ROP1 forward and ROP1 reverse were used for the synthesis of the *ROP1* (AA037935, nts 1-502) specific probe by PCR (Chapter 2).

4.2.4 Uracil incorporation assay

The UPRT activity was measured by the *T. gondii* uptake of ³H-uracil as explained in Chapter 3.

4.2.5 Detection of the expression of double-stranded RNA homologous to uracil phosphoribosyl transferase by reverse transcription polymerase chain reaction

In order to investigate the expression of the *dsUPRT*, a reverse transcription polymerase chain reaction (RT-PCR) procedure was used to analyze the expression of the sense and antisense RNA components of the *dsUPRT*. Total

RNA purified from either the parasite line or the RH parasites and treated with RNase-free DNase was used for RT-PCR under the conditions explained in the general methods (Chapter 2). The cDNA was reverse transcribed from the treated total RNA as the following. The BamHIUP oligonucleotide primer was used to reverse transcribe the antisense *UPRT* RNA after annealing at its complementary site (position 724 of *UPRT* gene). The AgeIUP oligonucleotide primer was used to reverse transcribe the sense *UPRT* RNA after annealing at its complementary site (position 1 of the *UPRT* gene). The RT reaction products were subsequently used for PCR amplification with the primer pairs (BamHIUP and AgeIUP).

4.2.6 Quantification of the level of double-stranded RNA homologous to uracil phosphoribosyl transferase by quantitative reverse transcription and polymerase chain reaction

4.2.6.1 Preparation of the competitive standard

In order to prepare the RNA standards for the quantitative competitive reverse transcription and polymerase chain reaction (QC-RT-PCR), the plasmid pUC19UPRT was digested with *HincII* restriction endonuclease to delete 80 nts within the *UPRT* ORF. The digested pUC19UPRT plasmid was then religated to generate the plasmid pUC19UPRT Δ *HincII* which was used to produce (by PCR) DNA templates for the synthesis of sense and antisense *UPRT* RNA internal standards. The RNA standards were synthesized by *in vitro* transcription using T7 RNA polymerase as described in the general methods (Chapter 2). The RNA standards used for the QC-RT-PCR were either the sense or the antisense RNAs.

4.2.6.2 Quantitative competitive reverse transcription polymerase chain reaction

Various concentrations (0.2 to 100 fg) of *UPRT* RNA standards were separately added to purified and DNase treated total RNA (2 µg) prior to reverse transcription (RT) reactions (50 µl). The cDNA was reverse transcribed from the treated total RNA as the following. The UpstreamHincII oligonucleotide primer was utilized to reverse transcribe the antisense *UPRT* RNA and antisense standard RNA after annealing at its complementary site (position 459 of the *UPRT* gene) on these strands. The DownstreamHincII oligonucleotide primer was used to reverse transcribe the sense strand of the *UPRT* RNA and sense standard RNA after annealing at its complementary site (position 701 of the *UPRT* gene) on these strands. The RT reaction products of the sense strand of the *UPRT* RNA and the internal RNA standards were subsequently used for PCR amplification with the primer pairs UpstreamHincII and DownstreamHincII. For each RT, at least two independent PCR reactions were performed. The RT-PCR products of either the sense or antisense strand of the *UPRT* RNA and the RNA standards with the expected sizes of 242 and 162 nt, respectively were resolved by electrophoresis on 1.5% ethidium bromide stained agarose gels. The band intensities of the resolved products were quantified using the Alpha Imager. The intensities of the band of the RNA standard vs. the band of the sense or antisense *UPRT* RNA was measured for each reaction were subsequently calculated to obtain a ratio. The log values of the ratios were then plotted vs. the log of the RNA standard amounts.

4.2.7 Transformation and plasmid rescue

Purified genomic DNA (10-20 μg) was transformed into competent XL1-1 Blue strain by the heat shock method as in the general methods (Chapter 2).

4.3 RESULTS

4.3.1 Generation a stable parasite line resistant to 5-fluoro-2'-deoxyuridine

The parasites exhibiting FDUR resistance (FDUR^r) phenotype emerged from the transformation using p30/11UP30/11 while none resulted from transformation with the control plasmid p30/11CAT. The generated FDUR^r parasites which were called Ui parasite line still exhibited sensitivity to chloramphenicol. Mock electroporations using the buffer lacking DNA performed in order to exclude the possibility of any random FDUR^r phenotype upon transformation did not produce any viable parasites in the presence of FDUR.

Dose-dependent studies were performed in order to determine the FDUR concentration which causes 50% parasite lethality (LD₅₀). In addition to the FDUR, 6-thioxanthine was selected as a control for the study. The Ui parasites exhibited an LD₅₀ of $50 \pm 5 \mu\text{M}$ FUDR, while the RH parental parasites had an LD₅₀ of $2.0 \pm 0.5 \mu\text{M}$ FUDR, (25-fold less than that of the Ui parasites, Fig. 4.1A). The high FDUR tolerance exhibited by the Ui parasites indicated that the *UPRT* was down-regulated in these parasites. The RH and Ui parasites showed LD₅₀ values of 40 ± 8 and $28 \pm 5 \mu\text{M}$ 6-thioxanthine, respectively. Both Ui and

RH were apparently sensitive to 6-thioxanthine, indicating that *HXGPRT* was not affected by the expression of the *dsUPRT* (Fig 4.1B).

4.3.2 Detection of *in vivo* produced double-stranded RNA homologous to uracil phosphoribosyl transferase

The p30/11UP30/11 plasmid was engineered to express *dsUPRT* in order to specifically silence the *UPRT* gene, presumably by an RNAi induced degradation of the target mRNA. It was therefore important to first investigate whether the *dsUPRT* was produced by the *Ui* parasites. Our attempts to detect the *dsUPRT* or its intermediates by northern blot analysis were not successful although large amounts (up to 25 µg) of total RNA were used. We thus used an RT-PCR procedure to detect the sense and the antisense RNA of the *dsUPRT*. When the sense strand of the *UPRT* gene was selected for analysis of expression during the RT reactions, PCR products of the expected size (724 bp) were detected for both the RH and *Ui* parasites (Fig. 4.2, lanes 4 and 5, respectively). When the antisense strand of the *UPRT* gene was analyzed during the RT reactions, no products were obtained for the wild type parasites (Fig. 4.2, lane 6). These results thus indicated that no antisense *UPRT* mRNA was naturally expressed. A PCR band of the expected size (724 bp) was revealed in samples isolated from the transformed parasites (lane 7), indicating that only the *Ui* parasites, but not the RH parasites, expressed both the sense and the antisense RNAs of the *UPRT* gene. To rule out the presence of genomic DNA contamination, control experiments were conducted where the total RNA preparations were directly subjected to PCR. No

products were detected from the RNA samples of both strains of the parasites (Fig. 4.2, lanes 1 and 2).

4.3.3 Measurement of the steady state levels of the uracil phosphoribosyl transferase transcript

The steady state levels of the *UPRT* mRNA were assessed in the transgenic *Ui* parasites, in comparison to the wild type strain. Total RNA was isolated from the RH and *Ui* parasites and subjected to northern blot analysis. When the *UPRT* specific probe was utilized, the hybridization signal revealed a single 2.2 kb band corresponding to the *UPRT* transcript in the RNA sample isolated from the RH parasites (upper panel, RH, Fig. 4.3). No signal was detected in the RNA sample from the *Ui* parasites (upper panel, *Ui*, Fig. 4.3). The undetectable *UPRT* mRNA levels in the *Ui* parasites confirmed that the corresponding gene was specifically down-regulated by the action of the *dsUPRT*. To ensure that equivalent amounts of RNA were used, the blot was stripped and re-probed for the house-keeping gene *ROP1*. The probe specific to *ROP1* revealed a single 2.1 kb band of equivalent intensity from both RNA samples (lower panel, Fig 4.3).

4.3.4 Assessment of the uracil phosphoribosyl transferase activity

In order to confirm that the attenuation of the *UPRT* expression caused lowered level of gene products, the *UPRT* activity of the *Ui* parasites was monitored and compared to that of the parental parasites. The wild type parasites

were able to assimilate ^3H -uracil at a value of 23952 ± 3594 cpm (RH, Fig. 4.4). The Ui parasites could still incorporate uracil at a value of 1138 ± 107 cpm, (Ui, Fig. 4.4). The low ^3H -uracil uptake by the Ui parasites indicated that the UPRT activity was inhibited. The repressed UPRT activity was in concordance with the FDUR^r phenotype of the Ui parasites.

4.3.5 Analysis of the genomic organization of the parasite line

The down-regulation effect mediated by the dsRNA is likely to be exerted at the post-transcriptional level. Therefore, the gene organization of the targeted gene should remain intact (Sharp, 2001). We consequently examined the genomic arrangement of the Ui parasite line. Genomic DNA isolated from the parasite line and parental parasites were digested with *EcoRI* or *BamHI* restriction endonucleases and subjected to Southern blot analysis. When the *UPRT* specific probe was used for detection, 4.8 and 13.4 kb bands corresponding to the digested *UPRT* genomic locus were revealed for the RH genomic DNA samples digested with *EcoRI* and *BamHI*, respectively (Fig. 4.5, lanes 1, 3 and 4, 6, respectively). In the samples from the transgenic parasite line, an additional band was revealed for each digestion (lanes 2 and 5). We speculated that the additional band could be derived from the plasmid used for generating the parasite line. To verify this speculation, trace amounts of the plasmid p30/11Up30/11 were mixed with genomic DNA from the RH parasites and then digested with same restriction endonucleases. The digestion products were resolved alongside the samples described earlier (lanes 1-6 vs. lanes 7-10). The digestion pattern for the plasmid

and RH genomic DNA mixtures was identical to those of the Ui genomic DNA (lanes 7 and 8). In addition, the sizes of the additional lower bands were identical to those of the digested plasmid (lanes 9 and 10). This demonstrated that these bands were derived from plasmid p30/11Up30/11.

4.3.6 Stability of the parasite line in the absence of 5-fluoro-2'-deoxyuridine

Southern blot analysis suggested that the transforming plasmid did not undergo genomic integration but was rather maintained as extra-chromosomal DNA. It thus was interesting to investigate whether this plasmid would persist after the withdrawal of FDUR from the parasite culturing medium.

4.3.6.1 Analysis of genomic DNA from different propagations of the parasite line

The stability of the Ui parasites with the FDUR^r phenotype was examined during propagation. The parasites were continuously cultured onto HFF monolayers with no FDUR. In addition, a control set of the Ui parasites was similarly propagated but in the presence of media supplemented with the FDUR. The initial Ui parasites maintained in the presence of the FDUR was termed passage zero (P0). The parasites from each passage were harvested and their DNAs were purified and subjected to Southern blot analysis. Using the *UPRT* probe for detection, two bands of 13.4 kb and 4.8 kb were revealed for the sample from P0 (Fig. 4.6, lanes 1 and 6). In order to estimate the amount of the plasmid

(the 4.8 kb band) maintained in each passage, the signals from the plasmid as well as the genomic locus band were quantified. The ratio of light units from the plasmid signal to that from the genomic band from the same sample ($I_{5\text{-kb}}/I_{13.5\text{-kb}}$) was calculated for all passages. To standardize the analysis, the $I_{5\text{-kb}}/I_{13.5\text{-kb}}$ values were normalized so that the value obtained from P0 was almost one. The control P0 passages grown in the presence of FDUR (P0, lanes 1 and 6, Fig. 4.6A) showed a normalized ratio of 1.1 ± 0.1 . This value decreased gradually as the passage number increased until it was almost or equal to zero for P8 and P10 (P8 and P10, Fig. 4.6B). The 4.8 kb plasmid band gradually disappeared during passage in the absence of the FDUR until it was undetectable for P8 and P10 (P8 and P10, Fig. 4.6A). When 10^4 parasites from P10 were used to infect HFF grown in media containing 5 μM FDUR, the parasites were not able to lyse their host indicating that these parasites were no longer FDUR^r. Thus, the transformed parasites maintained the plasmid under a selection pressure. Without this selection pressure, approximately 20% of the plasmid was lost per passage (Fig. 4.6B).

4.3.6.2 Transformation using genomic DNA from the parasite line and plasmid rescue

To confirm that the transformed plasmid was maintained as episomal DNA, a plasmid rescue experiment was performed. Different amounts (10 to 20 μg) of isolated DNA from the P0 parasites were used in the transformation of competent *E. coli*, XL-1 Blue strain. Approximately 2.9 ± 0.3 cfu/ μg DNA of

ampicillin-resistant *E. coli* colonies were obtained from two independent experiments.

4.3.6.3 Correlation of the steady state levels of the uracil phosphoribosyl transferase transcript and the homologous double-stranded RNA

We then investigated the steady state levels of the expressed *dsUPRT* and its homologous mRNA throughout sequential passages. The level of the *dsUPRT* produced in the P0 transformed parasites was quantified in forms of either sense or antisense RNAs (as described in the experimental procedures). Figure 4.7A shows an image of a typical agarose gel resolving the PCR products from the QC-RT-PCR, in which the intensities of the sense or antisense *UPRT* RNA bands (242 bp) are inversely proportional to the concentrations of the RNA standard. The intensities of the standard RNA band vs. the band of *dsUPRT* (as either the sense or antisense RNA) measured for each reaction were subsequently calculated to obtain a ratio. The log values of the ratios were then plotted vs. the log of the RNA standard amounts. Figure 4.7 (Panels B and C) shows the plots for the estimation of the amounts of the sense and the antisense RNA respectively. The amounts of expressed dsRNA in the form of either antisense or sense RNA were determined from the fitted equations, when $y = 0$ or when the ratio of the band intensities (standard vs. sense or antisense) equals to one as per Hayward-Lester *et al.*, 1996. When the sense RNA was selected for analysis of expression by QC-RT-PCR, the amount of the sense RNA was estimated at 120.4 ± 9.6 fg/ μ g

μg total RNA were isolated from 10^4 parasites. Similarly, when the antisense RNA was the RNA selected for analysis by QC-RT-PCR, the amount of the antisense RNA was estimated to be $57.9 \pm 9.4 \text{ fg}/\mu\text{g}$ total RNA or approximately 8 ± 1 copies per parasite (Fig. 4.7C). Due to the residual trace amounts of the endogenous mRNA that would have also been amplified with the RT-PCR, the level of the sense strand is higher than that of the antisense strand. It is therefore estimated that approximately 8 ± 1 copies of dsRNA were maintained at steady state conditions by the P0 per parasite and were actually enough to confer FDUR resistance. The amount of the *dsUPRT* expressed in each passage was estimated as such by QC-RT-PCR based on the level of antisense *UPRT* RNA detected. The graphical representation and its linear equation for the determination of the *dsUPRT* expressed in the P3 and P5 parasites are depicted in Fig. 4.8A and 4.8B, respectively. The estimated copy numbers of the dsRNA were recalculated per μg of total RNA in order to take into account the difference in the RNA yields between passages (Fig. 4.9A). Approximately 6.38×10^5 dsRNA copies per μg of total RNA were expressed in the P0 transformed parasites, 3.12×10^5 dsRNA copies per μg of total RNA in the P3 parasites, and 1.18×10^5 dsRNA copies per μg of total RNA in the P5 parasites. As for P7 and P9, the *dsUPRT* amounts were at non-detectable levels (Fig. 9A).

The steady state levels of the *UPRT* mRNA in each passage or propagation were assessed by dot blot analyses. The blots were first probed with the *UPRT* specific then stripped and re-probed with the *ROP1* specific probe. The relative amounts of the mRNAs in the total RNA were consequently estimated from the

quantified signals which were revealed by the individual probes. The *UPRT* specific probe revealed the hybridization signals for samples of the P0, P7 and P9. Comparable hybridization signals were revealed for all samples on the dot blot when the *ROP1* specific probe was used (Fig. 4.9B, the inset). In order to standardize for the amounts of the *UPRT* mRNA for each sample, the ratios of the *UPRT/ROP1* signals were calculated and used for comparison. Since there were no signals detected for passages 0, 1 and 3 using the *UPRT* specific probe (Fig. 4.8B, the inset), the *UPRT/ROP1* ratios were calculated as zero. The *UPRT/ROP1* ratios of the tested samples were all depicted in a histogram (Fig. 4.9B). The histogram shows that the P0 parasites had equivalent amounts of the *UPRT* mRNA and the *ROP1* mRNA (*UPRT/ROP1* ratio of one). The P9 parasites exhibited an unusually high *UPRT* level as compared to that of the *ROP1*. When the profile of the *UPRT* mRNA levels was compared to that of the dsRNA expressed (Fig. 4.9A vs. 4.9B), it was evident that the amounts of the *UPRT* mRNA and the *dsUPRT* expressed were inversely proportional. The higher the level of the expressed *dsUPRT*, the lower the level of the *UPRT* mRNA was (P0, P3 and P5). On the other hand, when the *dsUPRT* level was negligible, the level of the *UPRT* mRNA was as high as those of the RH strain which has an intact *UPRT* expression (P7 and P10).

4.4 DISCUSSION

In this chapter, we described the generation and characterization of a stable transgenic *T. gondii* parasite line expressing *dsUPRT*, called Ui. We

demonstrated that *dsUPRT* was expressed and could alter the pattern of *T. gondii* *UPRT* gene expression. The Ui parasites exhibited FDUR resistance (FDUR^r) phenotype. The down-regulated expression of the *dsUPRT* was sufficient to confer resistance to FDUR. The FDUR^r was a direct result of the lower steady state level of the *UPRT* mRNA in the transformed parasites as compared to that of the RH wild type strain (Fig. 4.3). It is likely that the expressed *dsUPRT* could induce the degradation of the *UPRT* mRNA, giving rise to the decreased UPRT activity.

Further characterization of the Ui parasites revealed interesting features. First, these parasites expressing *dsUPRT* seemed to maintain a putative extra-chromosomal DNA. Southern blot analysis using the *UPRT* specific probe showed a DNA fragment of approximately 4.8 kb only in the Ui parasites (Fig. 4.5). This interesting finding prompted us to investigate whether the Ui parasites expressing the dsRNA might behave similarly to transformed *E. coli*. When grown in the absence of a selection pressure, the cultured *E. coli* loses the transforming plasmid which harbors the resistance gene for the used compound. The FDUR was therefore removed from the culture media of the Ui parasites. Interestingly, the putative DNA fragment gradually disappeared through propagations of the parasite line. When the DNA isolated from the Ui parasites grown under the selection pressure was introduced into competent *E. coli*, a number of ampicillin resistant colonies were formed, further confirming that the putative DNA fragment corresponds to the transforming plasmid. The plasmids which were rescued from the parasite line were probably modified in such a way

that the ORF was recognized by both bacteria and *T. gondii*. Thus, the plasmids were accommodated, replicated and expressed in both organisms. It will be useful to develop the plasmid(s) into a versatile episomal shuttle vector such as that previously reported by Black and Boothroyd (Black and Boothroyd, 1998). This episomal shuttle vector could then be used as a transforming vector that would replicate independently without any interruption of the genomic arrangement of *T. gondii*.

Secondly, the expression of the *dsUPRT* in the parasite line maintained its 'FDUR' phenotype. Although the dsRNA expression could not be detected by northern blot analysis, QC-RT-PCR was used to individually estimate the amount of both the sense and antisense RNAs. The estimated amounts of antisense RNA were used to represent the stoichiometric ratios of the dsRNA expressed in each parasite passage. The estimated amount of the dsRNA expressed in the transformed parasites decreased progressively with each passage. This was in concordance with the gradual disappearance of the putative extra-chromosomal DNA. This correlation suggests that the extra-chromosomal DNA is the template for the synthesis of the dsRNA homologous to the *UPRT* mRNA. A low amount of the DNA template would result in an insufficient amount of the expressed dsRNA to trigger the degradation of the *UPRT* mRNA (*i.e.* passages 7 to 10, Fig. 4.6). For example, the P5 parasites carried the transforming plasmid at approximately 50% of the amount maintained in the P0 transformed parasites (Fig. 4.6B). The P5 parasites produced approximately 1.18×10^5 dsRNA copies per μg of total RNA (Fig. 4.8A) or 2 copies of dsRNA per parasite. The *UPRT*

mRNA of the P5 parasites was kept at a very low or almost non-detectable level (Fig. 4.9B and the inset). We could therefore deduce that at least 2 copies of dsRNA should be intracellularly maintained by *T. gondii* to confer the FDUR^r phenotype (Fig. 4.9A).

In this study, we demonstrated that intracellular dsRNA could down-regulate the expression of the homologous gene in *T. gondii*. Although the down-regulation effect was fully elucidated, there was no evidence about the involvement of siRNA intermediates. Further studies should aim at investigating whether these dsRNA intermediates are produced in *T. gondii*.

Figure 4.1

Tolerance of the parasite line to 5-fluoro-2'-deoxyuridine

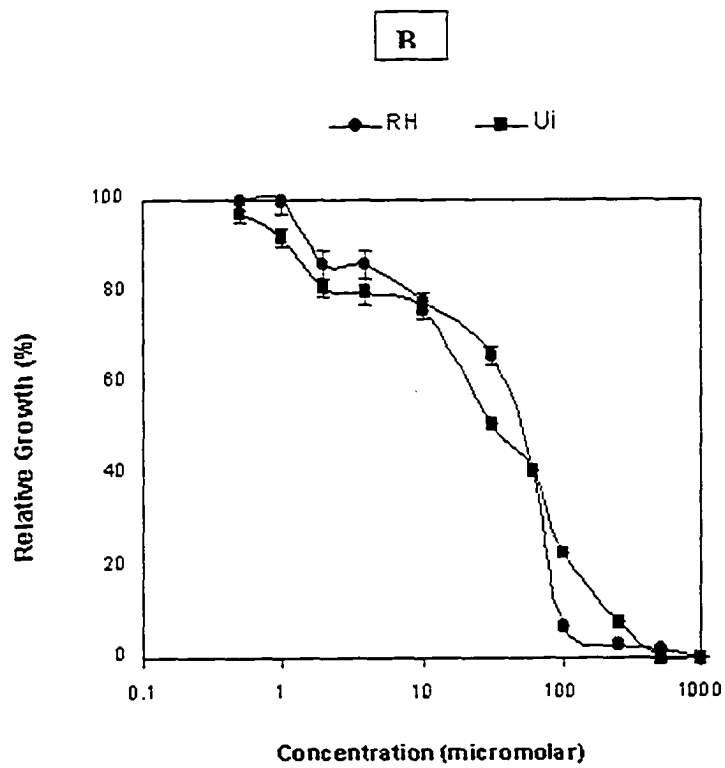
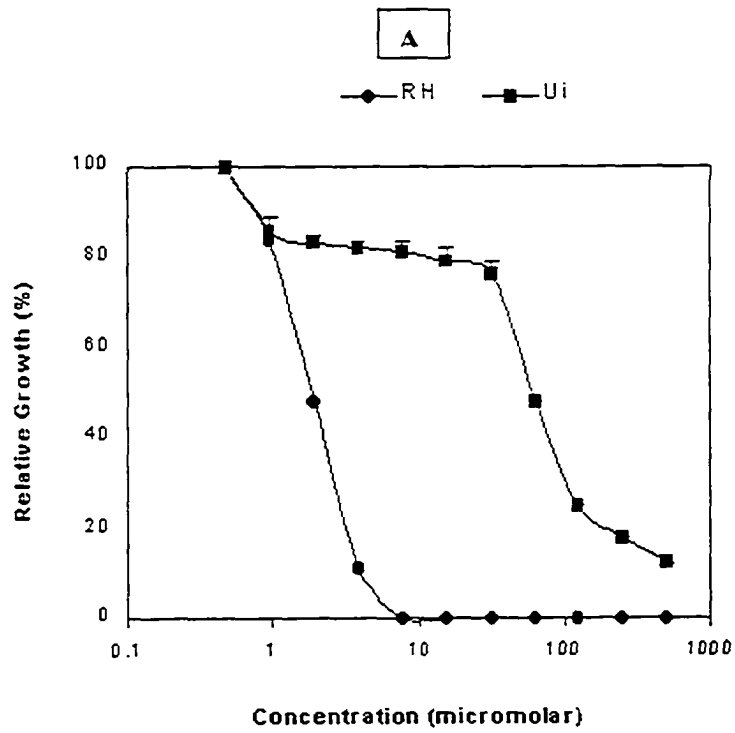


Figure 4.1. The growth of RH and Ui parasites was monitored in the presence of either **A:** FDUR or **B:** 6-thioxanthine. The media were supplemented with various concentrations of either FDUR or 6-thioxanthine. The LD₅₀ values were deduced from plotting the (%) growth of parasites as function of the concentration of the tested compound. The LD₅₀ values for FDUR are 50 ± 5 and 2.0 ± 0.5 μM for the Ui and RH wild type, respectively. The LD₅₀ values for 6-thioxanthine are 28 ± 5 and 40 ± 8 μM for the Ui and RH, respectively.

Figure 4.2

Detection of the expression of double-stranded RNA homologous to uracil phosphoribosyl transferase in the parasite line

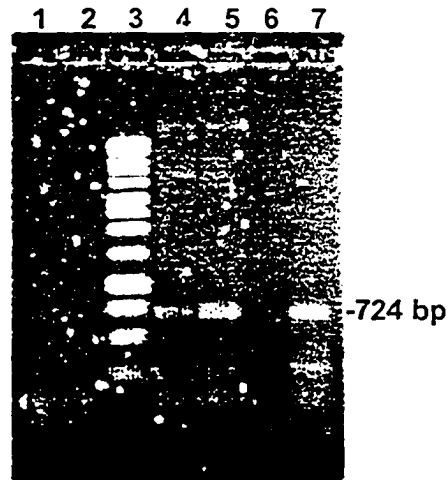


Figure 4.2. An image of the agarose gel resolution of the PCR and RT-PCR products. The PCR products from the amplifications using *AgeIUP* and *BamHIUP* primers and total RNAs isolated from the RH strain and the P0 transformed parasites are in lanes 1 and 2, respectively. The expected size of the band was 724 bp when this primer pair was used. The 1-kb DNA marker is in lane 3. The RT-PCR products are in lanes 4 to 7. Lanes 4 and 6 are the RT-PCR products amplified from the sample isolated from the RH strain. Lanes 5 and 7 are the RT-PCR products amplified from the sample isolated from the P0 transformed parasites. The oligonucleotide *AgeIUP* was used during the RT step for the samples in lanes 4 and 5, while the oligonucleotide *BamHIUP* was used during the RT step for the samples in lanes 6 and 7.

Figure 4.3

**Assessment of uracil phosphoribosyl transferase transcript steady state
level in the parasite line**

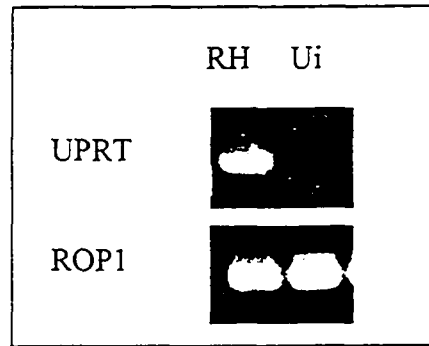


Figure 4.3. Total RNA samples isolated from Ui and RH parasites were subjected to northern blot analysis using either *UPRT* or *ROPI1* as probes to reveal the steady state level of the transcripts encoding *UPRT* and *ROPI1*, respectively.

Figure 4.4

Uracil phosphoribosyl transferase activity and the uracil uptake assay

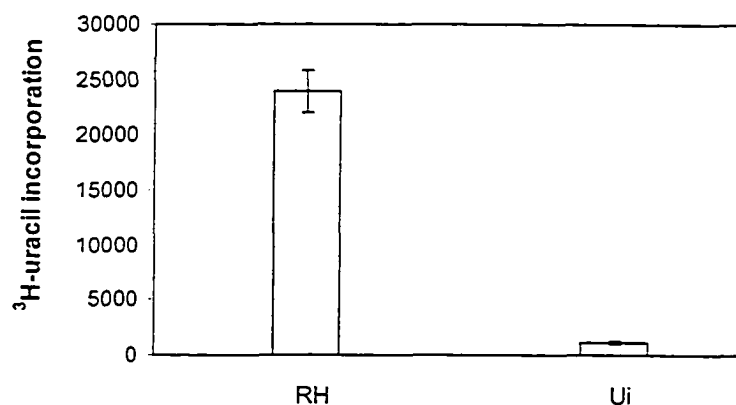


Figure 4.4. The level of ³H-uracil assimilated by intracellular *T. gondii* was measured to verify the enzymatic activity of UPRT in parasites expressing dsUPRT (Ui, 1138 ± 107 cpm) and the wild type parasite (RH, 23,952 ± 3594 cpm). At least three independent experiments were performed. The error bars represent deviation from the mean.

Figure 4.5

Analysis of the genomic organization of the parasite line

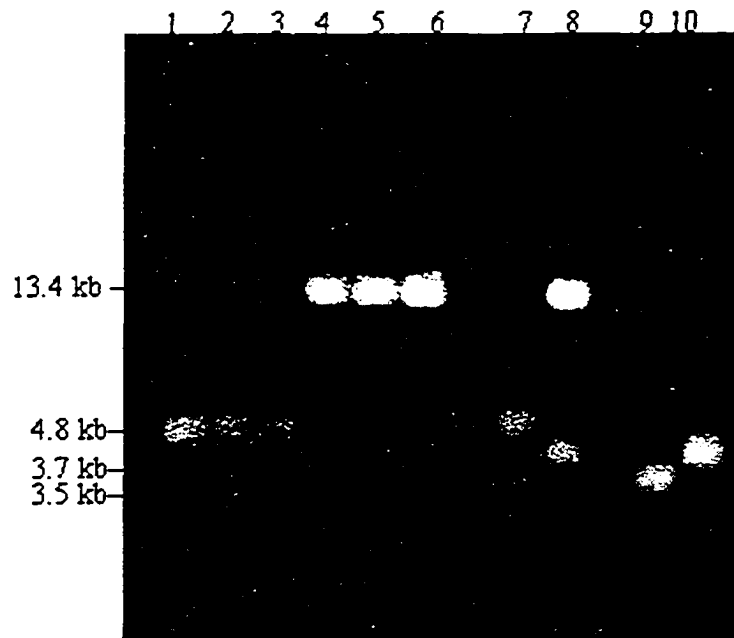


Figure 4.5. Genomic DNA isolated from RH wild type parasites and the Ui parasites were digested with either *EcoRI* or *BamHI* and subjected to southern blot analysis. The bands were revealed by using a *UPRT* probe. The numbers on the left indicate the estimated sizes of DNA fragments in kb. Lanes 1 to 3 are *EcoRI* -digested samples of the RH, Ui and RH parasites, respectively. Lanes 4-6 are *BamHI* -digested samples of RH, Ui and RH, respectively. Lanes 7 and 8 are *EcoRI* and *BamHI* digested DNA mixtures of genomic DNA isolated from the RH wild type and plasmid p30/11Up30/11. Lanes 9 and 10 are *EcoRI* and *BamHI* digested DNA of plasmid p30/11Up30/11.

Figure 4.6

Stability of the parasite line in the absence of 5-fluoro-2'-deoxyuridine

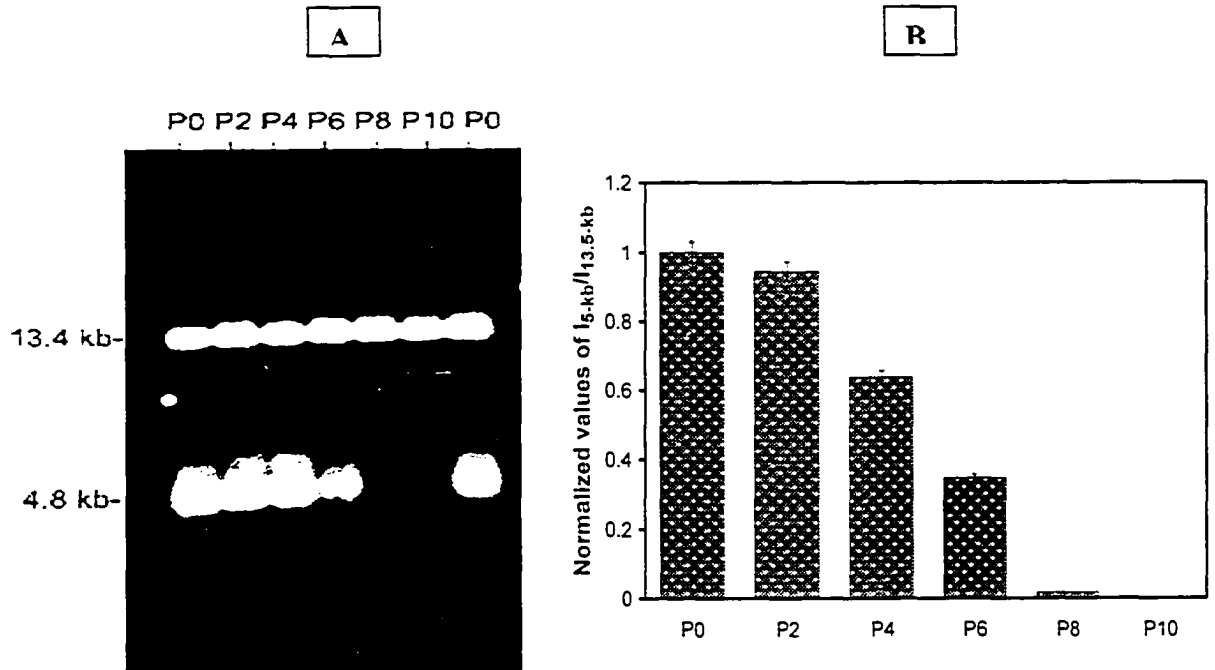


Figure 4.6. A. An image of a Southern blot in which hybridization signals were revealed using the *UPRT* probe. The DNA was isolated from *Ui* parasites grown in the absence of the FDUR for 10 passages (P2 to P10), and then digested with *Bam*HI. The control (P0) was the transformed parasites grown in the presence of FDUR. **B.** Quantitative analysis of the band patterns shown in A. The chemiluminescence light units of the lower band were quantified relative to the upper band; the values were normalized so that the value obtained from P0 was equivalent to one.

Figure 4.7

Measurement of the expression level of the double-stranded RNA homologous to uracil phosphoribosyl transferase in the parasite line

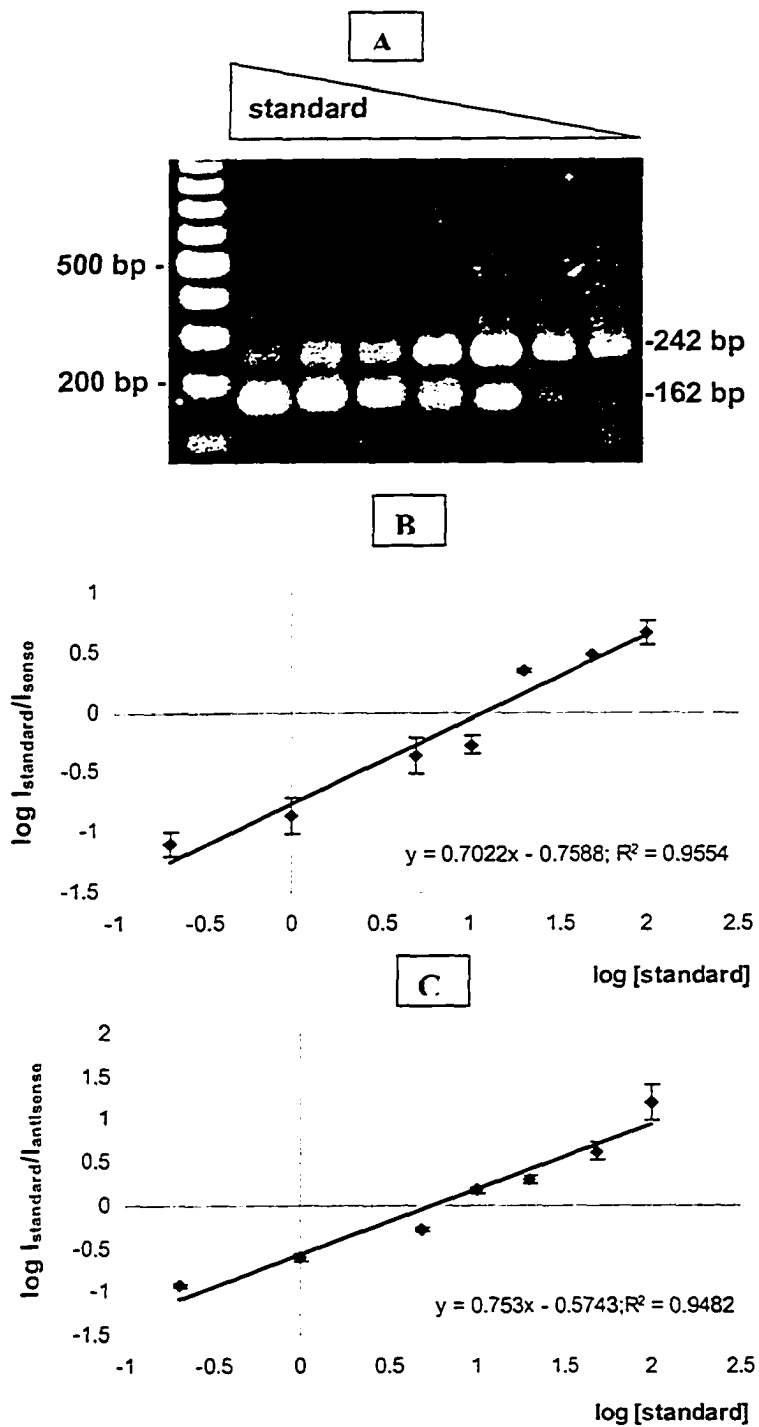


Figure 4.7. A. Image of an agarose gel resolution of typical competitive RT-PCR products. Fixed amounts of total RNA isolated from the P0 transformed parasites were mixed with decreasing amounts of the RNA standard and subjected to RT-PCR. The sizes of the expected bands were 162 and 242 bp for the internal RNA standard and the target RNA, respectively. **B and C.** A graphical representation and its linear equation used in the estimation of the sense RNA (**B**) or antisense RNA (**C**) of the *dsUPRT* produced by the P0 transformed parasites. The intensities of the band of either the sense RNA or antisense RNA and of the standard RNA band resolved by the agarose gel electrophoresis were quantified and calculated for each reaction to obtain a ratio ($I_{\text{standard}}/I_{\text{sense or antisense}}$). The log values of the ratios were then plotted vs. the log of the RNA standard amounts. Approximately 120.4 ± 9.6 fg of the sense RNA (**B**) and 57.9 ± 9.4 fg of the antisense RNA (**C**) were detected in one μg of total RNA isolated from the P0 parasites.

Figure 4.8

Measurement of the expression level of the double-stranded RNA homologous to uracil phosphoribosyl transferase in different propagations of the parasite line in the absence of 5-fluoro-2'-deoxyuridine

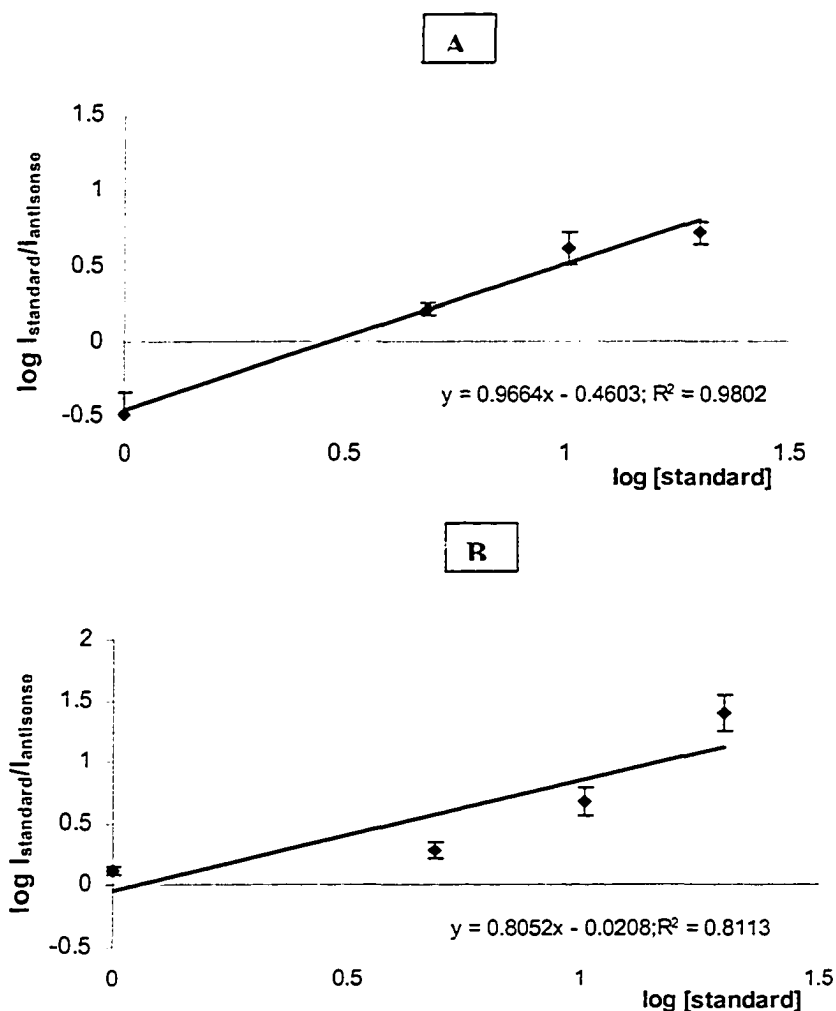


Figure 4.8. A graphical representation and its linear equation used in the estimation of the antisense RNA produced by the third propagation P3 of the parasite line in the absence of FDUR. Approximately 26.9 ± 4.4 fg (A) and 9.6 ± 1.6 (B) of the antisense RNA were detected in one μ g of total RNA isolated from the P3 and P5 parasites, respectively.

Figure 4.9

The correlation of the uracil phosphoribosyl transferase transcript and homologous double-stranded RNA expression levels

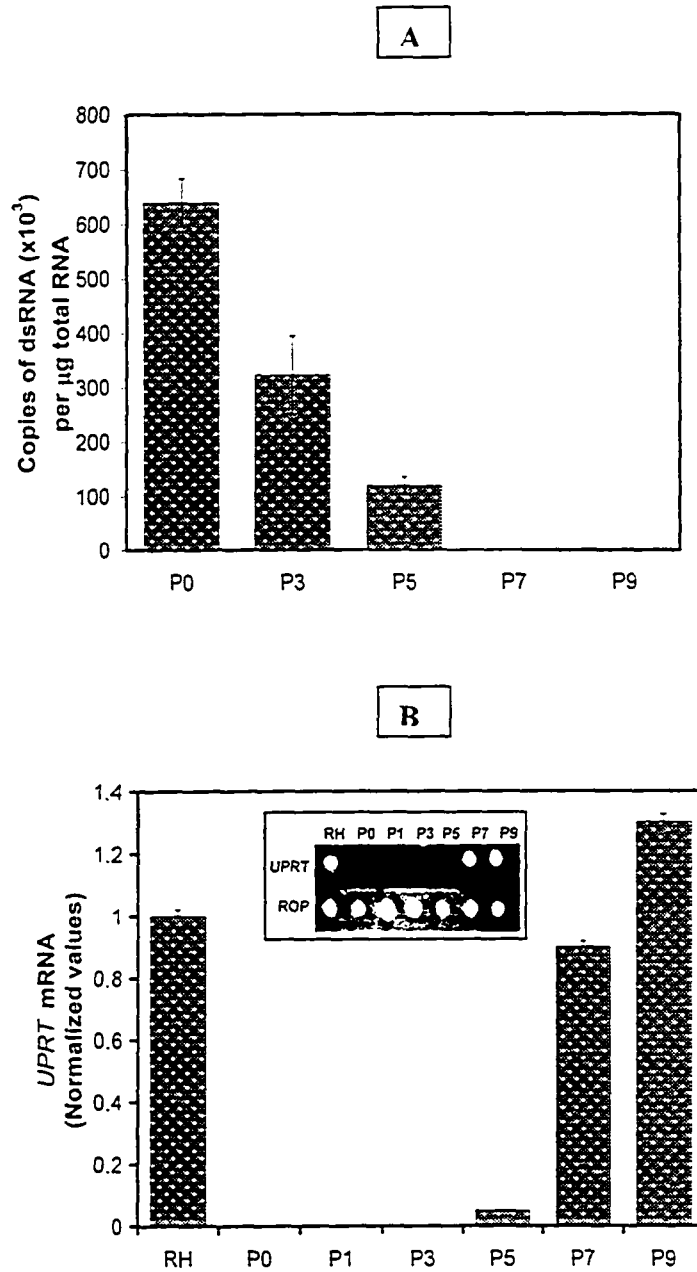


Figure 4.9. The levels of the double-stranded RNA and mRNA corresponding to the uracil phosphoribosyl transferase gene. **A.** The histogram illustrates the difference in the copy number of dsRNA produced by the transformed parasites (P0) and subsequent passages without the selection pressure (P3 to P9). **B.** The histogram shows the normalized level of the *UPRT* mRNA revealed using the dot blot analysis which was hybridized to probes specific to *UPRT* and *ROPI*. The inset is an image of a dot blot revealed by the individual probes.

CHAPTER 5
FUNCTIONAL ANALYSIS OF LACTATE DEHYDROGENASES IN
TOXOPLASMA GONDII

SUMMARY

In *Toxoplasma gondii*, lactate dehydrogenase is encoded by two independent and developmentally regulated genes *LDH1* and *LDH2*. These genes and their products have been implicated in the control of a metabolic flux during parasite differentiation. In order to investigate the significance of *LDH1* and *LDH2* in this process, we generated stable transgenic parasite lines in which the expression of these two expressed isoforms of lactate dehydrogenase was knocked down in a stage-specific manner. These *LDH* knock-down parasites exhibited variable growth rates in either the tachyzoite or the bradyzoite stage, as compared to the parental parasites. Their differentiation processes were impaired when the parasites were grown under *in vitro* conditions. *In vivo* studies in a murine model system revealed that tachyzoites of these parasite lines were unable to form significant number of tissue cysts and to establish a chronic infection. Importantly, all mice which were initially infected with tachyzoites of either of the four *LDH* knock-down lines survived a subsequent challenge with tachyzoites of the parental parasites (10^4), a dose that usually causes 100% mortality, suggesting that live vaccination of mice with the *LDH* knock-down tachyzoites can confer protection against *T. gondii*. Thus, we conclude that *LDH* expression is essential for parasite differentiation. The knock-down of *LDH1* and *LDH2*

expression gave rise to virulence-attenuated parasites that were unable to exhibit a significant brain cyst burden in a murine model of chronic infection.

5.1 INTRODUCTION

Lactate dehydrogenase (LDH) is a glycolytic enzyme that catalyzes the interconversion of pyruvate to lactate. This enzyme plays an indispensable role when glycolysis becomes the only pathway to provide energy under anaerobic conditions (Kavanagh *et al.*, 2000). LDH is considered as a potential anti-parasitic drug target because its unique structural and kinetic properties differ from those of human host cells (Kavanagh *et al.*, 2000, Dando *et al.*, 2001, Winter *et al.*, 2003). Among reported LDH sequences, those of *T. gondii* and all members of the *Plasmodium* genus carry a pentapeptide insertion into the enzyme active site (Winter *et al.*, 2003). The activity of LDHs is generally inhibited by an excess of pyruvate. However, this property is greatly reduced in *Plasmodium*- and *Toxoplasma* LDHs (Dando *et al.*, 2001, Winter *et al.*, 2003).

In *T. gondii*, two LDH isoforms are present; LDH1 and LDH2. The genes encoding the isoforms show 64% nucleotide sequence identity, and their gene products share 71% amino acid sequence identity (Parmley *et al.*, 1995). The genes encoding LDH1 and LDH2 isoforms are developmentally regulated. The mRNA of *LDH2* is detected in the bradyzoite stage only, while the transcript of *LDH1* is found in both bradyzoites and tachyzoites. The *LDH1* gene product is only expressed in tachyzoites, while that of *LDH2* is expressed in only bradyzoites. It is speculated that LDH1 is replaced by LDH2 during development

from tachyzoites to bradyzoites as a consequence of post-transcriptional induction of *LDH2* (Parmley *et al.*, 1995, Yang and Parmley, 1997). During differentiation, *T. gondii* modifies its morphology and energy metabolism to adapt to its surrounding environment. Aerobic respiration and glycolysis are functional in tachyzoites, while glycolysis is the only energy source in bradyzoites (Dando *et al.*, 2001, Denton *et al.*, 1996). Therefore, LDH, which is important for anaerobic respiration, might be a promising target for developing drugs for chronic toxoplasmosis.

Over the last few years, effective methods of transfection and targeted disruption of genes has made *T. gondii* amenable to genetic manipulations (Black and Boothroyd, 1998, Donald and Roos, 1998). In addition to these conventional gene manipulations, we previously reported that the introduction of double-stranded RNA (dsRNA) can lower the expression of *T. gondii* genes (Al-Anouti and Ananvoranich, 2002, Al-Anouti *et al.*, 2003, Chapter 3). In this study, we report the first success in knocking-down the expression of the essential genes *LDH1* and *LDH2* in *T. gondii*. Significantly, we have provided the evidence that the expression of *LDH1* and *LDH2* is essential for parasite development. The knock-down of *LDH1* and *LDH2* expression gave rise to virulence-attenuated parasites that were unable to exhibit a significant brain cyst burden in a murine model of chronic infection.

5.2 Experimental Procedures

5.2.1 *Toxoplasma gondii* and cell culture

All cell and parasite culture experiments were carried out as described in the general methods. Generation of LDH knock-down parasites was performed using the hypoxanthine-xanthine-guanine phosphoribosyl transferase (HXGPRT)-deficient (Δ HXGPRT) *T. gondii*, strain PLK (Roos *et al.*, 1994, AIDS Research and Reference Reagent Program, NIH).

5.2.2 Plasmid construction and transformation

5.2.2.1 Bradyzoite-specific expression plasmids

A DNA fragment (993 bp) encompassing the *LDH2* promoter region, referred to as L2, was amplified by PCR from genomic DNA isolated from *T. gondii* PLK strain using the oligonucleotides *KpnI*LDH2(sense) and LDH2(antisense). The fragment was cloned into pBluescript SK+ (Stratagene) at *KpnI* and a blunted *XhoI* site. The second L2 fragment was produced by PCR using the oligonucleotides *SacI*LDH2(sense) and *XbaI*LDH2(antisense) and was cloned between *SacI* and *XbaI* sites. Portions of *LDH1* and *LDH2* ORF (nucleotides 1-487, accession number U35118 and U23207, respectively) were amplified by PCR from plasmids pMAL-C2-LDH1 and pMAL-C2-LDH2 (obtained from Dr. Parmley, Palo Alto Medical Foundation, CA) and cloned at *SmaI* site. The 1.8 kb HXGPRT minigene was isolated from plasmid pTUB5mycGFPHXGPRT (obtained from Dr. Dominique Soldati, Imperial

College London, UK) by *SacII* digestion and subcloned into the constructed plasmids. The resultant plasmids which had two L2 fragments arranged in a head-to-head fashion flanking *LDH1* and *LDH2* cDNA were named pL2-LDH1-L2 and pL2-LDH2-L2, respectively. The restriction maps of constructed plasmids are depicted in the Appendix.

5.2.2.2 Tachyzoite-specific expression plasmids

The plasmid p30/11UP30/11, which contains the ORF of uracil phosphoribosyl transferase (*UPRT*, Al-Anouti and Ananvoranich, 2002), was removed by digestion with *NsiI* and *AgeI*. The *LDH1* and *LDH2* ORF portions were then cloned separately by blunt end ligation to replace the *UPRT* cDNA. The resultant plasmids had two modified SAG1 promoters arranged in a head-to-head fashion flanking either *LDH1* or *LDH2* coding region. The 1.8 kb HXGPRT minigene was cloned at *SacII* site to give rise to plasmids p30/11LDH130/11 and p30/11LDH230/11. The restriction maps of constructed plasmids are depicted in the Appendix.

5.2.2.3 Generation of stable parasite lines

The resultant plasmids were individually introduced into *PLKΔHXGPRT* parasites by electroporation as described in the general methods. Stable populations were selected using 25 µg/ml mycophenolic acid and 50 µg/ml xanthine which were added to the culture media (Donald and Roos, 1998). Electroporation with p30/11LDH130/11 and pL2LDH1L2 gave rise to transgenic

parasite lines TL1T and BL1B, which produce dsRNA homologous to *LDH1* in the tachyzoite and bradyzoite stage, respectively. Electroporation with p30/11LDH230/11 and pL2LDH2L2 resulted in the generation of parasite lines TL2T and BL2B, which express dsRNA homologous to *LDH2* in the tachyzoite and bradyzoite stage, respectively. Four transgenic parasite lines were generated, namely TL1T, TL2T, BL1B and BL2B. For clarity, T and B refer to the tachyzoite- or the bradyzoite-specific expression, respectively, while L1 and L2 refer to the *LDH1* and *LDH2*, respectively.

5.2.3 Southern and northern blot analysis

Southern and northern blot analysis were performed as explained in the general methods. The digoxigenin (DIG)-labeled DNA probes specific to uracil phosphoribosyl transferase (*UPRT*) and rhoptry protein 1 (*ROP1*) were produced by PCR as described in chapter 3. For the detection of enolase 2 (*ENO2*) mRNA, primers 5ENOx and 3ENOx were used for the synthesis of the *ENO2* specific probe. The oligonucleotides LDH1-5'-UTR and LDH2-5'-UTR specific to *LDH1* and *LDH2* mRNA were synthesized (Sigma Genosys) and subjected to tailing reactions using terminal transferase. The reactions were performed at 37°C for 1 h in a 20 µl volume containing 100 pmol of the oligonucleotide, 25 mM Tris-HCl pH 6.6, 0.2 M potassium cacodylate, 5 mM CoCl₂, 50 µM DIG-dUTP, 0.5 mM dATP and 25 u of terminal deoxynucleotidyl transferase (Roche).

5.2.4 Detection of double-stranded RNA homologous to lactate dehydrogenase by reverse transcription and polymerase chain reaction

Reverse transcription (RT) reactions were carried out under the conditions explained in the general methods. For the detection of *LDH1* antisense RNA, the oligonucleotide LDH-ORF(sense) was used as the RT primer. In parallel, for the detection of *LDH2* antisense RNA, the oligonucleotide LDH2forward was utilized as the RT primer. The subsequent PCR was performed as in the general methods primers [LDH-ORF(sense) and 3LDH-ORF(antisense) for RT-PCR of *LDH1* antisense RNA or LDH2forward and LDH2reverse for RT-PCR of *LDH2* antisense RNA]. Control experiments were conducted by directly subjecting RNA preparations to PCR. The sequences of all primers are listed in Appendix B.

5.2.5 Synthesis of double-stranded RNA and hairpin RNA by *in vitro* transcription

The sequence of T7 RNA polymerase promoter (17 nt long) was incorporated into the 5'-end of the DNA templates by PCR using T7 promoter containing oligonucleotides specific to the targeted genes (Appendix B). For the synthesis of dsRNA homologous to *LDH1* and *LDH2*, plasmids pMAL-C2-LDH1 and pMAL-C2-LDH2 (Parmley and Yang, 1997) were used as templates. For the synthesis of dsRNA homologous to *ROP1*, *UPRT* and *GFP*, pBS-ROP1 (obtained from NIH-AIDS reagents), pUPRT (obtained from Dr. Ullman, Oregon Health and Science University, USA) and pGFP-N1 (Clontech) were used respectively as template plasmids. The primer pairs: T7on5'LDH1 and T7on3'LDH1,

T7on5'LDH2 and T7on3'LDH2, T7on5'ROP1 and T7on3'ROP1, T7on5'UPRT and T7on3'UPRT, and T7on5'GFP and T7on3'GFP were used in individual PCR reactions for the production of the T7 RNA polymerase promoter-bearing DNA templates. Resultant DNA templates were then *in vitro* transcribed into corresponding dsRNAs as explained in the general methods. The dsRNAs homologous to *LDH1* (nt 1-487, accession number U35118), *LDH2* (nt 1-487, U23207), rhoptry protein 1 *ROP1* (nt 1-502, AA037935), uracil phosphoribosyl transferase *UPRT* (nt 1-724, U10246) and green fluorescent protein *GFP* (nt 1-500, AF420592) were obtained. The *ROP1*, *UPRT* and *GFP* genes were used as controls. The *ROP1* gene was chosen because it is an endogenous housekeeping gene that does not share any sequence similarity with *LDH1* nor *LDH2*. The *UPRT* gene was included because it is an endogenous non-essential gene that was successfully knocked-down in previous studies (Al-Anouti and Ananvoranich, 2002, chapter 3). The *GFP* gene was used because it is exogenous and completely unrelated to *T. gondii* genes. The hairpin RNA (hpRNA) is an RNA structure that consists of a 21 bp long RNA duplex with a 5'-hydroxyl terminus and a 2-nt 3'-overhang (McManus *et al.*, 2002). For the synthesis of hpRNA homologous to *LDH1*, the oligonucleotides hpLDH1 and T7 were heated at 95°C for 2 min in a buffer containing 10 mM Tris-HCl pH 8.0 and 10 mM MgCl₂ and were slowly cooled down to allow for annealing. The annealed oligonucleotides were subsequently used to produce hairpin RNA by *in vitro* transcription. Similarly, the oligonucleotides hpLDH2 and T7 were used to produce hairpin RNA homologous to *LDH2*.

5.2.6 Electroporation of double-stranded RNA and measurement of *Toxoplasma gondii* growth

Parasites were freshly harvested from infected HFF cells and subjected to electroporation with dsRNA as explained in the general methods. Parasite growth was subsequently measured by the ³H-uracil or ³H-hypoxanthine incorporation assay as described in Chapter 3.

5.2.7 Immunofluorescence assay

Parasites were inoculated onto HFF monolayers grown on glass slides. Cultures containing tachyzoites were then allowed to grow for 2-3 days, while intracellular bradyzoites were cultured for 4 days before analysis. All experiments were set up in duplicate and repeated at least twice. Cells were fixed with 3% paraformaldehyde in phosphate buffered saline (PBS) for 10 min and then permeabilized with 0.2% Triton X-100 in PBS for 15 min. Cells were then blocked with 3% bovine serum albumin (BSA) in PBS for 1 h at room temperature (Yahiaoui *et al.*, 1999). Slides were then incubated for 1 h with either the rabbit LDH1 or LDH2 antiserum (diluted 1:500). For cyst staining, *Dolichos biflorus* agglutinin conjugated to FITC (diluted 1:300, Sigma) was added for 1 h. After three washes with PBS, cells were incubated for 1 h with goat anti-rabbit IgG conjugated to rhodamine (diluted 1:5000, Molecular Probes). Staining of the nuclei was carried out by incubation in the presence of 4',6-diamidino-2-phenylindole (DAPI, Sigma) for 1 h, and three washings with PBS (Yahiaoui *et al.*, 1999). After drying, slides were overlaid with fluoromount and

examined with a Leica DMIRB microscope. All images were taken with a cooled Q-Imaging CCD camera using the Improvion Openlab software.

5.2.8 Lactate dehydrogenase enzymatic assay

Tachyzoites and bradyzoites (10^7 parasites) were harvested and lysed in 1 ml of a solution containing 50 mM HEPES pH 7.4 containing 20% glycerol, 0.25% Triton X-100 and 0.5 mM PMSF protease inhibitor. Cell-free lysates were obtained by centrifugation for 10 min at 14,000xg, and kept at -80°C until use. Protein concentrations were determined using the Bio-rad protein assay kit (BIO-RAD) with BSA (Promega) as standard. LDH enzymatic assays were carried out at 37°C in a final volume of 1 ml (Denton *et al.*, 1996). Reactions were initiated by the addition of 1.6 mM pyruvate (Sigma) to a mixture containing 100 mM Tris pH 7.4, 200 mM NaCl, 0.2 mg/ml NADH (Sigma), and 30 μg protein extract. All assays were monitored at 340 nm for the change in absorbance related to the change in the concentration of NADH (Denton *et al.*, 1996). To confirm the specificity of the reactions, control assays that lacked protein extracts were carried out.

5.2.9 Polyacrylamide gel electrophoresis and western blot analysis

Approximately 10^7 tachyzoites and bradyzoites were collected and boiled in a sodium dodecyl sulfate (SDS)-loading buffer (6.25 mM Tris-HCl, pH 6.8, 2% SDS, 10% sucrose, 0.05% Bromophenol blue and 1 mM 2-mercaptoethanol) for 10 min. The samples were resolved on a 9% SDS- polyacrylamide gel as in the

general methods, and subsequently transferred to a nitrocellulose membrane by electro-blotting (BIO-RAD) for 2 h at 80 mV (Sambrook, 1989). The blots were then incubated in a solution containing the polyclonal antibody specific to LDH1 or LDH2, for 1 h at room temperature. The secondary antibody (anti-rabbit IgG conjugated to horseradish peroxidase) was subsequently used (Sambrook, 1989). After washing with 20 mM Tris-HCl and 0.3% Tween-20, chemiluminescent detection was performed using the chemi-glow detection kit (Alpha Innotech). Control samples were LDH1 and LDH2 fusion proteins prepared from bacteria harboring plasmids pMAL-C2-LDH1 and pMAL-C2-LDH2. The bacterial cultures were induced with 1 mM isopropyl thiogalactopyranoside (IPTG) for 4 h, and collected (Yang and Parmley, 1997). Crude protein extracts containing LDH1 and LDH2 fusion proteins were obtained after sonication in a buffer containing 100 mM Tris-HCl pH 7.6 and were run along with parasite protein lysates on 9 % SDS-polyacrylamide gels.

5.2.10 Experimental infections in mice

These experiments were performed by Dr. Stanislas Tomavo (Molecular Parasitology and Biological Chemistry, University of Science and Technology, Lille, France). Purified tachyzoites from the parental PLK Δ HXGPRT described above, TL1T, TL2T, BL1B and BL2B were inoculated into groups of 5 female 8-9 week-old BALB/c mice at 10^3 or 10^4 parasites per mouse and monitored until death or survival for one or two months. To check that surviving mice were infected and immune response had developed in the infected mice, the serum of

each mouse was tested against the total extract antigens prepared from the parental parasites using western blots. In order to assess whether the primary infection of mice with TL1T-, TL2T-, BL1B- and BL2B-tachyzoites conferred protection against the parental parasites, infected mice which survived after 30 days post-inoculation were challenged with the parental parasites (10^4 tachyzoites per mouse) and then monitored for death or survival for 30 days.

In vivo cyst formation was determined by harvesting mouse brain at 8 weeks after infection. Cysts were purified using Percoll gradients. After resuspension of the pellets in PBS in a final volume of 100-200 μ l, the purified cysts were counted using inverted phase microscopy.

5.3 RESULTS

5.3.1 Down-regulation of the expression of lactate dehydrogenase by *in vitro* produced double-stranded RNA

We first verified whether the expression of *LDH1* and *LDH2* can be down-regulated following the introduction of homologous dsRNA. Northern blot analysis was utilized to assess the effect of dsRNA on the target LDH transcript. Equal amounts of tested dsRNAs (4 μ g) specific to *LDH1*, *LDH2*, *ROP1*, *GFP* or *UPRT* were individually introduced into filter-purified parasites by electroporation. At 24 h following electroporation, the total RNAs were isolated and subsequently used for northern blot analysis. A control electroporation (mock) was performed using the buffer lacking dsRNA. When the steady state levels of the constitutively expressed and non-target gene enolase 2 (*ENO2*) were

analyzed by northern blot, single bands were revealed (upper panel, Fig. 5.1). When the *ENO2* probe was removed and the blot was hybridized to the probe specific to *LDH1*, transcripts of 1.8 kb were revealed from all samples. The sample isolated from *LDH1* dsRNA electroporation exhibited relatively less abundance, as compared to other samples (second panel, Fig. 5.1). When the probe specific to *LDH2* was used on the same blot following the *LDH1*-probe removal, no signal was detected in all samples tested (third panel), confirming that *LDH2* was not expressed at this growth stage. Again, the *LDH2* probe was removed prior to the next hybridization. The probe specific to *ROP1* revealed transcripts of approximately 2.1 kb in all samples tested, and the hybridization signal was lower in the sample isolated from *ROP1* dsRNA electroporation (fourth panel, Fig. 5.1). Similarly, the *UPRT* specific probe showed a 2.2 kb band corresponding to *UPRT* transcripts, with the signal of the sample isolated from the *UPRT* dsRNA electroporation having less intensity (bottom panel, Fig. 5.1). Hence, we demonstrated that the down-regulation induced by dsRNA exhibited high specificity toward target genes.

5.3.2 Reduced parasite growth with lowered lactate dehydrogenase expression

We consequently verified whether the lowered expression of *LDH1* or *LDH2* would affect the parasite viability and proliferation. Nucleotide incorporation assays with ³H-uracil or ³H-hypoxanthine were used for this assessment. It has been reported that a single-stranded RNA with a hairpin structure (hpRNA) can

be used in place of dsRNA, to invoke RNAi in other systems (Elbashir *et al.*, 2001 and McManus *et al.*, 2002). Thus, we also designed and synthesized hpRNA containing the sequence specific to the unique region of the *LDH1* or *LDH2* ORF, called hpLDH1 and hpLDH2, respectively. These hpRNAs have the nucleotide sequences homologous to *LDH1* (nt 251-272) and *LDH2* (nt 248-269), respectively. Equal amounts (4 μg) of tested RNAs were individually introduced into the parasites *via* electroporation. After 24 h, the incorporation of ^3H -hypoxanthine or ^3H -uracil was monitored. Mock electroporations with the buffer alone were performed as controls. The mock electroporated parasites were able to infect HFF cells and incorporate both ^3H -hypoxanthine and ^3H -uracil ($64,000 \pm 4900$ and $70,200 \pm 6100$ cpm, respectively, mock, Fig. 5.2A), while the host HFF could not incorporate ^3H -hypoxanthine nor ^3H -uracil (420 ± 17 and 583 ± 12 cpm, respectively, HFF, Fig. 5.2A). Parasites electroporated with dsRNA homologous to *LDH1* assimilated less ^3H -hypoxanthine and ^3H -uracil compared to the mock ($44,400 \pm 3200$ and $42,000 \pm 3500$ cpm, respectively, LDH1 dsRNA, Fig. 5.2A). The reduction in nucleotide assimilation indicated that intact *LDH1* gene expression is needed for optimal parasite growth. In contrast, electroporation with dsRNA homologous to *LDH2* did not lower ^3H -hypoxanthine nor ^3H -uracil incorporation ($62,000 \pm 5800$ and $72,500 \pm 7800$ cpm, respectively, LDH2 dsRNA, Fig. 5.2A), while electroporation with either hpLDH1 or hpLDH2 had no effect on the uptake of both ^3H -hypoxanthine and ^3H -uracil (Fig. 5.2A). An equal amount of dsRNA homologous to *ROP1* was assayed for its effect on parasite growth. The electroporation of dsRNA homologous to *ROP1* had an insignificant

effect on ^3H -hypoxanthine and ^3H -uracil incorporation ($62,000 \pm 7300$ and $64,100 \pm 5100$ cpm, respectively, ROP1 dsRNA, Fig. 5.2A). This is as expected because *ROP1* knockout has no effect on tachyzoite growth (Soldati *et al.*, 1995).

We previously reported that transient down-regulation upon the introduction of *in vitro* synthesized dsRNA is dose-dependent (Al-Anouti *et al.*, 2003, Chapter 3). Hence, it was interesting to know whether the effect of *LDH1* down-regulation could be enhanced by increasing the amount of dsRNA. When 10 μg of *LDH1* dsRNA were electroporated into purified tachyzoites, no enhancement of the down-regulation was observed (Fig. 5.2B). When the concentrations of *LDH1* dsRNA were lowered (as low as 0.04 μg), the nucleotide incorporation was similar to that of the mock electroporation, thus indicating that the threshold of *LDH1* knock-down is reached when 4 μg of dsRNA was used (Fig. 5.2B).

5.3.3 Generation of lactate dehydrogenase knock-down parasite lines

In order to investigate the physiological roles of *LDH1* and *LDH2* in parasite development, we primarily aimed to lower *LDH1* expression in a tachyzoite-specific manner, and to lower *LDH2* expression in a bradyzoite-specific manner. The two transgenic parasite lines generated for this purpose were TL1T and BL2B, respectively. However, in order to gain a better insight into the knock-down effect and the *LDH* expression pattern, we generated two additional transgenic parasite lines, BL1B and TL2T. In BL1B, *LDH1* expression was knocked down in the bradyzoite conditions; while in TL2T, *LDH2* expression was

knocked down in the tachyzoite conditions. The data obtained in the following sections pertain to the characterization of the transgenic parasite lines.

5.3.3.1 Analysis of the genomic arrangement of the parasite lines

The genomic arrangement of these transgenic parasite lines were investigated using Southern blot analyses. Figure 5.3A shows a Southern blot analysis using the *LDH1* probe. A 12.2 kb-DNA band was detected in the sample isolated from the parental parasites and digested with *BamHI* (Fig. 5.3A, lane 1). This single band corresponds to the digested genomic locus of the *LDH1* gene. Additional bands were detected in the *BamHI*-digested DNA samples isolated from the transgenic parasite lines (Fig. 5.3A, lanes 2-5). Similar results were obtained when the *PstI*-digested DNA samples were used for the analysis. A single 3 kb band was revealed for the sample isolated from the parental parasites (Fig. 5.3A, lane 6), whereas additional bands were detected for the samples isolated from the transgenic parasite lines (Fig. 5.3A, lanes 7-10). The *LDH1* probe was removed and the blot was hybridized with the *LDH2* probe. A 9.2 kb band of the *BamHI* digested *LDH2* genomic locus was detected in the sample isolated from the parental parasites (Fig. 5.3B, lane 1), indicating no cross-hybridization of the *LDH2* probe to *LDH1* fragment. In addition to this band, the digested samples obtained from the transgenic parasite lines showed extra bands (Fig. 5.3B, lanes 2-5). Likewise, the *PstI* digested samples isolated from the parental parasites showed 3 different bands of 1.3, 1.8 and 2.2 kb in size (Fig. 5.3B, lane 6). The samples isolated from the transgenic parasite lines and digested

with the same restriction endonuclease showed additional random bands (Fig. 5.3B, lanes 7-10). The digestion patterns revealed by the *LDH1* and *LDH2* individual probes indicated that the transgenes, expressing dsRNA, were integrated into the genomes of the parasite lines.

5.3.3.2 Detection of the expression of double-stranded RNA homologous to lactate dehydrogenase and the transcription profile of the target mRNAs in the parasite lines

The constructed plasmids used for the generation of the parasite lines were engineered to express *dsLDH1* or *dsLDH2* in a stage-specific manner. Therefore, it was important to investigate whether the corresponding dsRNA was expressed in the transgenic parasite lines and in a stage-specific fashion as designed. In order to specifically detect the expressed antisense RNA strands of the dsRNAs, total RNA was isolated from tachyzoites or bradyzoites of the transgenic parasite lines and the parental parasites, and then subjected to the RT reactions. The RT reactions were carried out using a specific primer, which allowed only the antisense strands of *LDH1* or *LDH2* to be reverse-transcribed into cDNAs, which were then subjected to PCR. No band of expected size (487 bp) was detected when the samples isolated from the parental parasites were tested, clearly indicating that there was no natural *LDH1* antisense (lanes 2 and 3, Fig. 5.4A) or natural *LDH2* antisense (lanes 8 and 9) present in *T. gondii*. The expected band corresponding to the designed antisense *LDH1* RNA was detected in samples from TL1T-tachyzoites and TL1T-bradyzoites (lanes 4 and 5, Fig.

5.4A) and in BL1B bradyzoites (lane 7). An unexpected band (approximately 200 bp) was detected in BL1B- tachyzoites (lane 6), when the conditions for the specific detection of the antisense *LDH1* RNA were used. The expected band corresponding to the designed antisense *LDH2* RNA was detected in the samples from TL2T-tachyzoites (lane 10) and in BL2B-bradyzoites (lane 13), but not TL2T-bradyzoites (lane 11), BL2B-tachyzoites (lane 12) nor in samples from TL1T and BL1B (not shown). Unexpected bands (400 and 200 bp) were observed in the sample from BL2B-bradyzoite (lane 13). These bands (lanes 6 and 13, Fig. 5.4A) are presumably non-specific PCR products.

The steady state level of the *LDH1* and *LDH2* mRNAs in the knock-down parasite lines were then assessed. The dot blot analyses were performed using *LDH1* and *LDH2* gene specific probes (Fig. 5.4B). The *ROP1* specific probe was used to allow a normalization of signals obtained from *LDH1* and *LDH2* specific probes. For comparison, the ratios of *LDH1/ROP1* and *LDH2/ROP1* were calculated for each sample. It was observed that the ratio between *LDH1/ROP1* remained constant (1/1) for the tachyzoites (T) and bradyzoites (B) of the parental, TL2T and BL2B parasites and for the TL1T-bradyzoites and the BL1B-tachyzoites. It was as expected because *LDH1* mRNA is expressed constitutively in tachyzoites and bradyzoites, although the LDH1 product is formed only in tachyzoites (Parmley *et al.*, 1995). Reduced *LDH1/ROP1* ratios of 1.0/0.26 and 1.0/0.29 were observed for the TL1T-tachyzoites and the BL1B bradyzoites, respectively, indicating gene- and stage-specific knock-down of *LDH1* expression (Fig. 5.4B). When the signals from the *LDH2*-specific probe and *ROP1* probe

were measured and calculated, we detected negligible level of *LDH2* mRNA in the tachyzoites of all parasites including the parental, TL1T, BL1B, TL2T and BL2B parasites (Fig. 5.4B, bottom panel). The calculated ratios of *LDH2/ROP1* were approximately 1/1 for all tested bradyzoites were obtained, except the BL2B-bradyzoites, for which the ratio of *LDH2/ROP1* was 1.0/0.60, indicating that the expression of LDH2 was lowered only in the bradyzoite of BL2B parasite line (Fig. 5.4B).

5.3.3.3 Protein expression and enzymatic activities of lactate dehydrogenases of the parasite lines

In order to monitor the expressed gene products in the parental and knock-down parasite lines, western blot analyses were performed using polyclonal antibodies raised against LDH1 or LDH2 expressed isoforms (Yang and Parmley, 1997). Protein extracts obtained from the tachyzoites of tested parasites were immuno-blotted and incubated with the LDH1 antiserum (Fig. 5.5, upper panel). The lysate of TL1T-tachyzoites showed a decreased level of the expressed LDH1 isoform compared to those of the parental and other parasite lines. (Fig. 5.5, TL1T, upper panel). In parallel, the protein extracts obtained from the bradyzoites were immuno-blotted and incubated with the LDH2 antiserum (Fig. 5.5, lower panel). The extracts of TL2T and BL2B contained less of the LDH2 isoform. No significant difference was detected for the LDH2 expressed isoform in the samples of TL1T- and BL1B-bradyzoites. These findings clearly indicate that the knock-down of *LDH* expression is gene-specific. To further

confirm the attenuation of the LDH protein expression, the LDH enzymatic activity of the generated parasite lines and their parental parasites was compared. Cell-free lysates were prepared from the tachyzoites and bradyzoites of tested parasites. In order to standardize the obtained data, the LDH activity was calculated per mg of protein in the lysate ($\text{nmol}\cdot\text{min}^{-1}\cdot\text{mg}^{-1}$). The values of $809 \pm 142 \text{ nmol}\cdot\text{min}^{-1}\cdot\text{mg}^{-1}$ and $2730 \pm 529 \text{ nmol}\cdot\text{min}^{-1}\cdot\text{mg}^{-1}$ were obtained for the tachyzoites and bradyzoites of the parental parasites, respectively. The LDH activity of TL1T-tachyzoites was $349 \pm 68 \text{ nmol}\cdot\text{min}^{-1}\cdot\text{mg}^{-1}$ and significantly lower than those of the parental parasites. The values of 763 ± 124 , 794 ± 138 , and $738 \pm 132 \text{ nmol}\cdot\text{min}^{-1}\cdot\text{mg}^{-1}$ were obtained for the tachyzoites of TL2T, BL1B and BL2B parasite lines. The bradyzoite extracts showed a LDH activity of the values 1482 ± 232 and $2730 \pm 529 \text{ nmol}\cdot\text{min}^{-1}\cdot\text{mg}^{-1}$ for the BL2B and parental parasites, respectively. The TL1T-, TL2T- and BL1B-bradyzoites exhibited values of 2712 ± 518 , 2059 ± 502 and $3008 \pm 635 \text{ nmol}\cdot\text{min}^{-1}\cdot\text{mg}^{-1}$, respectively. These values are similar to that of the parental parasites. The human LDH is a secreted protein and its activity can therefore be detected in the cell media (Jijakli *et al.*, 1996). We thus tested whether the obtained data were partly derived from the secreted LDH upon cell lysis. The LDH assays were conducted using the parasite washes (i.e. prior to cell lysate preparation), and showed negligible values, indicating no host LDH contamination.

5.3.3.4 Phenotypic studies of the lactate dehydrogenase knock-down parasite lines

To characterize the phenotype of the *LDH* knock-down parasite lines, we examined the multiplication rates of tachyzoites and bradyzoites. Since *T. gondii* divides by a unique binary division, the number of parasites per vacuole reflects the division rate. The parental-, BL1B-, TL2T- and BL2B-tachyzoites multiplied at similar rates, of which 8 and 64 parasites/vacuole were obtained for most vacuoles, at times 48 and 96 h after infection (Fig. 5.6A and 5.6B, respectively). TL1T-tachyzoites grew more slowly. Values of 2 and 8 parasites/vacuoles at 48 and 96 h post-infection were scored. Under bradyzoite growth conditions, 32 parasites/vacuole were counted in most vacuoles of the parental parasites (Fig. 5.6C). It was detected that 8 parasites/vacuole for BL2B- and TL1T-bradyzoites and 26 parasites/vacuole for TL2T- and BL1B-bradyzoites were formed.

5.3.3.5 *In vitro* parasite differentiation

In order to evaluate whether the lowered *LDH* gene expression affects parasite differentiation, we investigated whether the *LDH* knock-down parasite lines could differentiate and form cysts *in vitro*. Fluorescein isothiocyanate (FITC)-conjugated *Dolichos biflorus* lectin, which specifically binds to the N-acetyl glucosamine moiety within the cyst wall, was used as a marker for the cyst wall development (Tomavo, 2001). The localization and abundance of LDH1 and LDH2 were monitored, along with the presence of the cyst wall, by immunofluorescence using LDH1- and LDH2-specific polyclonal antisera, raised

in rabbits. A rhodamine conjugated secondary antibody was used to reveal the signals of LDH1 and LDH2. The parasite lines were first grown as tachyzoites and subjected to immunofluorescence using the LDH1 antiserum (Fig. 5.7A, images 2 and 4). In order to estimate LDH1 protein level, the intensity of the fluorescence signal for the parental and transgenic tachyzoites were quantified and normalized with reference to the fluorescence signal for background. The ratio of the LDH1 signals from the tachyzoite parasite lines over those from the parental was calculated and plotted for each parasite line (Fig. 5.7B). We observed that the LDH1 ratio remained almost constant (1/1) for the parasites of TL2T, BL1B and BL2B lines. The ratio was reduced for TL1T-tachyzoites (1.0/0.32), indicating lower LDH1 protein expression (Fig. 5.7A, images 2, 4; and 5.7B). In parallel experiments, the transgenic parasite lines were cultured under bradyzoite-induced conditions and stained with the LDH2 antiserum in conjunction with FITC-labeled *Dolichos biflorus* lectin. The fluorescence signals for LDH2 were calculated, and the ratios were plotted for all parasite lines (Fig. 5.7C) as described for LDH1. The ratio of fluorescence signal for parasites of TL2T and BL1B were similar (1/1). For parasites of TL1T and BL2B lines, we observed lowered LDH2 ratios (1/0.8 and 1/0.28, respectively). Under these growth conditions, all parasite lines were positively stained with *Dolichos*, indicating that these parasites were surrounded by cyst walls. The parasites of the BL2B line showed a similar *Dolichos* staining pattern to that of the parental parasites, despite the reduced LDH2 signal (Fig. 5.7A, images 9, 10), indicating cyst formation *in vitro*.

We then further investigated whether TL1T-, BL1B-, TL2T- and BL2B-bradyzoites could convert back to tachyzoites. The TL1T-, BL1B-, TL2T- and BL2B-cysts were collected and treated with pepsin (0.1 mg/ml) for 10 min to digest the cyst walls. The treated parasites were then counted and allowed to infect the HFF monolayers. Released bradyzoites of the parental strain showed approximately 89% survival, as determined by Trypan blue staining of 2×10^5 parasites. The viability of the released TL1T- and BL2B-bradyzoites was significantly reduced compared to that of the parental (49% and 53%, when 6×10^4 and 7×10^4 parasites were stained, respectively). As for TL2T- and BL1B-bradyzoites, their survival scores were 61% and 68%, when 1×10^5 and 2×10^5 parasites were stained, respectively. When we used an equal number of the released bradyzoites for infection, the parental parasites were able to completely lyse their host fibroblasts in approximately 5-6 days. For TL1T and BL2B, the parasites were able to infect and lyse HFF monolayers in approximately 12-13 and 15-16 days, respectively. We observed that TL2T- and BL1B-released bradyzoites completely lysed the monolayers in approximately 9-10 and 8-9 days, respectively.

5.3.3.6 Assessment of the virulence of the parasite lines in mice

To explore the effect of *LDH1* and *LDH2* knock-down on parasite growth *in vivo*, TL1T, BL1B, TL2T and BL2B parasites were inoculated into female BALB/c mice at doses up to 10^3 tachyzoites. After 4-5 days of infection, all mice infected with the parental parasite (P) and *LDH* knock-down parasites

showed the same characteristic symptoms of disease. However, the groups of mice infected with the four knock-down parasite lines recovered faster than those infected with the parental parasite. At 14 days post-inoculation, infection with TL1T-, BL1B- and BL2B-tachyzoites was not lethal to the mice, while the infection with TL2T-tachyzoites and the parental parasites caused 20% and 60% mortality, respectively (Fig. 5.8A). When an independent experiment using a dose of 10^4 tachyzoites per mouse was performed, 40% and 100% mortality rates were observed at day 11 in mice infected with TL2T-tachyzoites and the parental parasite, respectively. In this case, 100% survival was again obtained in the groups of mice infected with TL1T, BL1B or BL2B (Fig. 5.8B), suggesting that *LDH* knock-down attenuated *T. gondii* virulence in mice. In order to ensure that the surviving mice had truly been infected, serum was collected 30 days post-inoculation and tested in western blot. A pool of the pre-immune sera from these same mice was also tested and failed to detect *T. gondii* antigens as expected. Numerous antigens of molecular masses ranging from 14 to 90 kDa were recognized by sera from mice surviving infection with TL1T, BL1B, TL2T and BL2B tachyzoites (Fig. 5.8C). Similar antigenic profiles were observed when the sera from the two mice surviving infection with 10^3 tachyzoites of the parental parasites (Fig. 5.8A) were tested (Fig. 5.8C, panel P, lanes 1 and 2). Except for an antigen of apparent molecular mass of 43 kDa which was not observed in four out of five mice infected with TL1T (panel TL1T, lanes 1-4) and one of the parental parasite (lane 1), numerous antigens of the same molecular masses were detected in all sera tested. To determine whether surviving mice had developed protective

immunity after 30 days post-infection, mice initially infected with TL1T, BL1B, TL2T and BL2B were challenged with 10^4 parental parasite tachyzoites. As shown in Fig. 5.8B (arrows), all mice infected with the *LDH* knock-down parasites (TL1T, BL1B, TL2T and BL2B) survived a subsequent challenge with 10^4 tachyzoites of the parental parasite, a dose that usually causes 100% mortality, suggesting that live vaccination of mice with the *LDH* knock-down tachyzoites can confer protection against *T. gondii*.

To determine whether *in vivo* cyst formation could occur in the *LDH* knock-down parasite lines, the surviving mice infected with 10^3 parasites from TL1T, BL1B, TL2T, BL2B and parental parasites, as described in Fig. 5.8A, were examined for the presence of cysts in the entire brain. Approximately 2-5 cysts per brain were detected in TL1T-, BL1B-, BL2B-infected mice, while about 20 cysts per brain were detected in TL2T-infected mice. The mice infected with the parental strain contained an average of 200 cysts per mouse brain (Fig. 5.8D). Identical results were obtained when the surviving mice infected with 10^4 tachyzoites were analyzed for the presence of cysts in the brain. Again, only very few cysts were detected, suggesting that unlike the parental strain, the *LDH* knock-down parasite lines were unable to produce a significant number of cysts *in vivo*.

5.4 DISCUSSION

Differentiation and encystation of *T. gondii* involves the coordinated expression of several genes. A broad spectrum of induction and suppression of

gene expression could be observed as developmental dynamics. Despite the amenability of *T. gondii* to genetic manipulation, silencing the expression of essential genes has proven difficult. Our previous studies have indicated that the introduction of dsRNA can be used as a powerful genetic tool for lowering the steady-state level of gene expression (Al-Anouti and Ananvoranich, 2001, Al-Anouti *et al.*, 2003, Chapter 3 and Chapter 4). In this study, we demonstrated that a similar approach can be used successfully for lowering *LDH1* and *LDH2* expression. Such effort was reported unattainable *via* conventional genetic manipulations (Cleary *et al.*, 2002). The ability to lower *LDH* expression has allowed us to investigate their significance in parasite development.

We initially demonstrated that the transient knock-down of *LDH* expression gave rise to an altered growth pattern for tachyzoites, as shown by the nucleotide incorporation assays (Fig. 5.2). The inhibition of *LDH1* gene expression in tachyzoites clearly decreased viability and proliferation. As expected, the *LDH2* dsRNA electroporation did not affect tachyzoite viability because *LDH2* is not expressed at this stage. This finding indicated that the introduction of dsRNA, without the presence of the target *LDH2* mRNA, did not interfere with the cell viability. The hpRNAs which targeted a unique sequence on either *LDH1* or *LDH2* mRNA did not lower *LDH* expression. However this finding was not indicative of an ineffectiveness of hpRNAs. We chose only a single site, which might not be accessible to the RISC complex. If other sites had been chosen, the knock-down might have occurred. We have attempted to transiently down-regulate *LDH2* expression in the bradyzoite stage by electroporation. However, no

conclusive data were obtained. It is likely that the introduction of dsRNA directly into bradyzoites by electroporation was not as efficient as that for tachyzoites.

Four transgenic parasite lines were generated and used for the investigation of the physiological roles and significance of *LDH1* and *LDH2* in the parasite development. TL1T and BL2B parasite lines were generated in order to monitor the down-regulation effect of *LDH1* and *LDH2* in a stage specific manner, following the pattern of the expressed isoforms. BL1B parasite line was used for investigating the outcome of lowering untranslated *LDH1* mRNA in bradyzoites. TL2T, on the other hand, was a control parasite line for the dsRNA expression in the absence of the target mRNA. Prior to the phenotypical studies, we characterized these parasite lines, in comparison to their parental line, *T. gondii*, strain PLKΔHXGPRT. We showed that these parasite lines expressed the *LDH1* and *LDH2* dsRNA, as designed. Detectable levels of *LDH1* dsRNA were expressed in TL1T-tachyzoites and BL1B-bradyzoites (Fig. 5.4A). Similarly, detectable levels of *LDH2* dsRNA were detected in TL2T-tachyzoites and BL2B-bradyzoites (Fig. 5.4A). As expected, the steady state levels of target mRNAs were lowered according to the dsRNA expression and RNAi silencing effect. The silencing effect was monitored by dot-blot analysis and western blot analysis (Fig. 5.4B and Fig. 5.5).

TL1T parasite line: TL1T tachyzoites exhibited impaired replication in HFF monolayer. The doubling time of TL1T-tachyzoites was twice that of the parental tachyzoites. It was recently reported that upon inhibiting LDH1 enzymatic activity by gossypol, the tachyzoite growth was reduced in cultured fibroblasts

(Kavanagh *et al.*, 2000, Dando *et al.*, 2001). Therefore, the TL1T phenotype is in concordance with these previous enzymatic and inhibition studies. Inhibiting LDH1 enzymatic activity gave rise to slower replication and growth. The finding that the TL1T parasites were unable to kill the mice with a dose that causes 100% mortality in the parental strain and were unable to develop a significant number of cysts *in vivo* indicated that the host immunity could clear these TL1T parasites more effectively and rapidly after an infection than wild-type parasites. More importantly, the infection with TL1T conferred protection against a new challenge with the parental strain at a dose that kills 100% of infected mice.

BL2B parasite line: It is not surprising that BL2B tachyzoites exhibited relatively normal growth similar to the parental parasites (Fig. 5.6A and 5.6B). As expected, BL2B-bradyzoites multiplied significantly slower than those of the parental parasites (Fig. 5.6B). The percentage survival of the pepsin-released parasites of BL2B-parasite line was low (49%), as compared to the parental parasite (89%). BL2B parasites were unable to develop a significant number of cysts *in vitro* (Fig. 5.6C, 5.7A) and *in vivo* (Fig. 5.8D), indicating that the BL2B parasites may be defective in the differentiation process. The fact that few mature cysts (only 2-5 cysts in the whole brain extract) were detected suggests that differentiation is likely completed by this parasite line but at very low efficiency. It was reported that an LDH activity, especially that of LDH2, could be required to acidify the cytosol and keep the parasite in its bradyzoite stage (Tomavo, 2001 and Denton *et al.*, 1996). The levels of expressed LDH2 and the steady state *LDH2* mRNA were lowered in BL2B, as compared to those of the parental

parasites (Fig. 5.5 and 5.4B). Thus, it is possible that normal functioning of the parasite requires sufficient levels of LDH2. The down-regulation of *LDH2* expression in BL2B-bradyzoites might be due to a combination of both RNAi and antisense effect. It is thus possible that lowered *LDH2* expression might have led to (i) an insufficient energy supply and (ii) suboptimal conditions required for the bradyzoite development and maintenance. In a murine model system, low efficiency in bradyzoite formation would have left some parasites in the tachyzoites stage to be cleared by the immune system. As observed for this parasite line, BL2B parasites could cause typical symptoms of disease, but are not lethal. Because only few cysts were obtained, we were unable to determine by electron microscopy whether they display a normal morphology. The fact that BL2B infection could confer protection against re-infection by *T. gondii*, indicates that the BL2B infection allows a protective immunity to develop.

BL1B parasite line: The expression of *LDH1* dsRNA in a bradyzoite specific manner gave rise to the lowered *LDH1* mRNA (Fig. 5.4B), indicative of the RNAi-knock-down of *LDH1* expression in the bradyzoite stage. BL1B exhibited a phenotype almost identical to that of the parental parasites. The BL1B-tachyzoites and -bradyzoites grew at a similar rate as those of the parental parasites. When *Dolichos* staining was used as the differentiation marker, BL1B was found to differentiate *in vitro*, similar to that of the parental parasites. *Dolichos* staining is specific to the cyst wall formation which takes place very early in the differentiation process (Soete *et al.*, 1993, Freyre, 1995). However, parasites released from the BL1B cysts exhibited less viability (only 68%

68% viability), as compared to the parental parasite (89% viability), suggesting an impairment in cyst development. In addition, the BL1B parasite line also failed to develop a significant number of cysts in the brains of mice. These findings suggest that the maintenance of *LDH1* mRNA level may be associated with the differentiation process, perhaps through maintenance of a micro-environmental balance. When we lowered *LDH1* mRNA in the bradyzoite stage, we might have offset the level of *LDH1* mRNA essential for (i) an optimal interaction with other cellular components important for the parasite differentiation, and/or (ii) parasite readiness to convert to tachyzoites. This notion requires further investigation. Approaches such as those of proteomics and microarray analysis would give better insight into the differences between the BL1B- and parental-bradyzoites.

TL2T parasite line: TL2T-tachyzoites produced *LDH2* dsRNA in the absence of the target mRNA (Fig. 5.4A). This parasite line has a similar growth pattern as the parental parasite line, indicating that the presence of dsRNA does not cause any harmful effect to the parasite growth (Fig. 5.6). The priming of RNAi system was not effective in lowering the *LDH2* expression, as seen by the absence of change in the level of *LDH2* mRNA in the TL2T-bradyzoites as compared to other three transgenic parasite lines (Fig. 5.4B). Nonetheless, the *LDH2* protein expression levels in the TL2T were lower than that in the parental line (Fig. 5.5). The fact that the steady state level of *LDH2* mRNA was unchanged, while expression of *LDH2* isoform was lowered, suggests that the down-regulation of *LDH2* expression in TL2T might not be due to down-regulation by RNAi, but instead due to an antisense effect. With an antisense

effect, translation of the target mRNA is blocked, without significant degradation of the message. This may explain why the mice infected with TL2T yielded fewer cysts in mice as compared to the mice infected with the parental strain. It should be noted that the number of cysts obtained in mice infected with TL2T was slightly higher than those generated by TL1T, BL1B and BL2B infection. The translational suppression by this putative antisense effect seems to be sufficient to attenuate the virulence of the parasite infection, but is not as efficient as that induced by mRNA degradation.

It is important to further investigate how *LDH2* dsRNA expression, particularly in the TL2T parasite line, initiates an antisense effect, not an RNAi effect. It has been reported that post-transcriptional regulation *via* antisense and RNAi share a common pathway, as those observed for the miRNA and siRNA, respectively (Voinnet, 2002). The degree of complementarity between the siRNAs or miRNAs and the mRNA target is the sole determinant of their function in mRNA degradation and/or translational repression (Doench *et al.*, 2003). The siRNAs recognize mRNA targets by precise complementary base-pair interactions leading to subsequent degradation of the target *via* an RNAi mechanism. On the other hand, miRNAs inhibit the translation of mRNAs *via* imprecise base-pair interactions (Hutvagner and Zamore, 2002). Both pathways share similar protein partners, RNase III and Argonaute family members (Hamilton *et al.*, 2002). It has been recently reported that *T. gondii* has RNAi-related genes: Dicer and Argonaute family members (Ullu *et al.*, 2004). The obtained the cDNA encoding putative Dicer and Argonaute have been recently obtained in Dr. Ananvoranich's

laboratory and their genes are currently being characterized. Thus it is highly likely that miRNA as well as siRNA pathways exist in *T. gondii*.

Since all *LDH* knock-down parasites are virulence-attenuated in the tested animal model, we question whether the transforming elements and their products (i.e. constructed plasmids and expressed dsRNAs) could be virulence attenuating factors. In order to answer this notion, we could further investigate whether other parasite lines expressing dsRNA unrelated to *LDH1* and *LDH2* are virulence-attenuated. However, this possibility is less likely because a parasite line expressing dsRNA homologous to *UPRT* exhibits normal growth and differentiation (Chapter 4, Al-Anouti *et al.*, 2003).

In conclusion, we have shown that the expression of *LDH1* and *LDH2* is essential for parasite development and growth. The generation of *LDH* knock-down parasites which are defective in their abilities to form cysts *in vivo* verifies the great potential of LDH as a target for designing future drugs that could block tissue cyst formation. The knock-down parasites might also serve as a useful basis for the development of vaccine strategies especially for livestock.

Figure 5.1

**The effect of double-stranded RNA homologous to
lactate dehydrogenase on the target transcript**

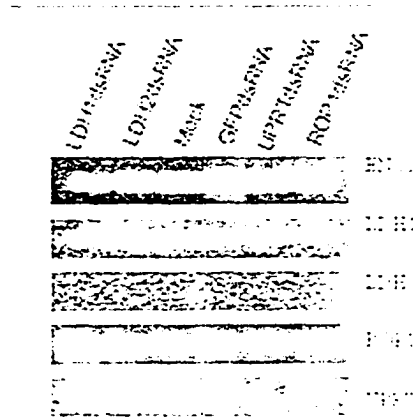


Figure 5.1. Assessment of the down-regulation effect of dsRNA by northern blot analysis. The dsRNA specific to *LDH1*, *LDH2*, *ROP1*, *UPRT* and *GFP* were individually electroporated into tachyzoites. Total RNA samples extracted from the parasites electroporated with the homologous dsRNA and the mock (buffer) were subjected to northern blot analysis. Chemiluminescent detection using the DIG-labeled probes (indicated for each panel) was used to reveal the steady state levels of the target transcripts as described in the Experimental Procedures.

Figure 5.2

The effect of double-stranded RNA homologous to lactate dehydrogenase on the growth of *Toxoplasma gondii*

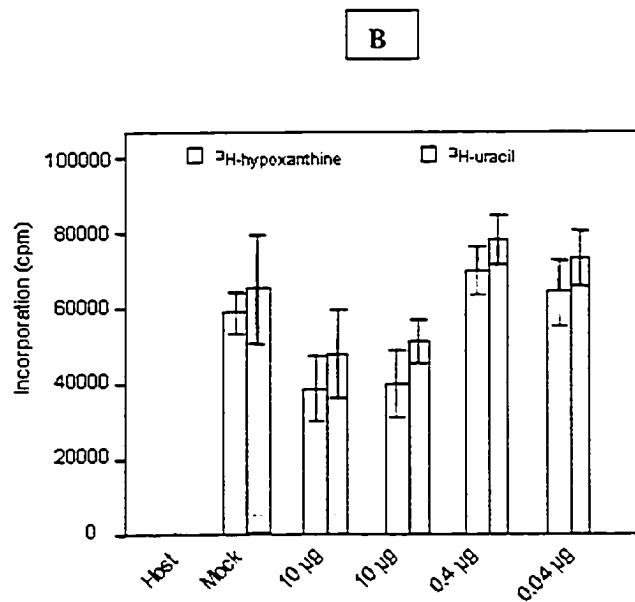
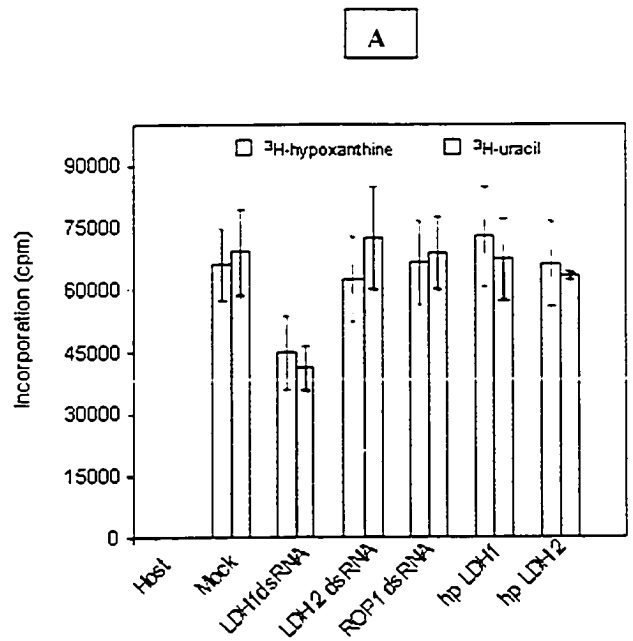


Figure 5.2. Inhibition of parasite growth by dsRNA homologous to *LDH*. **A.** The *in vitro* synthesized dsRNA homologous to *LDH1* and *LDH2* were individually electroporated into purified parasites. Four μg of each RNA species were tested, and the ^3H -uracil and ^3H -hypoxanthine assimilation assays were conducted 24 h following electroporation. The dsRNA homologous to non-target *ROP1* was used as a control. Mock electroporations were performed using the electroporation buffer with no RNA species. **B.** Dose dependence exhibited by dsRNA homologous to *LDH1*. Different concentrations of dsRNA homologous to *LDH1* (10, 4, 0.4 and 0.04 μg) were tested for their abilities to lower uracil and hypoxanthine incorporation.

Figure 5.3

Analysis of the genomic arrangement of the parasite lines

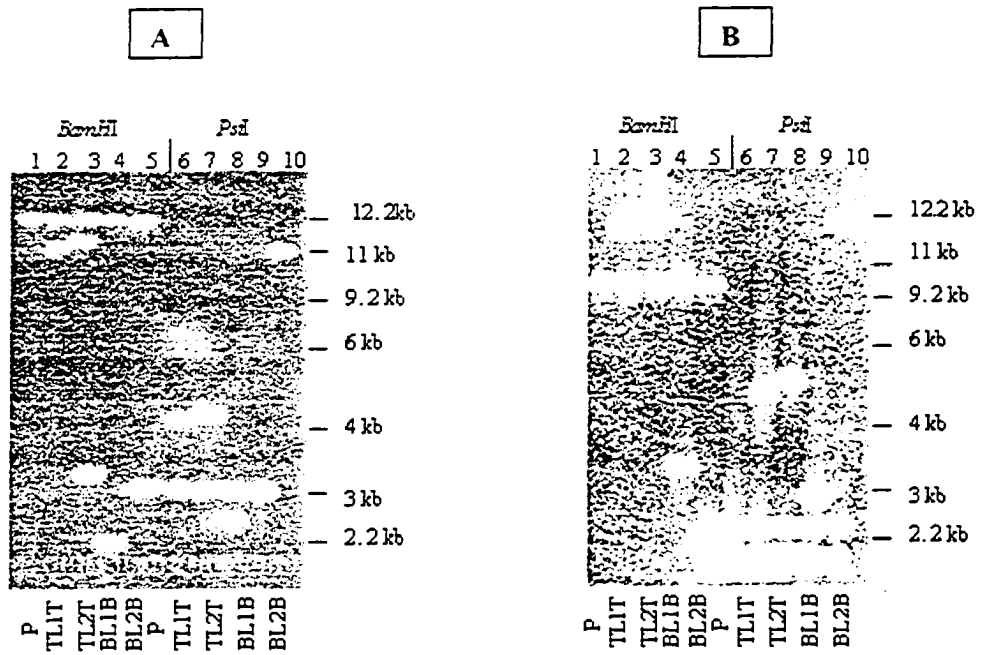


Figure 5.3. Southern blot analysis of genomic DNA isolated from the parental, TL1T, TL2T, BL1B and BL2B parasites. The isolated DNA was digested with either *Bam*HI or *Pst*I, and subjected to Southern blot analysis using a DIG-labeled *LDH1* cDNA fragment (A) or *LDH2* cDNA fragment (B).

Figure 5.4

Detection of the expression of double-stranded RNA homologous to lactate dehydrogenase and the transcription profile of the target mRNAs in the parasite lines

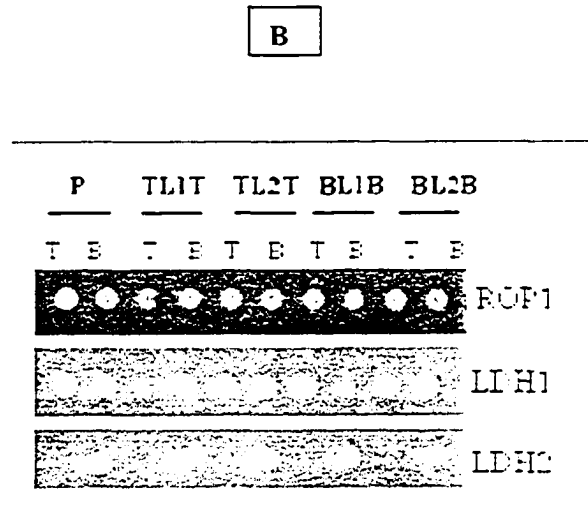
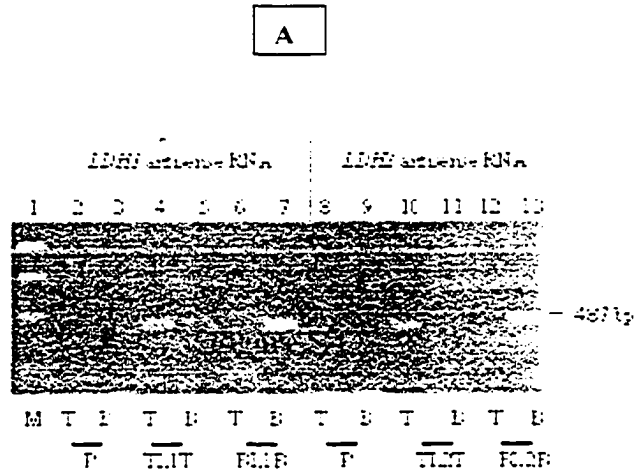


Figure 5.4. A. An image of an agarose gel resolving the RT-PCR products obtained using RNA samples extracted from the knock down parasites. The expected size of the RT-PCR product was 487 bp (as indicated) when using the primer pair LDH-ORF(sense) and 3LDH-ORF(antisense) or the primer pair LDH2forward and LDH2reverse. Lane 1 contains DNA markers of 1000, 750, 500 and 250 bp, respectively. The RT-PCR products amplified from the RNA samples isolated from the parental, TL1T and BL1B tachyzoites are in lanes 2, 4, and 6, respectively. The RT-PCR products amplified from the RNA samples isolated from the parental, TL1T and BL1B bradyzoites are in lanes 3, 5 and 7, respectively. The oligonucleotide primer LDH-ORF(sense) was used during the RT step for the samples in lanes 2-7. The RT-PCR products amplified from RNA samples isolated from parental, TL2T and BL2B tachyzoites are in lanes 8, 10, and 12, respectively. The RT-PCR products amplified from RNA samples isolated from the parental, TL2T and BL2B bradyzoites are in lanes 9, 11 and 13, respectively. The oligonucleotide primer LDH2forward was used during the RT step for the samples in lanes 8-13. **B.** *LDH1* and *LDH2* transcription profiles. Total RNA was extracted from the tachyzoites (T) and bradyzoites (B) of all four parasite lines along with the parental (P) and subjected to Dot-blot analysis. DIG-labeled probes specific to *LDH1* and *LDH2* 5'UTR were used to assess the steady state levels of the *LDH1* and *LDH2* target transcripts. A probe specific to *ROP1* was used to control for the amount of RNA per sample.

Figure 5.5

**Assessment of lactate dehydrogenase protein expression
in the parasite lines**

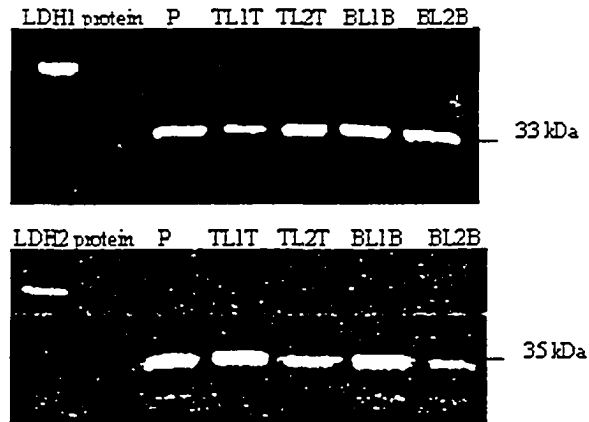


Figure 5.5. Western blot analysis of the expressed LDHs in the parasite lines. Images of western blots of tachyzoite protein extracts probed with the LDH1 antiserum (upper panel) and bradyzoite protein extracts probed with the LDH2 antiserum (lower panel). LDH1 and LDH2 fusion proteins were included as controls.

Figure 5.6

Growth and replication of the parasite lines

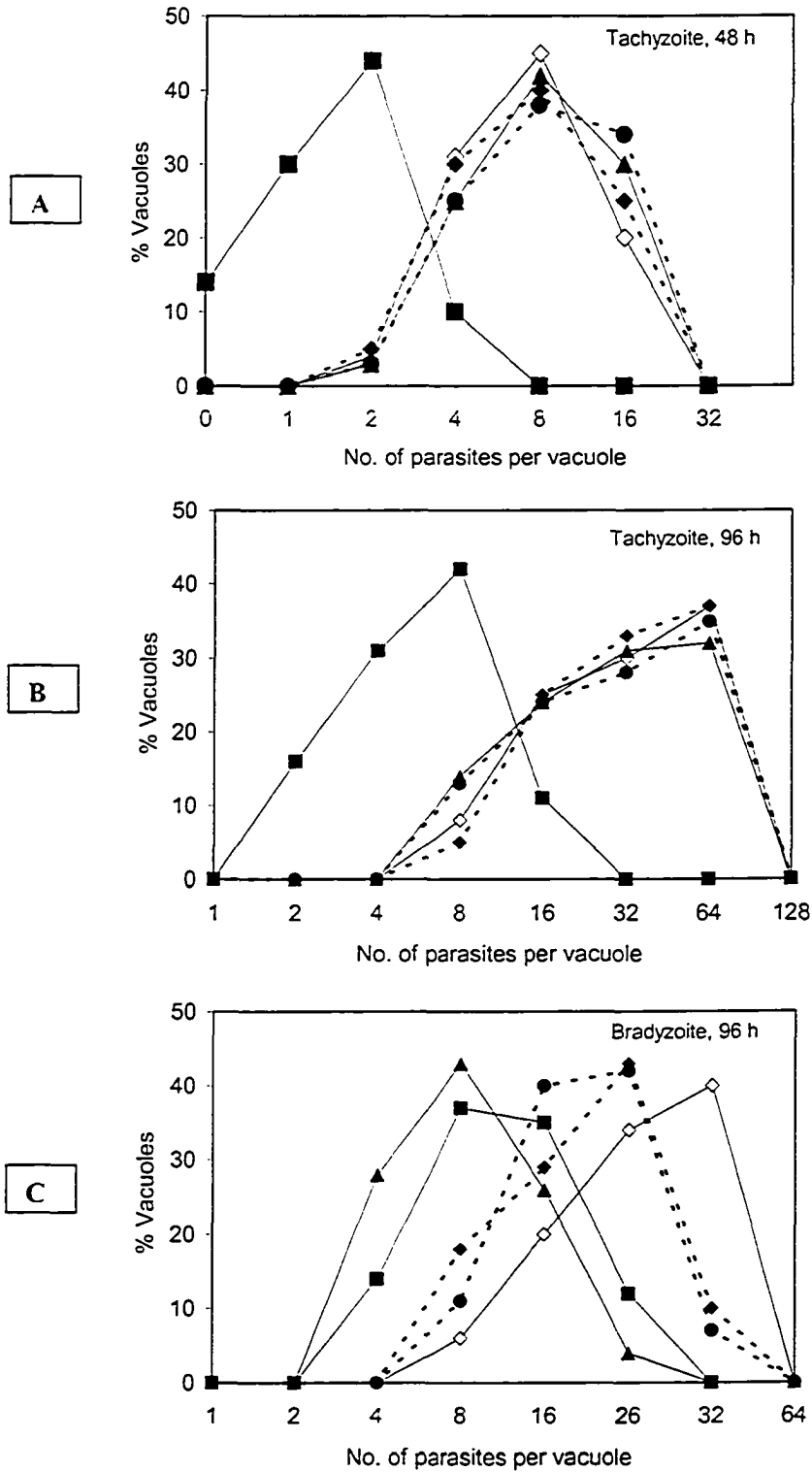


Figure 5.6. Parasite growth and replication. The percentage distribution of vacuole size (number of parasites/vacuole) was determined at 48 h (*A*) and 96 h (*B*) after infection with the parental and parasite lines grown under tachyzoite culture conditions, and at 96 h under bradyzoite differentiation conditions (*C*). The number of parasites per vacuole was counted for 100 vacuoles in two different experiments.

[-◇-, P; -■-, TL1T; -▲-, BL2B; -◆-, BL1B; -●-, TL2T]

Figure 5.7

In vitro differentiation of the parasite lines

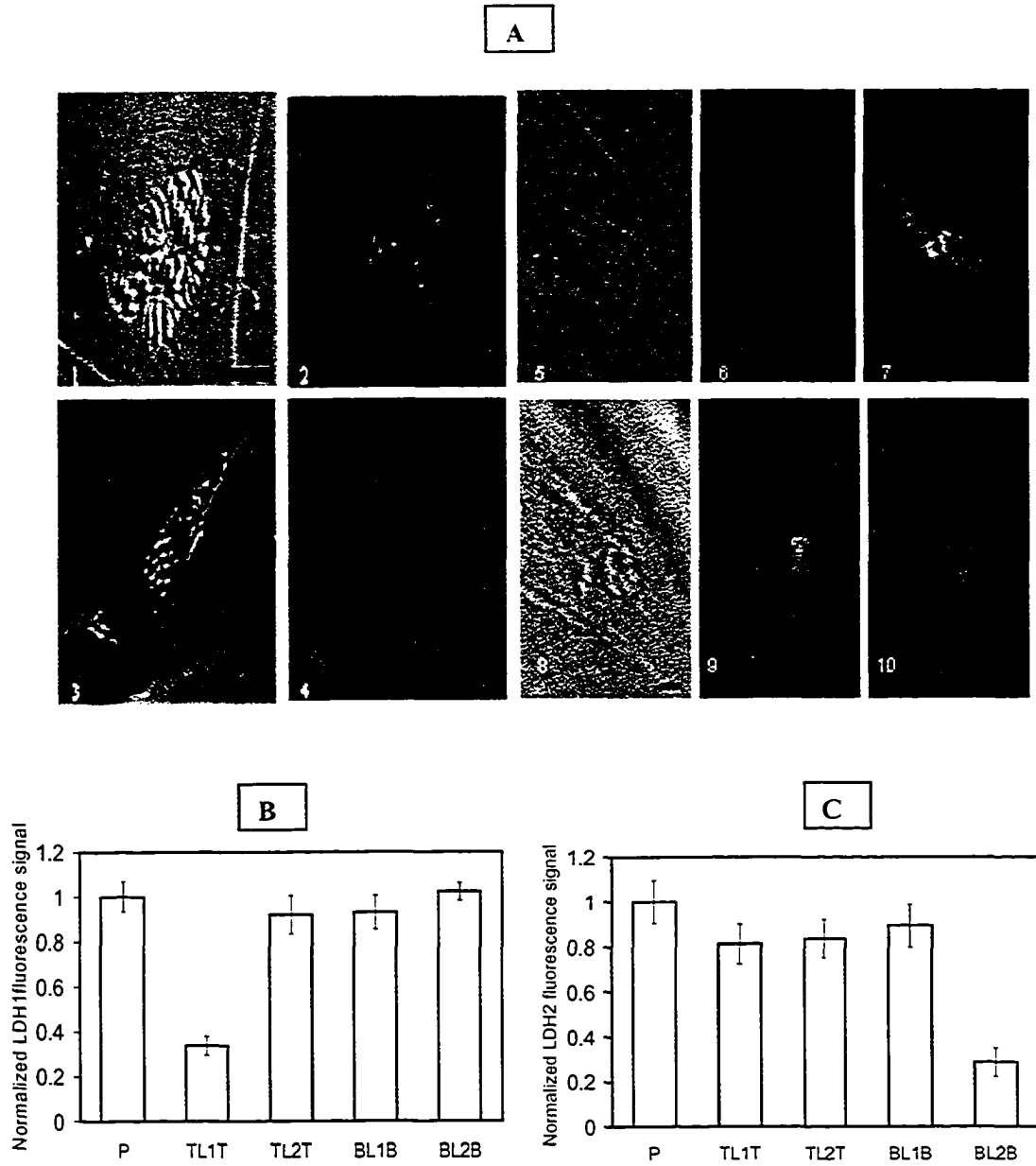


Figure 5.7. Differentiation of the stable parasite lines *in vitro*. **A.** The parental and knock-down parasite lines were grown in HFF monolayers under either tachyzoite- or bradyzoite-conditions. Nuclei were stained with DAPI (blue). The tachyzoites of the parental parasites (images 1 and 2) and TL1T line (images 3 and 4) were subjected to immunofluorescence assays using the LDH1 antiserum and a rhodamine conjugate (red) carried out as described in Experimental Procedures. FITC-labeled *Dolichos biflorus* agglutinin in conjunction with the LDH2 antiserum were used to stain the cyst wall of bradyzoites (green) and LDH2 (red) (images 5, 6 and 7) and BL2B-bradyzoites (images 8, 9 and 10). Bars on the micrographs are 10 μm (for images 3 and 4) and 20 μm (images 1, 2 and 5-10). **B.** Normalized fluorescence values from LDH1 staining for the parasite lines under tachyzoite culture conditions. **C.** Normalized fluorescence values from LDH2 staining when the parasites were induced to differentiate *in vitro* into bradyzoites.

Figure 5.8

Assessment of the virulence of the parasite lines *in vivo*

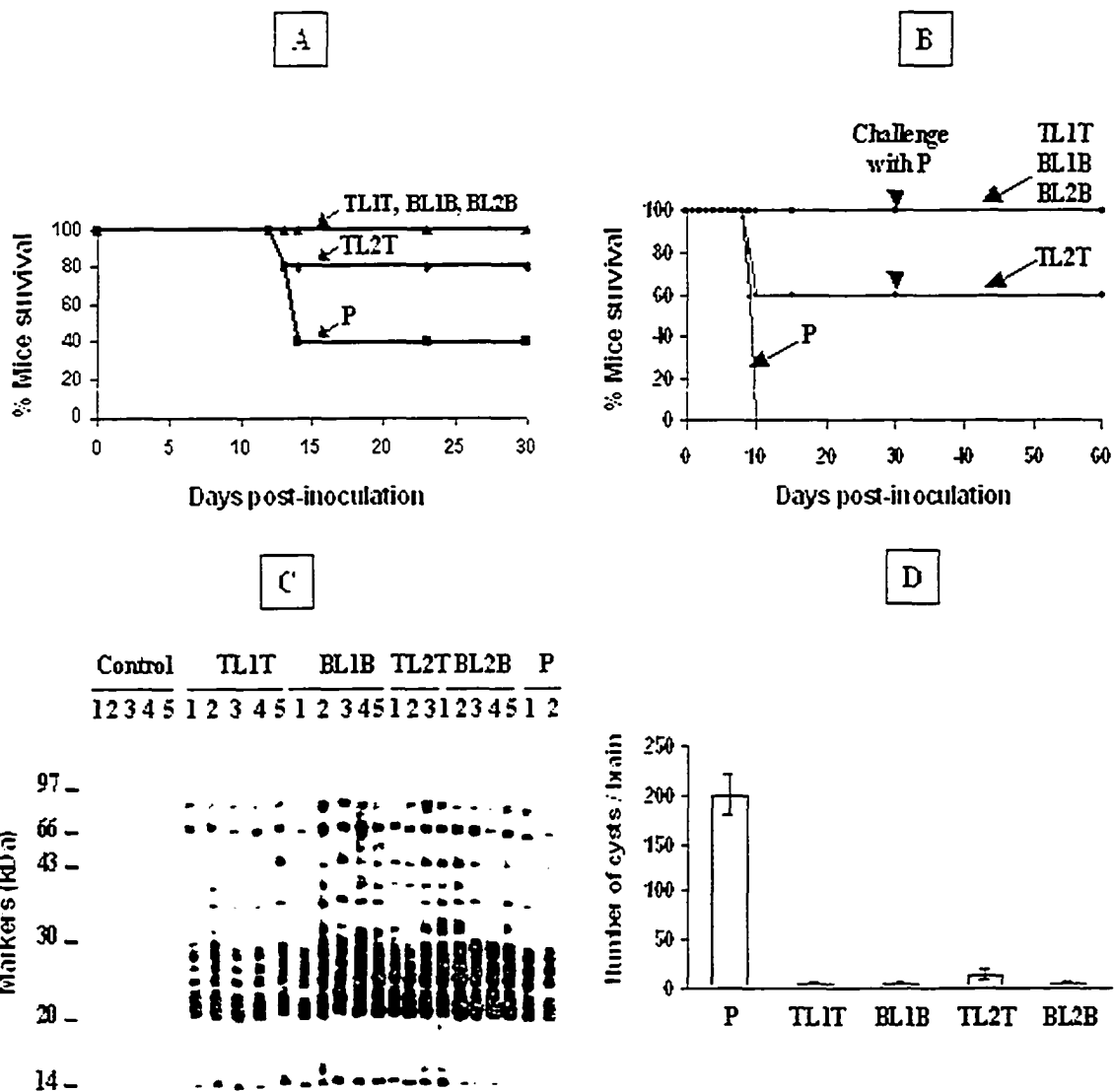


Figure 5.8. Experimental infections in mice *A.* The relative time-to-death of mice infected with TL1T, BL1B, TL2T, BL2B and parental (P) parasites were compared. Female BALB/c mice (groups of five) were inoculated with 10^3 tachyzoites, and mortality was monitored over 30 days. *B.* Comparative mortality of TL1T, BL1B, TL2T, BL2B and parental parasites. Female BALB/c mice (groups of five) were inoculated with 10^4 tachyzoites, and mortality rate was followed until 30 days post-infection. *C.* Western blots showing that all surviving mice displayed immune response by producing antibody against numerous *Toxoplasma* antigens. A pool of pre-immune sera of each tested group was in lanes 1-5 (control). Serum was taken from each infected and surviving mouse 30 days post-infection for TL1T, BL1B, TL2T, BL2B and parental (P), as indicated on the top of the blot. Protein markers are shown on the left. *D.* *In vivo* cyst development of TL1T, BL1B, TL2T, BL2B and parental parasites. The cysts were isolated from the brains of the living mice analyzed above. Average number of cysts per animal \pm standard error of the mean was shown.

GENERAL CONCLUSIONS

The main focus of this study is to elucidate the function of lactate dehydrogenase (*LDH*) which has been long hypothesized to be crucial for *Toxoplasma gondii* differentiation. We have developed a new strategy for this study which involved the use of double-stranded RNA (*dsRNA*) to down-regulate the target gene of interest. The originality and contribution of the research can be highlighted as the following:

1. It was the first to show that the introduction of double-stranded RNA can specifically lower the expression of homologous genes in *T. gondii*.
2. It suggested that RNA interference (*RNAi*) is functional in *T. gondii*.
3. It was the first to report a successful knock-down of *LDH* expression, an effort that had not been possible to attain by the conventional molecular methods available for *T. gondii*.
4. It significantly provided biochemical and molecular evidence for the significance of *LDH* expression in *T. gondii* differentiation and growth.
5. It was unique in the generation of parasite lines with attenuated virulence which could act as a basis for the development of live vaccination strategies for live stock particularly.
6. It verified the potential of *LDH* as a target for the development of future drugs that could prevent tissue cyst formation.

Future aspects that could stem from our work could be directed towards the following:

1. A more thorough characterization of the RNAi pathway in *T. gondii*. Future research should aim at investigating whether the small interfering RNA (siRNA) intermediate would be produced upon the introduction of the homologous dsRNA into *T. gondii*, and whether the siRNA intermediate would lead to the degradation of the homologous mRNA in the presence of parasite lysate or upon direct introduction into the parasite system. Also, the genes encoding putative Dicer and Argonaute family members identified within *T. gondii* genome could be expressed in order to characterize their products and verify whether they function in RNAi in a similar way to their homologs in other organisms.

2. A better understanding of the differentiation process in *T. gondii* and the molecular signals involved in the control of this process. It would be interesting to further confirm the metabolic and developmental role of LDH and find out whether functional complementation of LDH in the knock-down parasite lines would restore the growth rate, virulence and differentiation to normal. Using a similar approach to the one developed in our study, additional research could be performed in order to investigate the function of other developmentally regulated genes speculated to be important for *T. gondii* differentiation including enolases (*ENO1* and *ENO2*) and glucose 6-phosphate isomerase. A study that targets enolase or glucose 6-phosphate isomerase in addition to LDH would be a possible aspect for future investigations.

REFERENCES

- Al-Anouti F and Ananvoranich S. (2002) Comparative analysis of antisense RNA, double-stranded RNA and *delta* ribozyme-mediated gene regulation in *Toxoplasma gondii*. *Antisense and Nucleic Acid Drug Development* 12, 275-281.
- Al-Anouti F, Quach T and Ananvoranich S. (2003) Double-stranded RNA can mediate the suppression of uracil phosphoribosyltransferase expression in *Toxoplasma gondii*. *Biochemical and Biophysical Research Communication* 302, 316-323.
- Baker BF. (2002) The role of antisense oligonucleotides in the wave of genomic information. *Nucleosides Nucleotides Nucleic Acids* 20, 397-399.
- Baker BF and Monia BP. (1999) Novel mechanisms for antisense-mediated regulation of gene expression. *Biochimica and Biophysica Acta* 1489, 3-18.
- Banerjee D and Slack F. (2002) Control of developmental timing by small temporal RNAs. *BioEssays* 24, 119-129.
- Barker R, Meletev V and Zamecnick P. (1996) Inhibition of *Plasmodium falciparum* malaria using antisense oligonucleotides. *Proceedings of the National Academy of Science* 93, 515-518.
- Bastin P, Galvani A and Sperling L. (2001) Genetic interference in protozoa. *Research Microbiology* 152, 123-129.
- Bernstein E, Caudy A, Hammond S and Hannon G. (2001) Role for a bidentate ribonuclease in the initiation step of RNAi. *Nature* 409, 363-365.

Black M and Boothroyd J. (1998) Development of a stable episomal shuttle vector for *Toxoplasma gondii*. *The Journal of Biological Chemistry* 273, 3972-3979.

Bohne W, Heesemann J and Gross U. (1994) Reduced replication of *Toxoplasma gondii* is necessary for induction of bradyzoite-specific antigens: a possible role for nitric oxide in triggering stage conversion. *Infection and Immunology* 62, 1761-1777.

Bohne W and Roos DS. (1997) Stage-specific expression of a selectable marker in *Toxoplasma gondii* permits selective inhibition of either tachyzoites or bradyzoites. *Molecular and Biochemical Parasitology* 88, 115-126.

Bohne W, Wirsing A and Gross U. (1997) Bradyzoite-specific gene expression in *Toxoplasma gondii* requires minimal genomic elements. *Molecular and Biochemical Parasitology* 85, 89-98.

Boothroyd JC. (1998) Expressed sequence tag analysis of the bradyzoite stage of *Toxoplasma gondii*: identification of developmentally regulated genes. *Infection and Immunity* 66, 1632-1637.

Boothroyd JC, Black M, Bonnefoy S, Hehl A, Knoll LJ, Manger ID, Ortega-Barria E and Tomavo S. (1997) Genetic and biochemical analysis of development in *Toxoplasma gondii*. *Philosophy Society of London Biological Sciences* 352, 1347-1354.

Boothroyd JC, Black M, Kim K, Pfeferkorn E, Seeber F, Sibley D and Soldati D. (1995) Forward and reverse genetics in the study of the obligate intracellular parasite *Toxoplasma gondii*. *Methods in Molecular Genetics* 6, 3-29.

Bosher J and Labousse M. (2000) RNA interference: genetic wand and genetic watchdog. *Natural Cell Biology* 2, 31-36.

Brooks GA, Dubouchaud H, Brown M, Sicurello JP and Butz CE. (1999) Role of mitochondrial lactate dehydrogenase and lactate oxidation in the intracellular lactate shuttle. *Proceedings of the National Academy of Science* 96, 1129-1134.

Carthew R. (2001) Gene silencing by double-stranded RNA. *Current Opinions in Cell Biology* 13, 242-248.

Cleary MD, Singh U, Blader IJ, Brewer JL and Boothroyd JC. (2002) *Toxoplasma gondii* asexual development: identification of developmentally regulated genes and distinct patterns of gene expression. *Eukaryotic Cell* 3, 329-340.

Clemens J, Worby C, Simonson-Left N, Muda M, Maehama T, Hemmings B and Dixon B. (1999) Use of double-stranded RNA interference in *Drosophila* cell lines to dissect signal transduction pathways. *Proceedings of the National Academy of Science* 97, 6499-6503.

Cormack BP, Validivia RH and Falkow S. (1994) FACS-optimized mutants of the green fluorescent protein as a marker for gene expression. *Science* 102, 263-803.

Cottrell T and Doering T. (2003) Silence of the strands: RNAi in eukaryotic pathogens. *Trends in Microbiology* 11, 37-42.

Cubitt AB, Heim R, Adams SR, Boyd AE and Tsien RY. (1995) Understanding, improving and using green fluorescent proteins. *Trends in Biochemical Sciences* 20, 448-445.

Dando C, Schroeder ER, Hunsaker LA, Deck LM, Royer RE, Zhou X, Parmley SF and Vander Jagt DL. (2001) The kinetic properties and sensitivities to inhibitors of lactate dehydrogenases (LDH1 and LDH2) from *Toxoplasma gondii*: comparisons with pLDH from *Plasmodium falciparum*. *Molecular and Biochemical Parasitology* 118, 23-32.

Denton H, Roberts CW, Alexander J, Thong KW and Coombs GH. (1996) Enzymes of energy metabolism in the bradyzoites and tachyzoites of *Toxoplasma gondii*. *Microbiology Letters* 15, 103-108.

Doench JG, Petersen CP and Sharp PA. (2003) siRNAs can function as miRNAs. *Genes and Development* 17, 438-442.

Doherty E. (2000) Ribozymes structures and mechanisms. *Annual Reviews of Biomolecular Structures* 69, 597-615.

Doi N, Ueda R, Kumiko U and Saigo K. (2003) Short interfering RNA mediated gene silencing in mammalian cells requires Dicer. *Current Biology* 13, 41-46.

Donald RG, Roos DS. (1998) Gene knock-outs and allelic replacements in *Toxoplasma gondii*: HXGPRT as a selectable marker for hit-and-run mutagenesis. *Molecular and Biochemical Parasitology* 91, 295-305.

Donald R.G.K. and Roos D.S. (1995) Insertional mutagenesis and marker rescue in a protozoan parasite: cloning of the uracil phosphoribosyltransferase locus from *Toxoplasma gondii*. *Proceedings of the National Academy of Science* 92, 5749-5753.

Donald R.G.K, Carter D, Ullman B and Roos D.S (1996) Insertional tagging, cloning and Expression of the *Toxoplasma gondii* Hypoxanthine-Xanthine-Guanine Phosphoribosyltransferase gene. *The Journal of Biological Chemistry* 271, 14010-14019.

Dubey J. (1994) Toxoplasmosis. *Journal of American Veterinary Medicine Association* 205, 1593-1598.

Dubey JP, Lindsay DS and Speer CA. (1998) Structures of *Toxoplasma gondii* tachyzoites, bradyzoites and sporozoites and biology and development of tissue cysts. *Clinical Microbiology Reviews* 11, 267-299.

Dzierszinski F, Mortuaire M and Tomavo S. (2000) Targeted disruption of the surface antigen SAG3 gene in *Toxoplasma gondii* decreases host adhesion and drastically reduces virulence in mice. *Molecular Microbiology* 37, 574-582.

Dzierszinski F, Popescu O, Toursel C, Slomianny C, Yahiaoui B and Tomavo S. (1999) The protozoan parasite *Toxoplasma gondii* expresses two functional plant-like glycolytic enzymes. Implications for evolutionary origin of apicomplexans. *The Journal of Biological Chemistry* 274, 24888-24895.

Elbashir SM, Harborth J, Lendeckel W, Yalcin A, Weber K and Tuschl T. (2001) Duplexes of 21-nucleotide RNAs mediate RNAi in cultured mammalian cells. *Nature* 411, 494-498.

Filippov V, Solovyev S, Filippov M and Gill S. (2000) A novel type of RNase III family proteins in eukaryotes. *Gene* 245, 213-221.

Fire A, Xu S, Montgomery M, Kostas S, Driver S and Mello C. (1998) Potent and specific genetic interference by double-stranded RNA in *Caenorhabditis elegans*. *Nature* 391, 806-811.

Flores MV, Atkins D, Wade D, O'Sullivan WJ and Stewart TS. (1997) Inhibition of *Plasmodium falciparum* proliferation in vitro by ribozymes. *The Journal of Biological Chemistry* 272, 16940-16945.

Freyre A. (1995) Separation of *toxoplasma* cysts from brain tissue and liberation of viable bradyzoites. *Journal of Parasitology* 81, 1008-1010.

Gossen M and Bujard H. (1992) Tight control of gene expression in mammalian cells by tetracycline-responsive promoters. *Proceedings of the National Academy of Science* 89, 5547-5551.

Guerrier-Takada C, Gardiner K, Marsh T, Pace N and Altman S. (1983) The RNA moiety of ribonuclease P is the catalytic subunit of the enzyme. *Cell* 35, 849-857.

Hamilton A, Voinnet O, Chappell L and Baulcombe D. (2002) Two classes of short interfering RNA in RNA silencing. *EMBO Journal* 21, 4671-4679.

Hammond S, Bernstein E, Beach D and Hannon J. (2000) An RNA-directed nuclease mediates post-transcriptional gene silencing in *Drosophila* cells. *Nature* 404, 293-296.

Haner R and Hall J. (1998) The sequence-specific cleavage of RNA by artificial chemical ribonucleases. *Antisense Nucleic Acid Drug Development* 4, 423-430.

Hannon G. (2002) RNA interference. *Nature* 418, 244-251.

Hostomsky Z, Hughes SH, Goff SP, Le Grice SF. (1994) Redesignation of the RNase D activity associated with retroviral reverse transcriptase as RNase H. *Journal of Virology* 68, 1970-1971.

Hayward-Lester P, Oefner P and Doris A. (1996) Rapid quantification of gene expression by competitive RT-PCR and ion-pair reversed-phase HPLC. *Biotechniques* 20, 250-257.

Hutvagner G and Zamore P. (2002) RNAi: nature abhors a double-strand. *Science* 297, 2056-2060.

Jaeger L. (1997) The New World of ribozymes. *Current Opinions in Structural Biology* 7: 324–335.

Jen K and Gewirtz A. (2000) suppression of gene expression by targeted disruption of mRNA. *Stem Cells* 18, 307-319.

Jijakli H, Nadi AB, Cook L, Best L, Sener A, and Malaisse WJ. (1996) Insulinotropic action of methyl pyruvate: enzymatic and metabolic aspects. *Archives of Biochemistry and Biophysics* 335, 245-257.

Kavanagh KL, Elling RA and Wilson DK. (2004) Structure of *Toxoplasma gondii* LDH1: active-site differences from human lactate dehydrogenases and the structural basis for efficient APAD⁺ use. *Biochemistry* 43, 879-889.

Ketting R, Fischer S, Bernstein E, Sijen T, Hannon G and Plasterk R. (2001) Dicer functions in RNA interference and developmental timing in *C. elegans*. *Genes and Development* 15, 2654-2659.

Kissinger J, Gajira B, Li L, Paulsen I and Roos D. (2003) ToxoDB: accessing the *Toxoplasma gondii* genome. *Nucleic Acids Research* 31, 234-237.

Knoll LJ and Boothroyd JC. (1998) Isolation of developmentally regulated genes from *Toxoplasma gondii* by a gene trap with the positive and negative selectable marker hypoxanthine-xanthine-guanine phosphoribosyltransferase. *Molecular and Cell Biology* 18, 807-14.

Kruger K, Grabowski PJ, Asug AJ, Sands J, Dottsling DE and Cech TR. (1982) Self-splicing RNA: autoexcision and autocyclization of the ribosomal RNA intervening sequence of Tetrahymena. *Cell* 31, 147-157.

Kuwabara P and Coulson A. (2000) RNAi-Prospects for a General Technique for Determining Gene Function. *Parasitology Today* 16, 347-349.

LaCount D, Bruse S, Hill K and Donelson J. (2000) Double-stranded RNA Interference in *Trypanosoma brucei* using head-to-head promoters. *Molecular and Biochemical Parasitology* 111, 67-76.

Laemmli UK. (1970) Cleavage of structural proteins during the assembly of the head bacteriophage T4. *Nature* 227, 680-683.

Lamond AI and Sproat BS. (1993) Antisense oligonucleotides made of 2'-O-alkylRNA: their properties and applications in RNA biochemistry. *FEBS Letters* 325, 123-127.

Liu J, Carmell M, Rivas F, Marsden C, Thomson M, Song J, Hammond S and Hannon G. (2004) Rgonaute2 is the catalytic engine of mammalian RNAi. *Science* 305, 1437-1441.

Luft B and Remington J. (1992) Toxoplasmic encephalitis in AIDS. *Clinical Infectious diseases* 15, 24-222.

Malhorta P, Dasardadhi P, Kumar A, Mohammed A, Agrawal N, Bhatnagar R and Chauhan V.S. (2002) Double-stranded RNA-mediated gene silencing of cysteine proteases of *Plasmodium falciparum*. *Molecular Microbiology* 45, 1245-1254.

Manger ID, Hehl A, Parmley S, Sibley LD, Marra M, Hillier L, Waterston R, McManus M and Sharp P. (2002) Gene silencing in mammals by small interfering RNAs. *Nature Reviews of Genetics* 3, 737-747.

Marra M. (1998) Comparative analysis of wildtype and mutant GFP. *European Journal* 12, 287-289.

Meissner M, Brecht S, Bujard H and Soldati D. (2001) Modulation of myosin A expression by a newly established tetracycline repressor-based inducible system in *Toxoplasma gondii*. *Nucleic Acids Research* 29, 115-119.

Meissner M, Schluter D and Soldati D. (2002) Role of *Toxoplasma gondii* myosin A in powering parasite gliding and host cell invasion. *Science* 298, 837-840.

Melo EJ, Attias M and De Souza W. (2000) The single mitochondrion of tachyzoites of *Toxoplasma gondii*. *The Journal of Structural Biology* 130, 27-33.

Miller CM, Smith NC and Johnson AM. (1999) Cytokines, nitric oxide, heat shock proteins and virulence in *Toxoplasma*. *Parasitology Today* 10, 418-22.

McRobert, L. and McConkey, G.A. (2002) RNA interference inhibits growth of *Plasmodium falciparum*. *Molecular and Biochemical Parasitology* 119, 273-278.

Nakaar V, Ngo E and Joiner K. (2000) Selection based on the expression of antisense hypoxanthine-xanthine-guanine-phosphoribosyltransferase RNA in *Toxoplasma gondii*. *Molecular and Biochemical Parasitology* 110, 43-51.

Nakaar V, Samuel B, Ngo E and Joiner K. (1999) Targeted reduction of nucleoside triphosphate hydrolase by antisense RNA inhibits *Toxoplasma gondii* proliferation. *The Journal of Biological Chemistry* 274, 5083-5087.

Napoli C, Lemieux C and Jorgenson RA. (1990) Introduction of a chimeric chalcone synthase gene in petunia results in reversible cosuppression of homologous genes *in trans*. *Plant Cell* 2, 279-289.

Ngo H, Tschudi C and Ullu E. (1998). Double-stranded RNA induces mRNA degradation in *Trypanosoma brucei*. *Proceedings of the National Academy of Science* 95, 14687-14692.

Novina C and Sharp P. (2004) The RNAi revolution. *Nature* 430, 161-164.

Nykanen T, Haley B and Zamore P. (2001) ATP requirements and small interfering RNA structure in the RNAi pathway. *Cell* 107, 309-321.

Paddison P, Caudy A and Hannon G. (2002) Stable suppression of gene expression By RNAi in mammalian cells. *Proceedings of the National Academy of Science* 99, 1443-1448.

Parmley SF, Weiss LM and Yang S. (1995) Cloning of a bradyzoite-specific gene of *Toxoplasma gondii* encoding a cytoplasmic antigen. *Molecular and Biochemical Parasitology* 73, 253-257.

Parrish S and Fire A. (2001) Distinct roles for RDE-1 and RDE-4 during RNAi in *Caenorhabditis elegans*. *RNA* 7, 1397-1402.

Pfefferkorn ER, Schwartzman JD and Kasper LH. (1983) *Toxoplasma gondii*: use of mutants to study the host-parasite relationship. Ciba Foundation Symposium 99, 74-91.

Ravi K and Ahringer J. (2003). Genome-wide RNAi screening in *C. elegans*. *Methods* 30, 313-321.

Roos D, Donald RGK, Morrissette N and Moulton A.L.C. (1994) Molecular tools For genetic dissection of the protozoan parasite *Toxoplasma gondii*. *Methods in Cell Biology* 45, 27-63.

Sambrook J, Fritsch EF and Maniatis T. (1989). Molecular Cloning: A Laboratory Manual, 2nd Ed. Cold Spring Harbor Laboratory Press, Cold Spring Harbor, NY.

Schawrtzman J and Pfefferkorn ER. (1977) Pyrimidine synthesis by *Toxoplasma gondii*. *Journal of Parasitology* 67, 150-156.

Schumacher MA, Carter D, Scott DM, Roos DS, Ullman B and Brennan RG. (1998) Crystal structures of *Toxoplasma gondii* uracil phosphoribosyltransferase reveal the atomic basis of pyrimidine discrimination and prodrug binding. *Embryology* 15, 3219-3232.

Sharp P. (2001) RNA interference-2001. *Genes and Development* 15, 485-490.

Sharp P. (1999) RNAi and the double-stranded RNA. *Genes and Development* 13, 139-141.

Sheng J, Al-Anouti F and Ananvoranich S. (2003) Engineered *Delta* ribozymes can simultaneously knock down the expression of the genes encoding uracil phosphoribosyltransferase and hypoxanthine xanthine guanine phosphoribosyltransferase in *Toxoplasma gondii*. *The International Journal of Parasitology* 34, 253-263.

Sibley LD. (1993) Interactions between *Toxoplasma gondii* and its mammalian host cells. *Seminars in Cell Biology* 4(5), 35-44.

Sijen T, Fleenor J, Simmer F, Thijssen K, Parrish S, Timmons L, Plasterk R and Fire A. (2001) On the role of RNA amplification in dsRNA-triggered gene silencing. *Cell* 107, 465-476.

Sijen T and Kooter J. (2000) Post-transcriptional gene-silencing: RNAs on the attack or on the defense. *BioEssays* 22, 520-531.

Soete M, Camus D and Dubremetz JF. (1994) Experimental induction of bradyzoite-specific antigen expression and cyst formation by the RH strain of *Toxoplasma gondii* *in vitro*. *Experimental Parasitology* 78, 361-370.

Soete M, Fortier B, Camus D and Dubremetz JF. (1993) *Toxoplasma gondii*: kinetics of bradyzoite-tachyzoite interconversion *in vitro*. *Experimental Parasitology* 76, 259-264.

Soldati D and Boothroyd JC. (1995) A selector of transcription initiation in the protozoan parasite *Toxoplasma gondii*. *Molecular and Cell Biology* 15, 87-93.

Striepen B, He C, Matrajt M, Soldati D and Roos D.S. (1998) Expression, selection and organellar targeting of the green fluorescent protein in *Toxoplasma gondii*. *Molecular and Biochemical Parasitology* 92, 325-338.

Sui G, Affar B and Yang S. (2002) A DNA vector-based RNAi technology to suppress gene expression in mammalian cells. *Proceedings of the National Academy of Science* 99, 5515-5520.

Sun L, Cairns M, Saravolac E, Baker A and Gerlach W. (2000) Catalytic nucleic acids. *Pharmacological Reviews* 52, 325-346.

Svoboda P, Stein P, Hayashi H, and Schultz RM. (2000) Selective reduction of dormant maternal mRNAs in mouse oocytes by RNA interference. *Development* 127, 4147-4156.

Tabara H, Sarkissian M, Kelly W, Fleenor J, Fire A and Mello C. (1999) The rde-1 Gene, RNAi and Transposon silencing in *Caenorhabditis elegans*. *Cell* 99, 123-132.

Tanner NK. (1999) Ribozymes: the characteristics and properties of catalytic RNAs. *FEMS Microbiology Review* 23, 257-275.

Taylor ER, Seleiro EA and Brickell PM. (1996) Identification of antisense transcripts of the chicken insulin-like growth factor-II gene. *Journal of Molecular Endocrinology* 7, 145-154.

Tijsterman M, Ketting R and Plasterk R. (2002). The Genetics of RNA Silencing. *Annual Reviews of Genetics* 36, 489-519.

Tomavo S. (2001) The differential expression of multiple isoenzyme forms during stage conversion of *Toxoplasma gondii*: an adaptive developmental strategy. *International Journal of Parasitology* 31, 1023-1031.

Tschudi C, Djikeng A, Shi H and Ullu E. (2003) *In vivo* analysis of RNAi in *Trypanosoma brucei*. *Methods* 30, 304-312.

Tuschl T and Borkhardt A. (2002) Small interfering RNAs: a revolutionary tool for the analysis of gene function and gene therapy. *Gene* 2002 2, 158-167.

Tuschl T, Zamore P, Lehmann R, Bartel D and Sharp P. (1999). Targeted mRNA degradation by double-stranded RNA *in vitro*. *Genes and Development* 13, 3191-3197.

Ullu E, Tschudi C and Chakraborty T. (2004) RNAi in protozoan parasites. *Cell Microbiology* 6, 509-519.

Voinnet O. (2002) RNA silencing: small RNAs as ubiquitous regulators of gene expression. *Current Opinions in Plant Biology* 5, 444-451.

Wang Z, Morris J, Drew M and Englund P. (2000) Inhibition of *Trypanosoma brucei* gene expression by RNAi using an integratable vector with opposing T7 promoters. *The Journal of Biological chemistry* 275, 40174-41179.

Wianny F and Zernicka GM. (2000) Specific interference with gene function by double-stranded RNA in early mouse development. *Natural Cell Biology* 2, 70-75.

Winter VJ, Cameron A, Tranter R, Sessions RB, Brady RL. (2003) Crystal structure of *Plasmodium berghei* lactate dehydrogenase indicates the unique structural differences of these enzymes are shared across the *Plasmodium* genus. *Molecular and Biochemical Parasitology* 131, 1-10.

Wu J and Gerber MA. (1998) The inhibitory effects of antisense RNA on hepatitis B virus surface antigen synthesis. *Journal of Virology* 78, 641-647.

Yahiaoui B, Dzierszinski F, Bernigaud A, Slomianny C, Camus D and Tomavo S. (1999) Isolation and characterization of a subtractive library enriched for developmentally regulated transcripts expressed during encystation of *Toxoplasma gondii*. *Molecular and Biochemical Parasitology* 99, 223-235.

Yang D, Lu Brodsky F and Bishop M. (2002) Short RNA duplexes produced by hydrolysis with *Escherichia coli* RNase III mediate effective RNAi in mammalian cells. *Proceedings of the National Academy of Science* 99, 9942-9947.

Yang D, Lu H and Erickson J. (2000) Evidence that processed small dsRNAs may mediate sequence-specific mRNA degradation during RNAi in *Drosophila* embryos. *Current Biology* 10, 1191-1200.

Yang S and Parmley SF. (1995) A bradyzoite stage-specifically expressed gene of *Toxoplasma gondii* encodes a polypeptide homologous to lactate dehydrogenase. *Molecular and Biochemical Parasitology* 73, 291-294.

Yu S, DeRuijter L and Turner L. (2002) RNA interference by expression of short-interfering RNAs and hairpin RNAs in mammalian cells. *Proceedings of the National Academy of Science* 99, 6047-6052.

Zamore PD, Tuschl T, Sharp PA and Bartel DP. (2000) RNAi: double-stranded RNA directs the ATP-dependent cleavage of mRNA at 21 to 23 nucleotide intervals. *Cell* 101, 25-33.

Zeng Y and Cullen B. (2002) RNA interference in human cells is restricted to the cytoplasm. *RNA* 8, 855-860.

Zhang YW, Halonen SK, Ma YF, Wittner M and Weiss L. (2001) Initial characterization of CST1, a *Toxoplasma gondii* cyst wall glycoprotein. *Infection and Immunity* 69, 501-507.

APPENDIX A

General buffers and solutions used in the study

Buffer or solution	Constituents
Blocking solution	1 g blocking reagent in 100 ml maleic acid buffer
Cytomix	120 mM M KCl, 0.15 mM CaCl ₂ , 10 mM K ₂ HPO ₄ , KH ₂ PO ₄ , pH 7.6, 25 mM HEPES, pH 7.6, 2 mM EDTA, 5 mM MgCl ₂
Detection buffer	0.1 M Tris-HCl, and 0.1 M NaCl, pH 9.5
Dulbecco's phosphate-buffered saline (DPBS)	PBS buffer supplemented with 0.1 g/l Ca ⁺²
DNA gel loading	0.25% (w/v) Bromophenol Blue in 30% glycerol
Hybridization buffer	1% (w/v) blocking reagent, 0.5% sarcosyl and SDS, 4x SSC, and 5 mM sodium phosphate buffer, pH 7.0
Luri Bertani broth (LB broth)	10 g/l tryptone, 5 g/l yeast extract and, 0.17 M NaCl. The broth is sterilized by autoclaving for 15 min.
Maleic acid buffer	0.1 M maleic acid, and 0.15 M NaCl, pH 7.5
MOPS	20 mM MOPS, 5 mM NaCl, and 1mM EDTA pH 7.0
Phosphate-buffered saline (PBS)	0.14 M NaCl, 2.7 mM KCl, 10 mM Na ₂ HPO ₄ and 1.76 mM KH ₂ PO ₄ KH ₂ PO ₄ , pH 7.4
Resolving gel	9% acrylamide/bisacrylamide (37.5:1), 0.39 M Tris, pH 8.8, 0.1% SDS, 0.1% APS and 0.04% TEMED

RNA gel loading	50% formamide, 5.5% formaldehyde, 0.25% of each Bromophenol Blue and Xylene Cyanol, 20 mM MOPS, 5 mM NaCl, and 1 mM EDTA pH 7.0
Sodium chloride-sodium citrate (SSC)	3 M NaCl, 300 mM sodium citrate, pH 7.0
Stacking gel	5% acrylamide/bisacrylamide (37.5:1), 0.125 M Tris, pH 6.8, 0.1% SDS, 0.1% APS and 0.1% TEMED
SDS-PAGE destaining	45% methanol and 10% glacial acetic acid (v/v)
SDS-PAGE loading	25mM Tris, pH 6.8, 100 mM DTT, 2% SDS, 0.1% Bromophenol Blue and 10% glycerol
SDS-PAGE staining	2.5 g/l Coomassie blue in 40% methanol and 10% glacial acetic acid (v/v)
Tris EDTA buffer (TE)	10 mM Tris, pH 8.0, and 1 mM EDTA
Tris-glycine	25 mM Tris, pH 8.3, 0.25 M glycine and 0.1% SDS
Tris-Acetate-EDTA (TAE)	40 m Tris-acetate and 1 mM EDTA

APPENDIX B

Oligonucleotides used in the study

Primers for the synthesis of dsRNA DNA templates

T7on5'GFP	5'-TAATACGACTCACTATAGGTGAGCAAGGGC-3'
T7on3'GFP	5'-TAATACGACTCACTATAGGTACAGCTCGTCC-3'
T7on5'HX	5'-TAATACGACTCACTATAGGATGGCGTCCAAACCC-3'
T7on3'HX	5'-TAATACGACTCACTATAGGACCGGTGTCGACGTC-3'
T7on3'lacZ	5'-TAATACGACTCACTATAGGATTCCTGGCCGTC-3'
T7on3'lacZ	5'-TAATACGACTCACTATAGGTTTATGCAGCAACG-3'
T7on5'LDH1	5'-TAATACGACTCACTATAGGATGGCACCCGCA-3'
T7on3'LDH1	5'-TAATACGACTCACTATAGGCGTTTCGGCTCC-3'
T7on5'LDH2	5'-TAATACGACTCACTATAGGATGACGGGTACC-3'
T7on3'LDH2	5'-TAATACGACTCACTATAGGAAATCGTGCCGA-3'
T7on3'GFP mut2	5'-AAGAATTCTAATACGACTCACTATAGGAGAAGA-3'
T7on3'GFP mut2	5'-AAGAATTCTAATACGACTCACTATAGGTCTGCTA-3'
T7on5'ROP1	5'-TAATACGACTCACTATAGGGGAACATGGGCC-3'
T7on3'ROP1	5'-TAATACGACTCACTATAGGCGCCGAAAGCGT-3'
T7on5'UPRT	5'-TAATACGACTCACTATAGGATGGCGCAGGTC-3'
T7on3'UPRT	5'-TAATACGACTCACTATAGGCCAAAGTACCGG-3'

Primers for the synthesis of DIG-labeled probes

5ENOx	5'-ATGGTGGTTATCAAGG-3'
3ENOx	5'-CCAACGGGAGCGATC-3'
HXGPRT forward	5'-ATGGCGTCCAAACCCATTGAA-3'
HXGPRT reverse	5'-ACCGGTGTCGACGTCCTC-3'
LDH1-5'UTR	5'-AAATGGCACCCGCACTTG-3'
LDH2-5'UTR	5'-CCATGACGGGTACCGTTAGC-3'
ROP1-forward	5'-GGAACATGGGCCACAGG-3'
ROP1-reverse	5'-CGCCCAAAGCGTCTCTG-3'
AgeIUP	5'-CCAAAGTACCCGGTCACCG-3'
5BamHIUP	5'-CATTGGATCCATGGCGCAGGTCCCAGC-3'

Primers for the construction of plasmids

KpnILDH2sense	5'-CGGGTACCTCCGAGCATCTCTACTGTAGAAAGT-3'
LDH2antisense	5'-GGTACGAATGCCGAGCAGCGCAAAGAAAGT-3'
LDH-ORFsense	5'-ATGGCACCCGCACTGGT-3'
3LDH-ORFantisense	5'-GCGGAAGCGACCAGTCGA-3'
LDH2forward	5'-ATGACGGGTACCGTTAG-3'
LDH2reverse	5'-AAATCGTGCCGAATCTA-3'
SacILDH2sense	5'-CGGAGCTCTCCGAGCATCTCTACTGTAGAAAGT-3'
XbaILDH2antisense	5'-CGTCTAGAGTACGAATCGG-3'

Primers for the synthesis of hairpin RNA

hpLDH1	5'AGGTCGTAAGAGTACTCAGCACGCAAGCGTGCTGA GTACTCTTACGACCTATAGTGAGTCGTATTA-3'
hpLDH2	5'AAGGTCATACTGGTTTGCGCTCGTCAAGACGAGCG CAAACCAGTATGACCTATAGTGAGTCGTATTA-3'
T7	5'-TAATACGACTCACTATAGG-3'

APPENDIX C

Sequences of synthesized lactate dehydrogenase hairpin RNAs

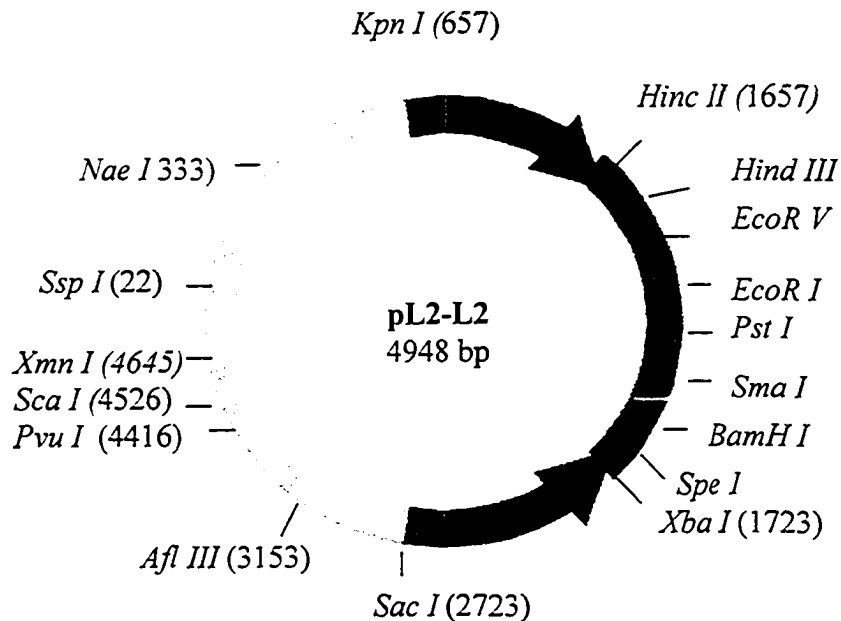
LDH1 hpRNA

g cgugcugaguacucuuacgaccuu OH
u
u c gcacgacucaugagaaugcugg PO₄

LDH2 hpRNA

g acgagcgcaaaccaguaugaccuu-OH
u
u c ugcucgcguuuggucauacucc-PO₄

APPENDIX D
Restriction map for plasmid pL2-L2



LDH2 promoter sequence (1kb)

```
tccgagcatctctactgtagaaagtaaaactatacctgctacacgagcttttgttgcaatgggtatt
taaagatccttagcatccgcttgcccctcttcgtctgtcaagcttaaactgctcggtccgctcagatt
accctcgtgaaggcaacgtgatcaacacggatctacacccctgttgcaaatctcggcagtgaggagc
gtgtgtgtgtgtgctgtgtgtgtgaaggggtacaccgccaccttgatttactagtgaggcggttgca
cctcgttcgtgacacgtgtggtcgcacctgtttcggggtaagcctgttttagctgccttcgtattgt
aaaaagggggttcggagcgaatcacctgatgtttgtctcaaaacctcgtggtacaccgacttgtt
tattccttctttcttctccacctccaactgcactcccgttcttctctctacaaccgcaacgaagt
gtgcacgctttgcaaggagctagcttagctgcatcatcactggctgatgatgggtgactctccagtc
acctggtgcccggaggtactgcccggagcatgctgctcccgttccagaaccagcggccggcggtgacaa
gcgtcgggctgaggcgtacaaataaccagaacttcttgcaacatgctctgCaggggagtgaaactg
cggacagggcggtgacgcgatatctgtaccggacgtggtcgatgccggcagagttttgtgcagctcc
ttccgaaaagggcacagaagacaatctggtggataaaaggagaacgttgtagcgtattccagaat
tatactcatgtgtgtggaacttctgagtaatgaagagacctgaatgtttaacttaaagtcgtgagg
agttaaacggcgtcgtgccaaaagttcaggcgtgtcgggtggcttttcgtagcaacatacttacgac
tttctttgcgctgctcggcattcgtac
```

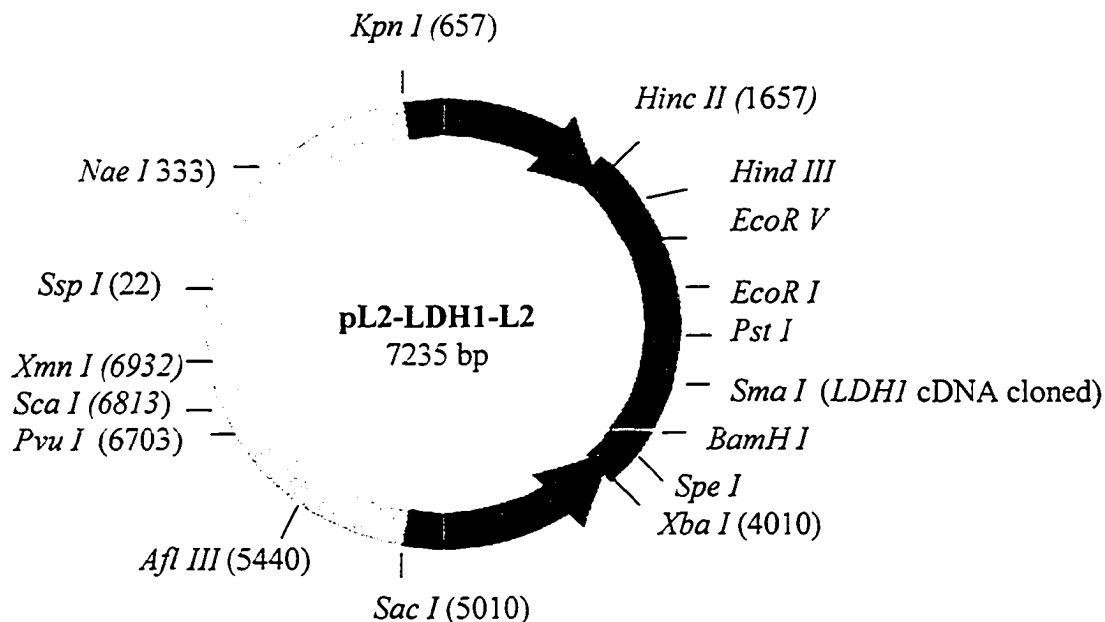
One **LDH2 promoter** was cloned between *sacI* 1759 and *XbaI* 1736

The second between *KpnI* 657 and blunted *XhoI*

The plasmid pL2-L2 is derived from pBluescript SK (+/-) backbone

APPENDIX E

Restriction map for plasmid pL2-LDH1-L2



LDH1 (GenBank accession number U35118)

```

Aaaatggcaccgcacttgtgagaggagaaagaaggtggccatgattggctctggcatgat
tgggtggcactatgggctacctgtgcgctctccgtgagctcgctgacgtcgttctctacgatg
ttgtcaaaggatgcccggggtaagcctcttgacctgagccatgtgacctccgtggctcgac
accaacgtttccgtccgtgctgagtactcttacgaggccgctcaccgggtgaggactgctg
tategttacccgctgctgaccaaggtgcccgggcaagcccgactccgagtgaggccgaaacg
atctgctcccgttcaactcgaagatcattcgcgagatcggtcagaacatcaagaagtactgc
cccaagaccttcatcatcgtggtcaccaaccgctggactgcatggtaagggttatgtgcca
ggcctctggcgtcccgaaccaacatgatctgcgggtatggcctgcatgctcgactctg
    
```

Arrows represent the **LDH2 promoter**

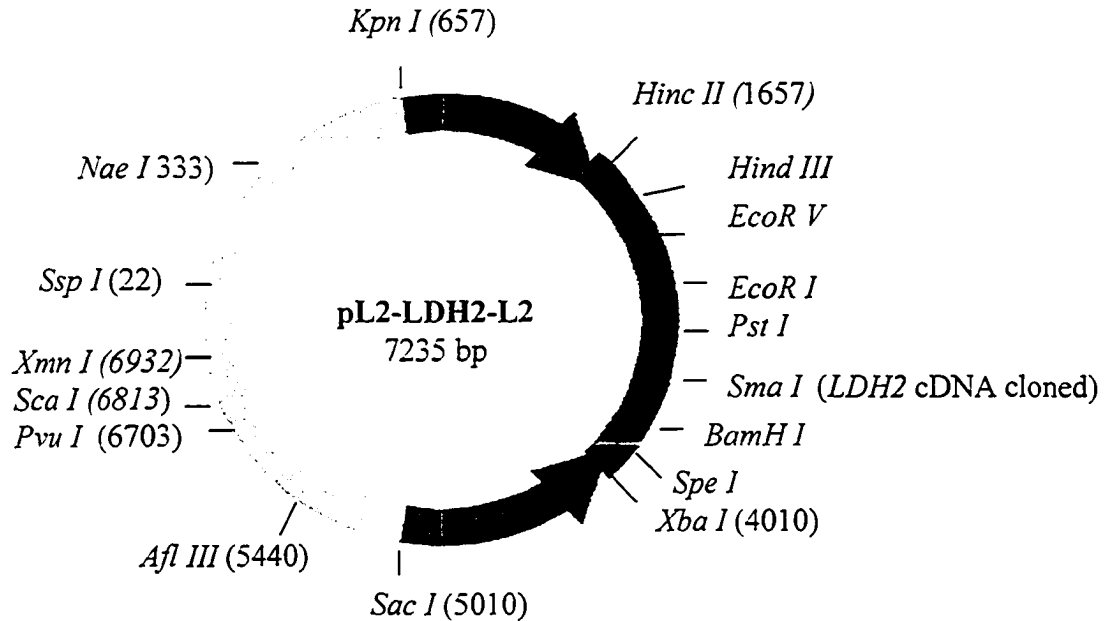
The **LDH1 cDNA** fragment (nt 1-487) was cloned at the blunt *SmaI* site

The HXGPRT cassette (1.8 kb) was cloned at *EcoRI* site

The plasmid pL2-LDH1-L2 is derived from plasmid pL2-L2

APPENDIX F

Restriction map for plasmid pL2-LDH2-L2



LDH2 (GenBank accession number U23207)

```

cttccaccatgacgggtaccgtagcagaagaaaaagattgcaatgattggttctggcatg
ataggaggaaccatgggctaccttgtgtgcttcgggagctagccgacgtcgtactattcga
cgttgtaacaggcatgccagaagggaaggcgttggatgattcacaggcgcacaagcattgctg
acacgaacgtgagcgtgacgagcgcacaaccagtatgagaagatcgccggatcggatgtcgta
ataataactgcagggtgaccaaggtaccggggaagagtgaacaggagtggagcagaaacga
cctttaccggtcaatgcaaaaatcattcgagaggtagcgcaggagtgagaagaagtactgcc
cgcttgcttttgaattg
tagtgacaaaccgcttgactgcatggtaaagtcttcatgaagcgagcgggttaccaaaa
aacatggtttgcggaatggcgaatgtgttagattcggc
    
```

Arrows represent the **LDH2 promoter**

The **LDH2 cDNA** fragment (nt 1-487) was cloned at the blunt *Sma*I site.

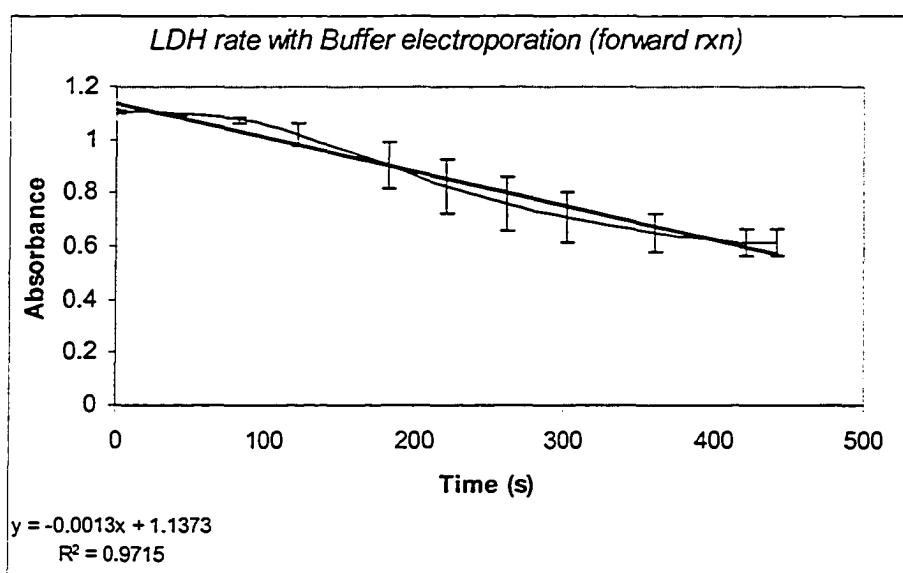
The HXGPRT cassette (1.8 kb) was cloned at *Eco*R I site

The plasmid pL2-LDH1-L2 is derived from plasmid pL2-L2

APPENDIX G

Measurement of lactate dehydrogenase enzymatic activity

To determine LDH activity in the forward reaction, the rate of the enzymatic reaction (R) is first calculated according to the spectrophotometric method by following the decrease in the absorbance due to NADH at 340 nm (Denton *et al.*, 1996). According to the Beer-Lambert equation ($A = \epsilon Cl$); where A is the absorbance at 340 nm, ϵ = the molar absorptivity characteristic of the material ($6.22 \text{ mM}^{-1} \cdot \text{cm}^{-1}$ for NADH), C is the concentration of the material in mmole/L and l is the optical path (1 cm); R is the slope of the graph obtained by plotting the change in absorbance versus time.



For this graph, $R = 1.3 \times 10^{-3}/\text{sec}$

Since $R = \Delta A/\text{sec}$; $R = \Delta A/(1/60) \text{ min} = \Delta[\text{NADH}] \times \epsilon \times l / (1/60) \text{ min}$

Therefore, $\frac{R \times 60/\text{min}}{\epsilon \times l} = \Delta[\text{NADH}]$ and $\Delta\text{moles of NADH} = \frac{R \times 60/\text{min} \times 10^{-3} \text{ L}}{\epsilon \times l}$

For this R value, $\Delta\text{moles of NADH} = \frac{1.3 \times 10^{-3} \times 60 \times 10^{-3}}{6.22 \times 1}$

The activity of LDH is calculated to be $12.54 \text{ nmol} \cdot \text{min}^{-1}$. Finally, the specific activity (activity per mg of protein in the lysate) is determined to be $809 \text{ nmol} \cdot \text{min}^{-1} \cdot \text{mg}^{-1}$; knowing that $15.5 \mu\text{g}$ protein extract was used in a final reaction volume of 1 mL.

VITA AUCTORIS
FATME AL-ANOUTI

Department of Chemistry and Biochemistry
University of Windsor
401 Sunset, Windsor, ON, N9B3P4

EDUCATION

2001- present	University of Windsor (ON, Canada)
1999-2001	Ph.D. candidate , Biochemistry M.Sc. , Clinical Chemistry
1995-1997	American University of Beirut (Lebanon)
1992-1995	M.Sc. , Microbiology and Immunology B.Sc. , Biological Sciences

EMPLOYMENT

1999-2005	University of Windsor (ON, Canada)
1994-1995	Research and teaching assistant National Laboratories for Medical Research (Lebanon)

AWARDS

- The University of Windsor Tuition Scholarship for the academic year 1999-2000.
- The University of Windsor Excellence award for scientific presentations, 2003.
- The University of Windsor Excellence award for scientific achievements, 2003.
- The Ontario Graduate Scholarship for the academic year 2003-2004.
- The Ontario Graduate Travel Award for the year 2003-2004
- The University of Windsor Excellence award for scientific achievements, 2003
- The Ontario Graduate Scholarship for the year 2004-2005.
- The University of Windsor Excellence award for scientific achievements, 2004.
- The Ontario Graduate Travel Award for the year 2004-2005.

VITA AUCTORIS
PUBLICATIONS

- Article by Al-Anouti, F., Parmley, S., Tomavo, S., and Ananvoranich, S. entitled as “The expression of lactate dehydrogenase is important for the cell cycle of *Toxoplasma gondii*”. *The Journal of Biological Chemistry* (2004), 279(50):52300-52311
- Article by Sheng, J., Al-Anouti, F., and Ananvoranich, S. entitled as “Engineered *Delta* ribozymes can simultaneously knock down the expression of the genes encoding uracil phosphoribosyltransferase and hypoxanthine xanthine guanine phosphoribosyltransferase in *Toxoplasma gondii*”. *The international journal of parasitology* (2004), 34(3):253-63.
- Article by Al-Anouti, F., Quach, T., and Ananvoranich, S. entitled as “Double-stranded RNA-mediated suppression of uracil phosphoribosyltransferase expression in *Toxoplasma gondii*”. *Biochemical and Biophysical Research Communications* (2003), 302, 316-323.
- Article by Lally, J., Al-Anouti, F., Bols, N., and Dixon, B. entitled as “Functional Characterization of CK-1, a Putative CC Chemokine from Rainbow Trout (*Onchorhynchus mykiss*)”. *Fish and Shellfish Immunology* (2003), 15(5):411-24.
- Article by Al-Anouti F. and Ananvoranich S. entitled as “Comparative Analysis of Antisense RNA, Double-Stranded RNA and *Delta* Ribozyme-Mediated Gene Regulation in *Toxoplasma gondii*”. *Antisense and Nucleic Acid Drug Development* (2002), 12, 275-281.

POSTER PRESENTATIONS

- Al-Anouti F., Al-Rayes M., Shamim G., Tomavo S., and Ananvoranich S. (September, 2003). RNAi for a functional analysis of metabolic enzymes in *Toxoplasma gondii*. The 15th annual molecular parasitology meeting, Woods Hole, Boston, USA-September, 2004.
- Al-Anouti F., Shamim G. and Ananvoranich S. RNAi for a functional analysis of Lactate dehydrogenase in *T. gondii*. The ninth annual meeting of the RNA society. University of Wisconsin, Madison-June, 2004.
- Al-Anouti, F., and Ananvoranich, S. (September, 2003). Knock-down of the expression of lactate dehydrogenase in *Toxoplasma gondii*. The 14th annual molecular parasitology meeting, Woods Hole, Boston, USA.
- Ananvoranich, S., Al-Anouti, F., and Sheng, J. (May, 2002) *In vivo* stability and efficacy of double-stranded RNA and *delta* ribozymes in *Toxoplasma gondii*. The 7th Annual Meeting of the RNA Society, Madison, Wisconsin, USA
- Lally, J., Al-Anouti, F., Gauley, J., Bols, N., and Dixon, B. (April, 2002). The Functional Characterization of CK-1, A Putative CC Chemokine from Rainbow Trout (*Onchorhynchus mykiss*). The 16th Annual Spring Meeting for the Canadian Society for Immunology, Collingwood, Canada.